

M2 macrophages as therapeutic targets: characterization and yeast-based gene delivery

Dissertation
zur Erlangung des Grades
des Doktors der Naturwissenschaften
der Naturwissenschaftlich-Technischen Fakultät
der Universität des Saarlandes

von
Michelle Seif

Saarbrücken
2016

Tag des Kolloquiums: 27.10.2016

Dekan: Prof. Dr. Guido Kickelbick

Berichterstatter: Prof. Dr. Alexandra K. Kiemer
Prof. Dr. Manfred J. Schmitt

Vorsitz: Prof. Dr. Andriy Luzhetskyy

Akad. Mitarbeiter: Dr. Matthias Engel

Contents

Table of Contents

Abbreviations	1
Abstract	5
1 Introduction	7
1.1 Macrophage heterogeneity and plasticity	9
1.1.1 Classically activated macrophages (M1).....	10
1.1.2 Alternatively activated macrophages (M2)	11
1.1.3 Tumor-associated macrophages	12
1.1.4 Inducing an M1 phenotype in macrophages by gene therapy	13
1.2 Silica nanoparticles	14
1.3 Yeast <i>Saccharomyces cerevisiae</i>	15
1.3.1 Recombinant <i>S. cerevisiae</i> in biotechnology.....	15
1.3.2 <i>S. cerevisiae</i> interaction with phagocytic cells.....	16
1.4 Aim of this work	17
2 Chapter I	19
2.1 Introduction	21
2.2 Results	22
2.2.1 Human monocyte-derived macrophages.....	22
2.2.2 Uptake of yeast by monocytes derived macrophages	24
2.2.3 Effect of <i>S. cerevisiae</i> on M-CSF and GM-CSF-differentiated macrophages polarization	27
2.3 Discussion	32
2.3.1 Characterization of GM-M Φ and M-M Φ	32
2.3.2 <i>S. cerevisiae</i> uptake by <i>in vitro</i> polarized macrophages.....	33
2.3.3 <i>S. cerevisiae</i> polarizes both M-CSF and GM-CSF-differentiated macrophages towards an M1-like phenotype	34
2.4 Conclusion	35

Contents

3	Chapter II	37
3.1	Introduction.....	39
3.2	Results.....	40
3.2.1	Polarization of human monocyte-derived macrophages.....	40
3.2.2	Uptake of yeast by differently polarized macrophages.....	43
3.2.3	<i>S. cerevisiae</i> uptake induces pro-inflammatory cytokine mRNA expression in M1 and M2c macrophages.....	45
3.2.4	<i>S. cerevisiae</i> delivers functional DNA and mRNA to human M1 and M2c macrophages.....	47
3.2.5	<i>S. cerevisiae</i> -mediated <i>MYD88</i> mRNA delivery repolarizes M2c macrophages towards a pro-inflammatory phenotype.....	49
3.2.6	<i>S. cerevisiae</i> -mediated <i>TNF</i> mRNA delivery repolarizes M2c macrophages towards a pro-inflammatory phenotype.....	53
3.3	Discussion.....	55
3.3.1	<i>In vitro</i> model of pro- and anti-inflammatory macrophages	55
3.3.2	Yeast uptake by differently polarized macrophages.....	56
3.3.3	Yeast mediated nucleic acids delivery to human macrophages	56
3.4	Conclusion	58
4	Chapter III	59
4.1	Introduction.....	61
4.2	Results.....	62
4.2.1	Silica nanoparticle toxicity	62
4.2.2	Uptake of nanoparticles and microparticles in <i>in vitro</i> polarized macrophages.....	63
4.2.3	Nanoparticle uptake in primary human alveolar macrophages (AM) and tumor-associated macrophages (TAM)	66
4.3	Discussion.....	68
4.3.1	Nanoparticles clearance.....	68
4.3.2	Macrophage polarization influences particle uptake.....	69
4.3.3	Silica nanoparticles uptake is enhanced in tumor-associated macrophages.....	71
4.4	Conclusion	72

Contents

5	Materials and methods	73
5.1	Cell culture	75
5.1.1	Human monocyte-derived macrophages (MDM)	75
5.1.2	THP-1 cell line	77
5.1.3	Cell counting and viability	77
5.2	Yeast preparation	78
5.2.1	Culture	78
5.2.2	Fluorescence labeling	79
5.2.3	Opsonization	79
5.2.4	Plasmid generation for yeast transformation	79
5.2.5	Transformation	79
5.3	Isolation of DNA	80
5.3.1	Plasmid DNA isolation	80
5.3.2	THP-1 DNA isolation	80
5.4	Agarose gel electrophoresis	81
5.4.1	Detection of DNA	81
5.4.2	Detection of RNA	81
5.5	RNA isolation and reverse transcription	81
5.5.1	RNA isolation	81
5.5.2	Measurement of RNA concentration	82
5.5.3	Alu PCR	82
5.5.4	Reverse transcription	83
5.6	Real Time RT-PCR	83
5.6.1	Primer and probes sequences	83
5.6.2	Standard dilution series	84
5.6.3	Experimental procedure	84
5.7	Western Blot	86
5.7.1	Preparation of protein samples	86
5.7.2	SDS-polyacrylamide gel electrophoresis (SDS-PAGE)	86
5.7.3	Blotting	87
5.7.4	Immunodetection	87
5.8	Flow cytometry	88

Contents

5.8.1	Antibodies	88
5.8.2	Cell staining and analysis	88
5.9	Uptake studies	89
5.9.1	Sample preparation	89
5.9.1	Uptake evaluation by fluorescence microscopy	89
5.9.2	Uptake quantification by flow cytometry	90
5.10	Cytokine measurement	90
5.11	Statistics	90
6	Summary and outlook	93
7	References	99
8	Publications	113
9	Acknowledgment	115

Abbreviations

Abbreviations

ACTB	Beta-actin
AM	alveolar macrophage
amp	ampicillin
AP-1	Activator protein 1
APC	Allophycocyanin
APS	ammonium persulfate
BHQ1	black hole quencher 1
bp	base pairs
BSA	bovine serum albumin
<i>C. Albicans</i>	<i>Candida albicans</i>
CD	cluster of differentiation
cDNA	complementary DNA
CEA	Carcinoembryonic Antigen
CFSE	carboxyfluorescein diacetate succinimidyl ester
CXCL	Chemokine (C-X-C motif) ligand
d/o	deficient
DAPI	4',6-diamidino-2-phenylindole
DC	dendritic cell
DMSO	dimethyl sulfoxide
DNA	deoxyribonucleic acid
DNase	deoxyribonuclease
dNTP	dATP, dCTP, dGTP or dTTP
dTTP	2'-deoxythymidine 5'-triphosphate
E. coli	Escherichia coli
EDTA	ethylenediaminetetraacetic acid
eGFP	green fluorescent protein
EtBr	ethidium bromide
FBS	fetal bovine serum

Abbreviations

Fc	fragment crystalline
FITC	fluorescein isothiocyanate
FSC	forward scatter
g	gram
GILZ	glucocorticoid -induced leucine zipper
Glipr1	Glioma pathogenesis-related protein 1
GM-CSF	Granulocyte-macrophage colony-stimulating factor
GMFI	geometric mean of fluorescence intensity
GM-M Φ	GM-CSF derived macrophages
GRAS	Generally recognized as safe
HCV	Hepatitis C virus
HLA	human leukocyte antigen
ICL1	isocitrate lyase
IFN	interferon
IKK- β	inhibitory protein κ B
IL	Interleukin
IL-1ra	IL-1 receptor antagonist
IRES	internal ribosomal entry site
IRF	IFN regulating factor
kb	kilo bases
kDa	kilo Dalton
l	litre
LB	Luria Bertani
LiAc	lithium acetate
LPS	lipopolysaccharide
M	molar
MCP-1	Monocyte chemoattractant protein-1
M-CSF	Macrophage colony-stimulating factor
MgCl ₂	Magnesium Chloride
min	minute
MLS1	malate synthase

Abbreviations

M-M Φ	M-CSF derived macrophages
MOI	multiplicity of infection
MPS	mononuclear phagocyte system
mRNA	messenger RNA
MTT	3-(4,5-dimethyl-thiazol-2-)-2.5-diphenyl tetrazolium bromide
MyD88	myeloid differentiation factor 88
M Φ	Macrophages
NaN ₃	Sodium azide
NF- κ B	nuclear factor- κ b
NK	Natural killer
<i>P. brasiliensis</i>	<i>Paracoccidioides brasiliensis</i>
PBMC	Peripheral blood mononuclear cells
PBS	phosphate buffered saline
PBST	phosphate buffered saline tween
PCR	polymerase chain reaction
PE	Phycoerythrin
PEG	polyethyleneglycol
PGK	phosphoglycerate kinase promoter
PI	Propidium Iodide
PMA	Phorbol 12-myristate 13-acetate
RNA	ribonucleic acid
RNase	ribonuclease
rpm	rounds per minute
RPMI	Roswell Park Memorial Institute
RT	reverse transcription
<i>S. cerevisiae</i>	<i>Saccharomyces cerevisiae</i>
SC	synthetic complete
SDS	sodium dodecylsulfate
SDS-PAGE	sodium dodecylsulfate polyacrylamide gel electrophoresis
SEM	standard error of the mean

Abbreviations

SFM	Serum Free Medium
shRNA	short hairpin RNA
SSC	sideward scatter
STAT	Signal Transducer and Activator of Transcription
TAM	tumor-associated macrophages
TBE	tris-borate EDTA buffer
TE	tris-EDTA buffer
TEMED	Tetramethylethylenediamin
TGF	transforming growth factor
TLR	toll-like Receptor
TNF- α	tumor necrosis factor- α
TRIF	TIR-domain-containing adapter-inducing interferon- β
Tris	α,α,α -tris-(hydroxymethyl)-methylamine
U	unit
ura	uracil
UV	ultra violet
V	volt
x g	x-fold gravitational force
[v/v]	volume per volume
[w/v]	weight per volume
μm	micrometer

Abstract

Abstract

Macrophages (M ϕ) are professional phagocytic cells responsible for internalizing and clearing particles and pathogens. The prevailing M ϕ phenotype largely depends on the local immune status of the host. Whereas M1-polarized M ϕ are considered as pro-inflammatory M ϕ , M2 M ϕ exhibit anti-inflammatory functions and promote tumor growth.

Yeast *Saccharomyces cerevisiae* is taken up by phagocytic cells and is a promising vehicle for nucleic acids vaccines. Herein, we aimed to study the response of human M ϕ to *S. cerevisiae* exposure and its potential use as a gene delivery system in M1 and M2 cells.

Oponized *S. cerevisiae* was taken up to the same extent by M1 and M2 M ϕ and induced an M1 like-phenotype in both cell types. Furthermore, yeast delivered functional nucleic acids to M ϕ , especially when constitutively biosynthesized mRNA was used. Interestingly, protein expression of the delivered nucleic acid was higher in M2 cells when compared with M1 M ϕ . Finally, the delivery of pro-inflammatory mediator mRNA to M2 M ϕ re-educated them towards an M1 phenotype.

Silica nanoparticles represent another potential delivery system. Interestingly, nanoparticle uptake was enhanced in M2 compared with M1 M ϕ . In contrast, the uptake of microparticles did not differ between M1 and M2 phenotypes.

Our results suggest the use of yeast- or nanoparticle-based gene delivery as promising approach for the treatment of pathologic conditions that may benefit from the presence of M1-polarized M ϕ , such as cancer.

Zusammenfassung

Makrophagen (M ϕ) sind professionelle Phagozyten und damit für die Aufnahme und den Abbau von Partikeln und Pathogenen verantwortlich. Der vorherrschende M ϕ -Phänotyp wird vom lokalen Immunstatus des Wirts bestimmt.

Abstract

Während M1-M ϕ Entzündungsreaktionen unterstützen, haben M2-M ϕ anti-inflammatorische Funktionen, können allerdings auch das Tumorwachstum fördern.

Der Hefestamm *Saccharomyces cerevisiae* wird von phagozytierenden Zellen aufgenommen und bietet so die Möglichkeit, DNA-Impfstoffe zu verabreichen. In dieser Arbeit wurde der Einfluss von *S. cerevisiae* auf den Makrophagen-Phänotyp sowie eine mögliche Verwendung als Genübertragungssystem untersucht.

Opsonierte Hefezellen wurden von M1- und M2-M ϕ im gleichen Ausmaß aufgenommen und riefen in beiden Zelltypen einen pro-inflammatorischen Phänotyp hervor. Darüber hinaus konnte *S. cerevisiae* zur Übertragung funktioneller DNA und mRNA genutzt werden. Durch Übertragung von mRNA, die für pro-inflammatorische Mediatoren kodierte, konnten M2-M ϕ erfolgreich in Richtung M1 repolarisiert werden.

Silica-Nanopartikel könnten ebenfalls ein nützliches Werkzeug zur Genübertragung darstellen. Interessanterweise zeigten M2-M ϕ eine höhere Kapazität zur Aufnahme von Silica-Nanopartikeln.

Zusammengefasst zeigen unsere Ergebnisse, dass Hefe- oder Nanopartikel-basierte Gentherapie einen vielversprechenden Ansatz zur Therapie von Erkrankungen darstellen könnte, die von der Anwesenheit von M1-M ϕ profitieren, wie z.B. Tumorerkrankungen.

1 Introduction

Introduction

Introduction

1.1 Macrophage heterogeneity and plasticity

Macrophages are a heterogeneous population of innate immune cells, distributed throughout the tissues of the body. They are professional phagocytic cells mainly responsible for ingesting and processing foreign materials and clearance of dead cells and debris. Macrophages express a panel of receptors (e.g. scavenger receptors, Toll-like receptors (TLRs), or Fc receptors) allowing them to detect aberrant signals. They can act as effector cells in inflammation and activate the adaptive immune system (Murray and Wynn, 2011).

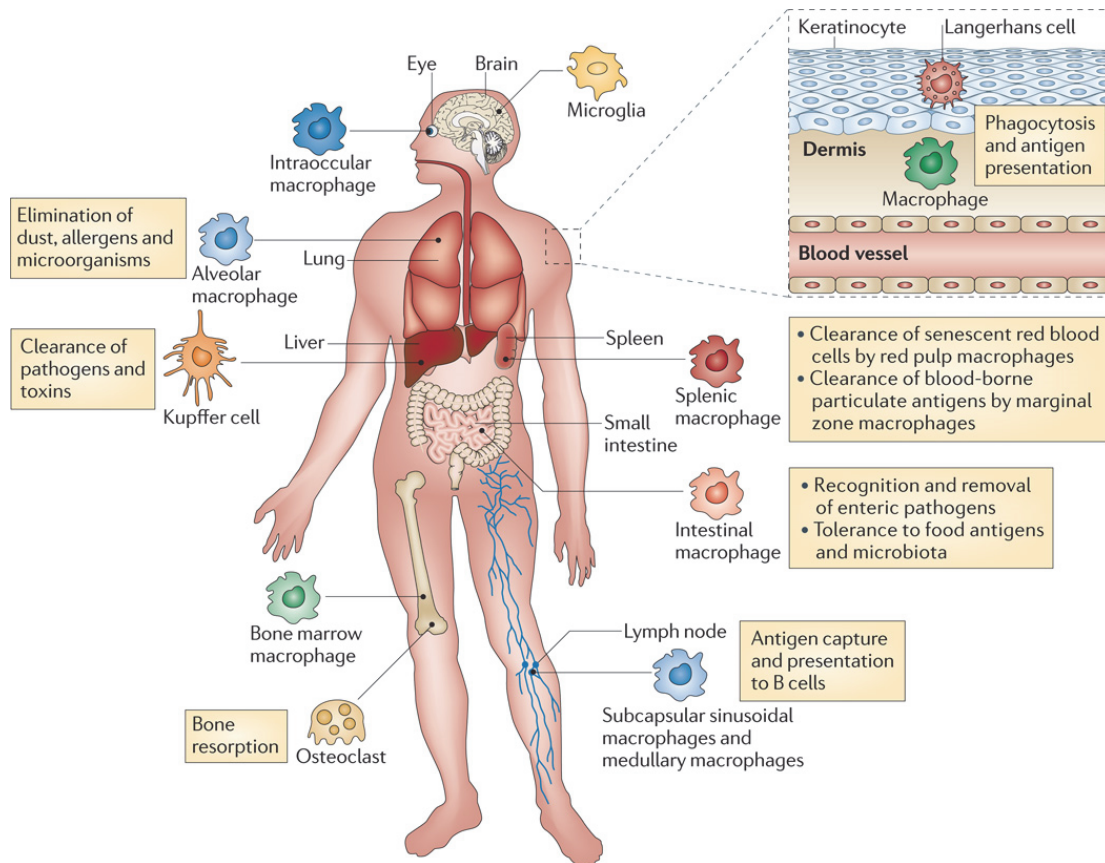


Figure 1: Macrophage distribution and functions. Macrophages are strategically located throughout the body. They fulfill several functions, mainly phagocytosis, cytokine secretion, and antigen presentation. Reprinted by permission from Macmillan Publishers Ltd: [Nat. Rev. Immunol.] (Murray and Wynn, 2011), copyright (2011).

Macrophages have a remarkable plasticity. Their functional phenotype can be dictated by the signals received from their micro-environment. With reference to Th1/Th2 polarization, two distinct activation states of macrophages have been

Introduction

suggested: the classically activated (M1) macrophage phenotype and the alternatively activated (M2) macrophage phenotype (Mills *et al.*, 2000; Mantovani *et al.*, 2004)

1.1.1 Classically activated macrophages (M1)

The M1 phenotype can be induced by different signals, such as granulocyte-macrophage colony-stimulating factor (GM-CSF) (Martinez *et al.*, 2014; Verreck *et al.*, 2004), the Th1 cytokine IFN- γ , the bacterial product lipopolysaccharide (LPS), or tumor necrosis factor (TNF)- α (Martinez *et al.*, 2014; Mantovani *et al.*, 2004). These stimuli trigger the expression of pro-inflammatory mediators and surface markers (e.g.: CD80, CD86, HLAII) in macrophages, which is mediated *via* several signal transduction pathways (Martinez *et al.*, 2014). For example, LPS is recognized by Toll-like receptor 4 (TLR4) and initiates distinct signaling cascades *via* the adapter molecules MyD88 (Myeloid differentiation primary response gene 88) or TRIF (TIR-domain-containing adapter-inducing interferon- β), which leads to the expression of high amounts of pro-inflammatory cytokines, mainly TNF- α , IL-6, IL-12, and interferons (Martinez *et al.*, 2014).

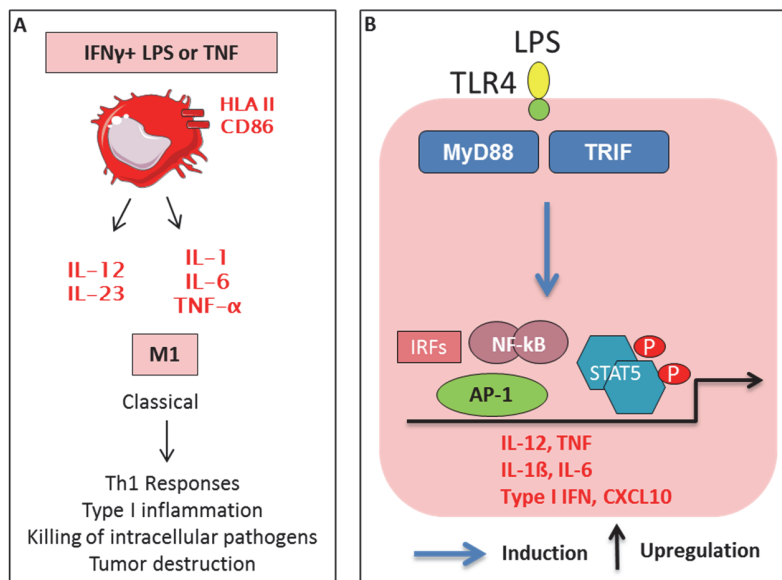


Figure 2: Classical activation of macrophages. (A) M1 stimuli, markers, and functions. (B) Key signaling mediators involved in LPS-induced activation. Modified after (Martinez *et al.*, 2014). Illustrations were obtained and modified from Servier Medical Art by Servier, <http://www.servier.com/Powerpoint-image-bank>, licensed under Creative Commons Attribution 3.0 Unported License, <http://creativecommons.org/licenses/by/3.0/>.

Introduction

M1 macrophages are essential for pathogen clearance, adaptive immune response activation, and tumor suppression, but they can also contribute to the pathogenesis of auto-immune and chronic inflammatory diseases (Murray and Wynn, 2011).

1.1.2 Alternatively activated macrophages (M2)

M2 macrophages are more diverse than M1 macrophages and can be divided into sub-groups depending on the stimuli inducing the phenotype. When alternatively activated macrophages were described for the first time they were induced by the Th2 cytokine IL-4 (Mills *et al.*, 2000). This phenotype was later called M2a and is characterized by a high expression of the mannose receptor (CD206) and the production of IL-1 receptor antagonist (IL-1ra). Macrophages stimulated simultaneously by immune complexes and agonists of Toll-like receptors (e.g.: LPS) are known as M2b. These cells express at the same time pro-inflammatory cytokines (e.g.: TNF- α and IL-6) and high levels of the anti-inflammatory cytokine IL-10 with low levels of IL-12. The anti-inflammatory cytokine IL-10 induces the M2c phenotype (Martinez *et al.*, 2014; Mantovani *et al.*, 2004). IL-10 administration leads to an inhibition of pro-inflammatory cytokine expression and to the production of anti-inflammatory mediators, such as IL-10 itself (Staples *et al.*, 2007) or GILZ (Berrebi *et al.*, 2003), as well as to the upregulation of the scavenger receptor CD163 (Rey-Giraud *et al.*, 2012). Recently, the macrophage colony-stimulating factor (M-CSF) was also considered as an M2 stimulus since it can also induce an anti-inflammatory phenotype (Martinez *et al.*, 2014; Verreck *et al.*, 2004).

Introduction

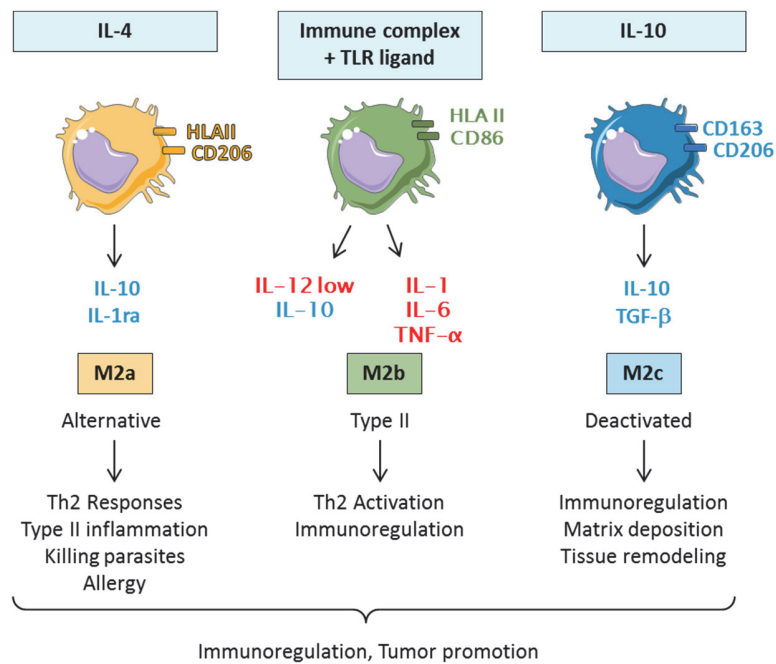


Figure 3: M2 macrophage sub-groups. M2 stimuli, markers, and functions. Modified after (Martinez *et al.*, 2014). Illustrations were obtained and modified from Servier Medical Art by Servier, <http://www.servier.com/Powerpoint-image-bank>, licensed under Creative Commons Attribution 3.0 Unported License, <http://creativecommons.org/licenses/by/3.0/>.

The M2 phenotype is critically involved in wound healing and anti-parasitic immunity but is also known to promote tumor growth (Murray and Wynn, 2011).

1.1.3 Tumor-associated macrophages

Macrophages are one of the major populations of infiltrating leukocytes in solid tumors. These tumor-associated macrophages (TAM) play an important role in tumor initiation, development, and metastasis. TAM are considered to be a polarized M2-like macrophage population with potent immunosuppressive functions (Ma *et al.*, 2010; Solinas *et al.*, 2009; Sica *et al.*, 2007). Both the presence of TAM and M-CSF overexpression are related to a poor prognosis, especially in ovarian, breast, uterine, prostate cancer and lung adenocarcinoma (Bingle *et al.*, 2002; Pollard *et al.*, 2004; Lin *et al.*, 2001; Zhang *et al.*, 2011). Also elevated numbers of tumor-associated macrophages were correlated with therapy failure since they contribute to drug-resistance and have a radioprotective effect (Tang *et al.*, 2013).

Introduction

Tumor associated macrophages originate from circulating blood monocytes recruited to the tumor sites by tumor-derived chemoattractants, mainly MCP-1 (Monocyte chemoattractant protein-1) and M-CSF (Sica *et al.*, 2006; Mantovani *et al.*, 2002). In the tumor microenvironment, M-CSF promotes monocyte survival and differentiation into macrophages (Lin *et al.*, 2001). The cytokines expressed at the tumor site, mainly M-CSF, IL-10, and TGF- β , promote macrophage polarization towards an M2c phenotype (Sica *et al.*, 2006). TAM have many M2 markers: they express low levels of pro-inflammatory cytokines, high levels of scavenger receptor A (CD204), CD163, and mannose receptor (Sica *et al.*, 2006; Mantovani *et al.*, 2002; Komohara *et al.*, 2014). TAM display several pro-tumoral functions, mainly suppression of adaptive immunity, matrix remodeling, promotion of neo-angiogenesis, maintenance of tumor growth and survival, and promotion of tumor invasion and metastasis (Sica *et al.*, 2006). Thus, targeting TAM and re-educating them from an M2 to an M1 phenotype is a promising approach for cancer therapy (Tang *et al.*, 2013; Stout *et al.*, 2009).

1.1.4 Inducing an M1 phenotype in macrophages by gene therapy

The plasticity of macrophages provides a basis for strategies aiming to re-educate TAM towards an M1 phenotype. Several strategies using nucleic acid therapy seeking to increase the expression of pro-inflammatory mediators in macrophages were described (Singh *et al.*, 2014). In a mouse macrophage cell line, the expression of IFN- γ under the control of a hypoxia promoter using an adenoviral vector led to the successful overexpression of IFN- γ mRNA and protein in a hypoxic environment (Carta *et al.*, 2001). Murine macrophages transfected with an IL-12 recombinant adenoviral vector secreted IL-12 and were characterized by an upregulation of HLA I and II. When injected into the tumor of a mouse prostate cancer model they enhanced the infiltration of T cells and NK cells, consequently increasing the survival of the mice (Satoh *et al.*, 2003). Macrophages transfected with the *Glipr1* (Glioma pathogenesis-related protein 1, a protein having pro-apoptotic activities in prostate and bladder cancer cells) gene in an adenoviral vector showed a high expression of CD40, CD80, HLAII,

Introduction

IL-12, and IL-6. When injected into the tumor of a metastatic prostate cancer mouse model, they resulted in significantly suppressed tumor growth and metastasis (Tabata *et al.*, 2011). In another tumor model, TAM were isolated from established tumors, and then infected with an adenovirus carrying dominant negative IKK β , followed by a reinjection into the tumor-bearing mice. A significant decrease in tumor burden was observed along with a higher expression of IL-12 and lower expression of IL-10 in macrophages (Hagemann *et al.*, 2008). In an *in vitro* model of human M1/M2 polarized macrophages, Krausgruber *et al.* showed that the forced expression of IRF5 (Interferon regulatory factor 5, a master regulator of M1 phenotype in macrophages) in M2 macrophages re-educated them to an M1 phenotype by inducing the expression of pro-inflammatory cytokines and costimulatory molecules (Krausgruber *et al.*, 2011). All these studies using adenoviruses showed promising results, but their application is limited due their complicated handling procedure and poor safety profile. Several promising non-viral delivery systems including lipoplexes, polyplexes, polymers, and lipid delivery systems were tested in studies targeting the inflammatory macrophage phenotype (Singh *et al.*, 2014).

1.2 Silica nanoparticles

Silica nanoparticles are used in several biomedical applications such as bio-sensing and imaging (Korzeniowska *et al.*, 2013). They also represent a promising non-viral gene delivery vector due to their versatility, low toxicity and high transfection efficiency (Knopp *et al.*, 2009). Several studies showed the possibility of using surface modified silica nanoparticles as gene delivery system (Knopp *et al.*, 2009). Cationic silica nanoparticles carrying eGFP DNA at their surface introduced intranasally to mouse showed higher eGFP expression in lung than the eGFP plasmid alone (Ravi Kumar *et al.*, 2004). Amino-surface functionalized silica nanoparticles binding plasmid DNA were injected into mouse brains to transfect neuronal-like cells. This approach showed equal or better transfection efficiency than viral vectors (Bharali *et al.*, 2005).

Introduction

1.3 Yeast *Saccharomyces cerevisiae*

1.3.1 Recombinant *S. cerevisiae* in biotechnology

Saccharomyces cerevisiae is a non-pathogenic yeast, which has been used for thousands of years in the food industry (Sicard and Legras, 2011). Recombinant *S. cerevisiae* expressing viral or cancer antigens is currently being tested as a vaccine vehicle. Respective preclinical and clinical trials were reviewed by Ardiani *et al.* (Ardiani *et al.*, 2010). Moreover, recent studies have shown that recombinant *S. cerevisiae* could be used as a live vector for nucleic acids vaccination. After recombinant yeast uptake, human monocyte-derived dendritic cells expressed the model gene enhanced green fluorescent protein (eGFP) and were able to process and present the antigen of the human cytomegalovirus phosphoprotein pp65 (Walch *et al.*, 2012). Furthermore, *S. cerevisiae* could also deliver shRNA *in vivo* after oral yeast administration (Zhang *et al.*, 2014).

Several attributes make *S. cerevisiae* a promising nucleic acid vehicle:

- (i) It can be administered orally and protect the transported material from degradation in the gut (Beier *et al.*, 1998; Kenngott *et al.*, 2016)
- (ii) Unlike bacterial and viral live vectors, *S. cerevisiae* is considered as a safe organism (GRAS notice (175, 604, 422) from the FDA “U.S. Food and Drug Administration”) and it is devoid of endotoxins and super antigens (Gellisen and Hollenberg, 1997; Walch *et al.*, 2012).
- (iii) It has shown to be more efficient in nucleic acid delivery than a comparable *Listeria*-based system (Walch *et al.*, 2012).
- (iv) Yeast can be easily genetically modified and can be rapidly grown to high cell density (Valenzuela *et al.*, 1982; Smith *et al.*, 1985).
- (v) Yeast can specifically target phagocytic cells (Beier *et al.*, 1998).

Introduction

1.3.2 *S. cerevisiae* interaction with phagocytic cells

The *S. cerevisiae* cell wall is mainly composed of mannosylated proteins, β -glucan, and chitin (Lesage *et al.*, 2006). These different components can be recognized by several receptors, mainly the mannose receptor (CD206) (Giaimis *et al.*, 1993), Dectin-1 (Brown and Gordon, 2001), and Toll-like receptors (especially TLR2/TLR6 and TLR4) (Uematsu and Akira 2008). These receptors have a differential expression on professional phagocytic cells.

Whole *S. cerevisiae* can activate human dendritic cells by increasing the expression of the surface markers CD80, CD83, and HLAII, and the secretion of the cytokines IL-12, TNF- α , IFN- γ , IL-8, IL-2, IL-13, IL-10 and IL-1 β (Remondo *et al.*, 2009)

The effect of some *S. cerevisiae*-derived components, such as β -glucan and zymosan on mouse macrophage polarization was recently described. While Liu *et al.* showed that β -glucan *via* its interaction with Dectin-1 induces an M1-like phenotype by down-regulating M2 markers, e.g. CD163 and IL-10, and up-regulating M1 markers, such as CD86, IL-12, and TNF- α (Liu *et al.*, 2016), Elcombe *et al.* reported that zymosan induces an M2b phenotype with a high expression of IL-10 and low levels of IL-12 (Elcombe *et al.*, 2013).

Introduction

1.4 Aim of this work

Macrophages are a heterogeneous and plastic cell population with two main phenotypes: pro-inflammatory classically activated macrophages (M1) and anti-inflammatory alternatively activated macrophages (M2). The macrophage phenotype can be both protective and pathogenic. Whereas M1-polarized macrophages are involved in host defense and have anti-tumor activity, M2 macrophages exhibit wound-healing properties, but also promote tumor growth. Re-educating macrophages from an M2 to an M1 phenotype is a promising approach for cancer therapy. Yeast (*Saccharomyces cerevisiae*) and silica nanoparticles represent interesting vehicles for numerous medical applications. Macrophages are the major cell population responsible for nanoparticle clearance and yeast phagocytosis *in vivo*. So far, studies on *S. cerevisiae* or silica nanoparticle interaction with macrophages did not consider the macrophage phenotype. The aim of the present study was to investigate the interaction between differently polarized macrophages and *S. cerevisiae* or silica nanoparticles, given their possible application to target and possibly re-educate macrophages from an M2 to an M1 phenotype.

I. *Saccharomyces cerevisiae* is a promising vehicle for the delivery of vaccines. It is well established that *S. cerevisiae* is taken up by professional phagocytic cells. However, the response of human macrophages to *S. cerevisiae* is ill-defined. Thus, the first chapter of this work focuses on characterizing the interaction between *S. cerevisiae* and M1- or M2-like macrophages.

II. Recent studies on novel vaccination strategies have shown that *S. cerevisiae* can deliver nucleic acids to phagocytic cells. Therefore, in the second part of the present study, we aimed to investigate the potential use of *S. cerevisiae* for nucleic acid delivery to human macrophages to re-educate M2 macrophages towards an M1 phenotype by yeast-based delivery of *MYD88* or *TNF* mRNA.

Introduction

III. Despite the increasing number of applications for silica nanoparticles, the influence of macrophage polarization on their uptake and thereby their clearance has not been characterized yet. In the third part of the present study, we aimed to examine the uptake potential of differentially polarized human macrophages for silica nanoparticles.

2 Chapter I

Saccharomyces cerevisiae polarizes both M-CSF and GM-CSF differentiated macrophages towards an M1-like phenotype

Chapter I

Chapter I

2.1 Introduction

Recently, the influence of *C. albicans* uptake on M1 and M2 macrophages has been studied. Reales-Calderón *et al.* reported that human macrophages differentiated *in vitro* by GM-CSF or M-CSF treatment respond differently to *C. albicans*. The exposure to *C. albicans* increased the production of IL-10 by M-CSF-differentiated macrophages but did not have any significant effect on the expression of IL-12, TNF- α , or IL-6. Interestingly, proteomic analysis suggests that interaction with *C. albicans* skews M1 macrophages towards an M2 macrophage phenotype (Reales-Calderón *et al.*, 2014).

Paracoccidioides brasiliensis represents another common pathogenic yeast strain that causes systemic mycosis in humans. In a recent study, the effect of *P. brasiliensis* infection on GM-CSF and M-CSF differentiated bone marrow-derived macrophages from the A/J and B10.A mouse strains were analyzed. Unlike M-CSF differentiated macrophages, GM-CSF-differentiated cells produced high levels of pro-inflammatory cytokines, i.e. IL-6 and TNF- α , as well as the anti-inflammatory cytokine IL-10 upon incubation with *P. brasiliensis*. These results suggest that M1-like macrophages, which are predominant in the B10.A, but not in the A/J strain, may contribute to an unbalanced early immune response against *P. brasiliensis* in B10.A mice (De Souza Silva *et al.*, 2015).

Despite a significant number of studies on yeast-macrophage interactions, little is known about the direct effect of *Saccharomyces cerevisiae* on macrophage polarization. In contrast to the yeast strains mentioned above, *S. cerevisiae* is non-pathogenic and is currently being tested as a vaccine vehicle.

In the present chapter, we characterized the influence of *S. cerevisiae* uptake on human macrophage polarization. We prepared M1- and M2-like macrophages by differentiating human peripheral blood monocytes using GM-CSF or M-CSF, respectively. Subsequently, we examined their uptake potential for fluorescently labeled *S. cerevisiae* and investigated the expression of M1 and M2 markers before and after yeast uptake.

2.2 Results

2.2.1 Human monocyte-derived macrophages

Human peripheral blood monocytes were differentiated into macrophages by GM-CSF- or M-CSF-treatment (GM-M Φ / M-M Φ) and the expression of 7 surface markers was analyzed by flow cytometry. As previously reported, GM-M Φ and M-M Φ shared similar expression level of HLA I (Rey-Giraud *et al.*, 2012) and CD80 (Figure 4). Notably, M-M Φ expressed higher levels of CD14, but a much lower amount of mannose receptors (CD206) than GM-M Φ (Rey-Giraud *et al.*, 2012; Xu *et al.*, 2006; Bender *et al.*, 2004). Moreover, GM-M Φ were characterized by elevated expression of the M1 markers CD86 and HLAII (Krausgruber *et al.*, 2011; Lawrence *et al.*, 2011; Sica *et al.*, 2012; Gordon *et al.*, 2005). In contrast, M-M Φ expressed higher levels of CD163, a known M2 marker (Biswas *et al.*, 2010; Krausgruber *et al.*, 2011; Heusinkveld *et al.*, 2011; Xu *et al.*, 2007). Taken together, the flow cytometric analysis confirmed that GM-M Φ display an M1-like phenotype, whereas M-M Φ resemble M2 macrophages.

Chapter I

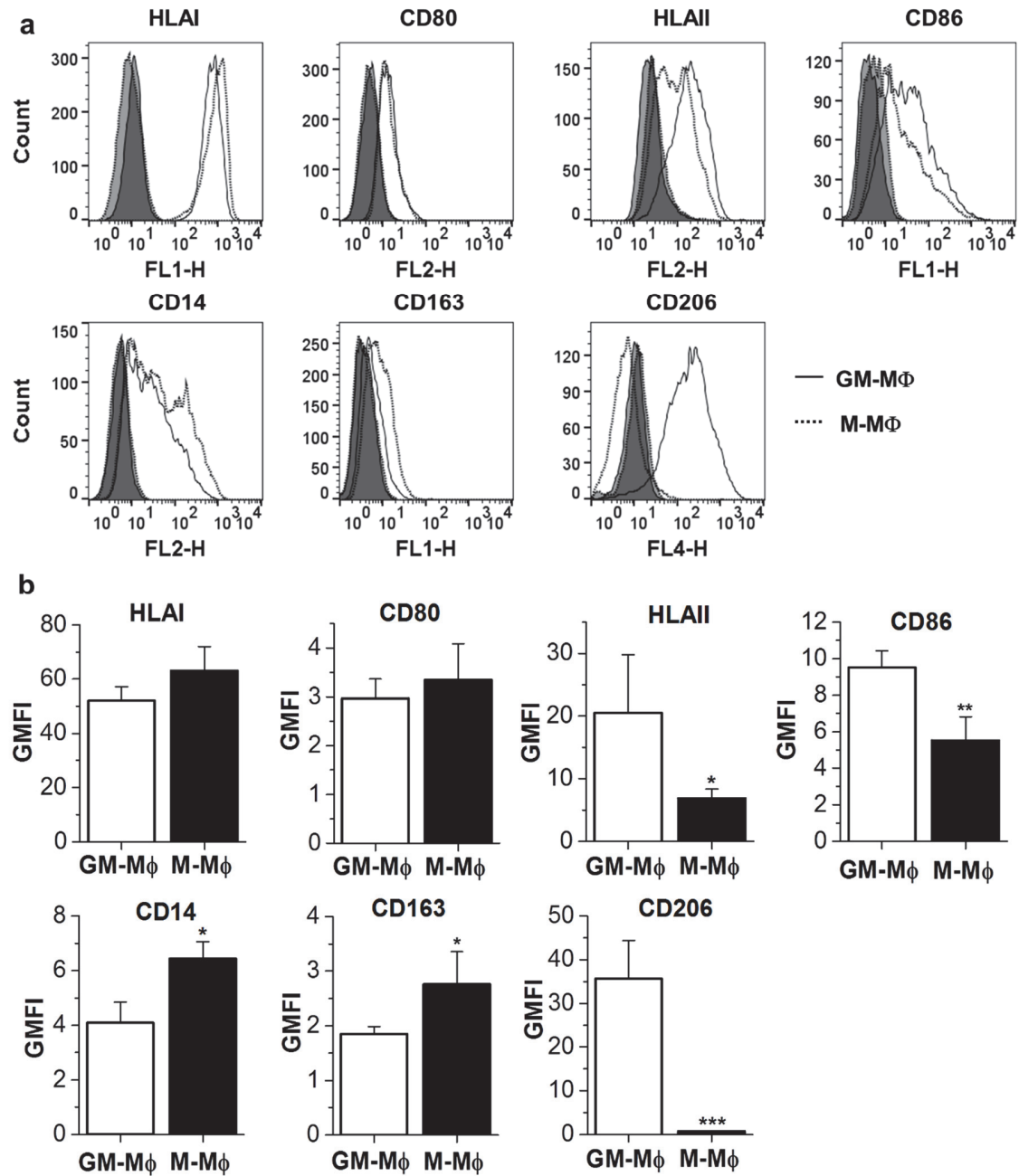


Figure 4: Characterization of monocyte-derived macrophages. Human peripheral blood monocytes were differentiated with either GM-CSF (GM-MΦ) or M-CSF (M-MΦ). Surface expression of HLA I, CD80, HLA II, CD86, CD14, CD163, and CD206 was analyzed by flow cytometry. (A) One representative histogram is shown. Dark gray: isotype control, white: specific staining. (B) GMFI values. Data represent GMFI means + SEM of obtained from 7 independent experiments with cells from different donors. p-values were generated by Mann-Whitney test except for CD14, where the two sample t-test was used. *p < 0.05, **p < 0.01, ***p < 0.001.

Chapter I

2.2.2 Uptake of yeast by monocytes derived macrophages

We then compared the ability of human GM-M Φ and M-M Φ to phagocytose *S. cerevisiae* S86c. Living yeast was stained with CFSE. Subsequently, yeast cells were left untreated or opsonized with human AB serum. As shown in Figure 5 A, both types of macrophages were able to take up untreated or opsonized *S. cerevisiae* at a multiplicity of infection (MOI) of 7 after co-incubation for 4 h. While 87% of GM-M Φ were CFSE positive reflecting a high yeast uptake efficiency, only 43.9% of M-M Φ were able to internalize untreated yeast within 4 h (Figure 5 B, C). Yeast opsonization with human serum did not affect yeast uptake by GM-M Φ but significantly increased yeast internalization by M-M Φ . When using opsonized yeast, no significant difference in yeast uptake was observed between GM-M Φ (85.6 ± 3.3) and M-M Φ (80.2 ± 0.8) (Figure 5 B, C). Since the experiments were conducted in serum free medium, opsonized yeast was used in the following experiments to ensure identical starting conditions that better match the *in vivo* situation.

To determine the optimal MOI for high uptake efficiency, macrophages were incubated for 4 h with opsonized yeast at various MOIs ranging from 1 to 11. The percentage of cells engulfing yeast was enhanced by increasing the MOI, reaching a plateau level at an MOI of 7 (Figure 6 A). Thus, we used MOI 7 in all further experiments.

Next, we determined the optimal incubation time for yeast exposure. Yeast cells were added at an MOI of 7, and macrophages were analyzed at different time points for CFSE positive cells by flow cytometry. The uptake efficiency was already high ($87.61 \pm 4.33\%$ for GM-M Φ and $82.6 \pm 1.75\%$ for M-M Φ) as early as 30 min after the co-incubation, reached a maximum at 2 h ($92.66 \pm 1.45\%$ for GM-M Φ and 83.5 ± 1.42 for M-M Φ) and a plateau phase afterward (Figure 6 B). Notably, yeast exposure did not show any toxic effect on macrophages at all MOIs tested (Figure 6 C).

Chapter I

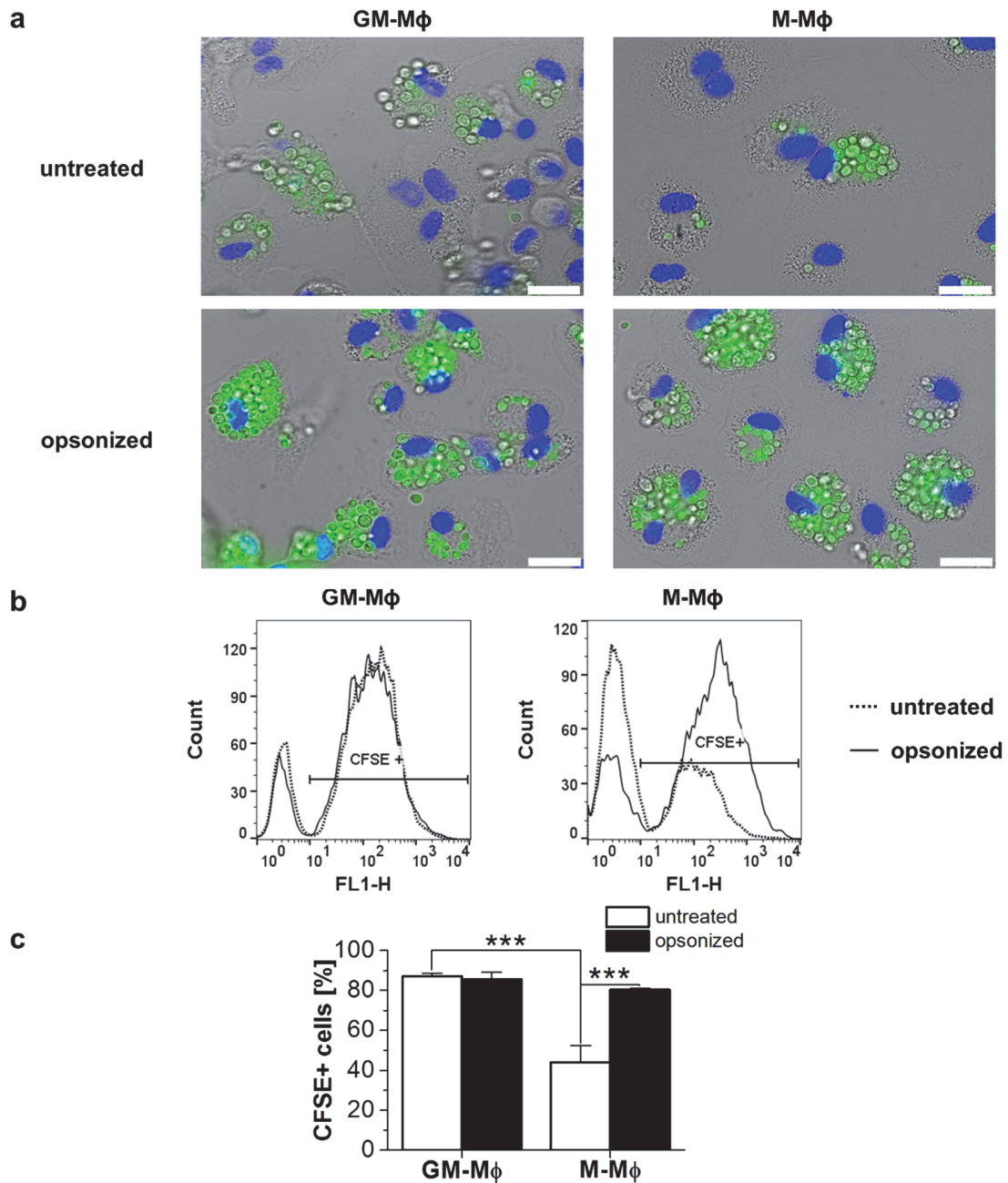


Figure 5: Uptake of *S. cerevisiae* by monocyte-derived macrophages. GM-M ϕ or M-M ϕ were incubated with untreated or opsonized *S. cerevisiae* at an MOI of 7 for 4 h. (A) Yeast uptake was verified by fluorescence microscopy. Green: *S. cerevisiae*, blue: nucleus, scale bar: 20 μ m. The percentage of CFSE+ macrophages was measured by flow cytometry. (B) One representative histogram is shown. (C) Percentage of CFSE+ macrophages. Data represent means + SEM from three independent experiments performed in duplicate. p -values were calculated by one-way ANOVA with Bonferroni's post hoc test. *** p < 0.001.

Chapter I

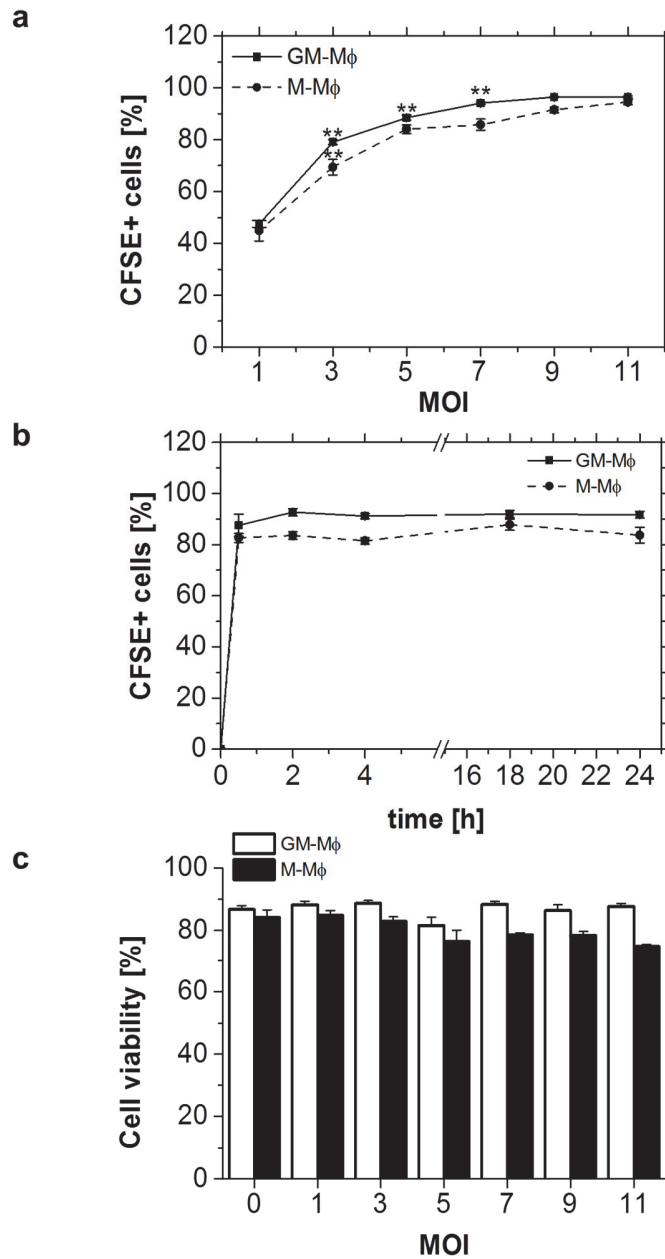


Figure 6: Characterization of *S. cerevisiae* uptake by GM-M Φ and M-M Φ . GM-M Φ or M-M Φ were incubated with opsonized *S. cerevisiae* (A) at varying MOIs for 4 h or (B) at an MOI of 7 for varying periods of time. Data are presented as the percentage of CFSE+ macrophages. (C) Cell viability was measured by PI staining. Data are presented as the percentage of living macrophages (PI negative). Data represent means + SEM of three independent experiments performed in duplicate. p-values were generated by Mann-Whitney test. **p < 0.01, ***p < 0.001. (*) MOI compared to the preceding MOI.

Chapter I

2.2.3 Effect of *S. cerevisiae* on M-CSF and GM-CSF-differentiated macrophages polarization

To study the effect of *S. cerevisiae* on macrophage polarization, GM-M Φ and M-M Φ were loaded with opsonized *S. cerevisiae* and the expression of M1 and M2 markers was analyzed.

The expression of surface markers on yeast-loaded macrophages was measured by flow cytometry and compared to unloaded cells (Figure 7 A). No changes were observed in HLA I and CD80 expression in yeast-loaded GM-M Φ (Figure 7 B). The M1 markers HLA II and CD86 were significantly upregulated after yeast uptake by GM-M Φ . In contrast, the M2 marker CD14 was downregulated. CD163 expression also tended to be decreased, although the effect was not statistically significant (Figure 7 B). The mannose receptor CD206 was also significantly downregulated (Figure 7 B).

Similarly, HLA II and CD86 were upregulated in M-M Φ after yeast uptake, whereas CD14 was significantly downregulated (Figure 8 B). Taken together, *S. cerevisiae* enhanced M1 surface marker expression in both GM-M Φ and M-M Φ while reducing M2 markers. Taking into consideration that the initial expression of these markers was higher in GM-M Φ , the M1 like-phenotype induced by yeast was more intense in GM-M Φ compared with M-M Φ .

Chapter I

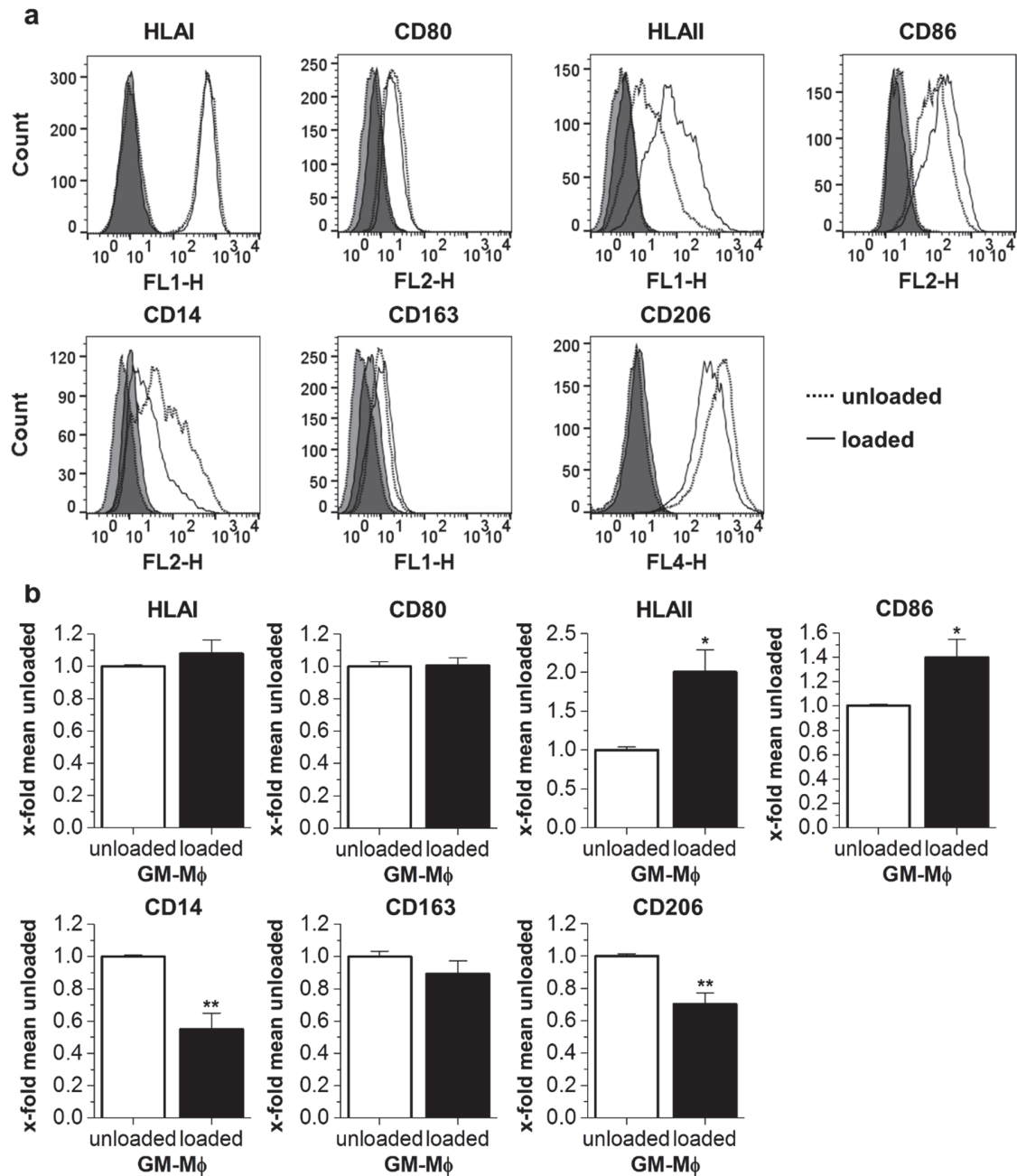


Figure 7: *S. cerevisiae* induces an M1 surface marker expression in GM-MΦ. GM-MΦ were incubated with opsonized *S. cerevisiae* at an MOI of 7 for 40 h. Surface expression of HLAI, CD80, HLAI, CD86, CD14, CD163 and CD206 was analyzed by flow cytometry. (A) One representative histogram is shown. Dark gray: isotype control, white: specific staining. (B) GMFI values. Data represent GMFI means + SEM of yeast-loaded cells normalized to the mean of GMFI values for unloaded cells. Data were obtained from 4 independent experiments performed in duplicate. p-values were generated by two sample t-test except for CD80 where Mann-Whitney was used. *p < 0.05, **p < 0.01.

Chapter I

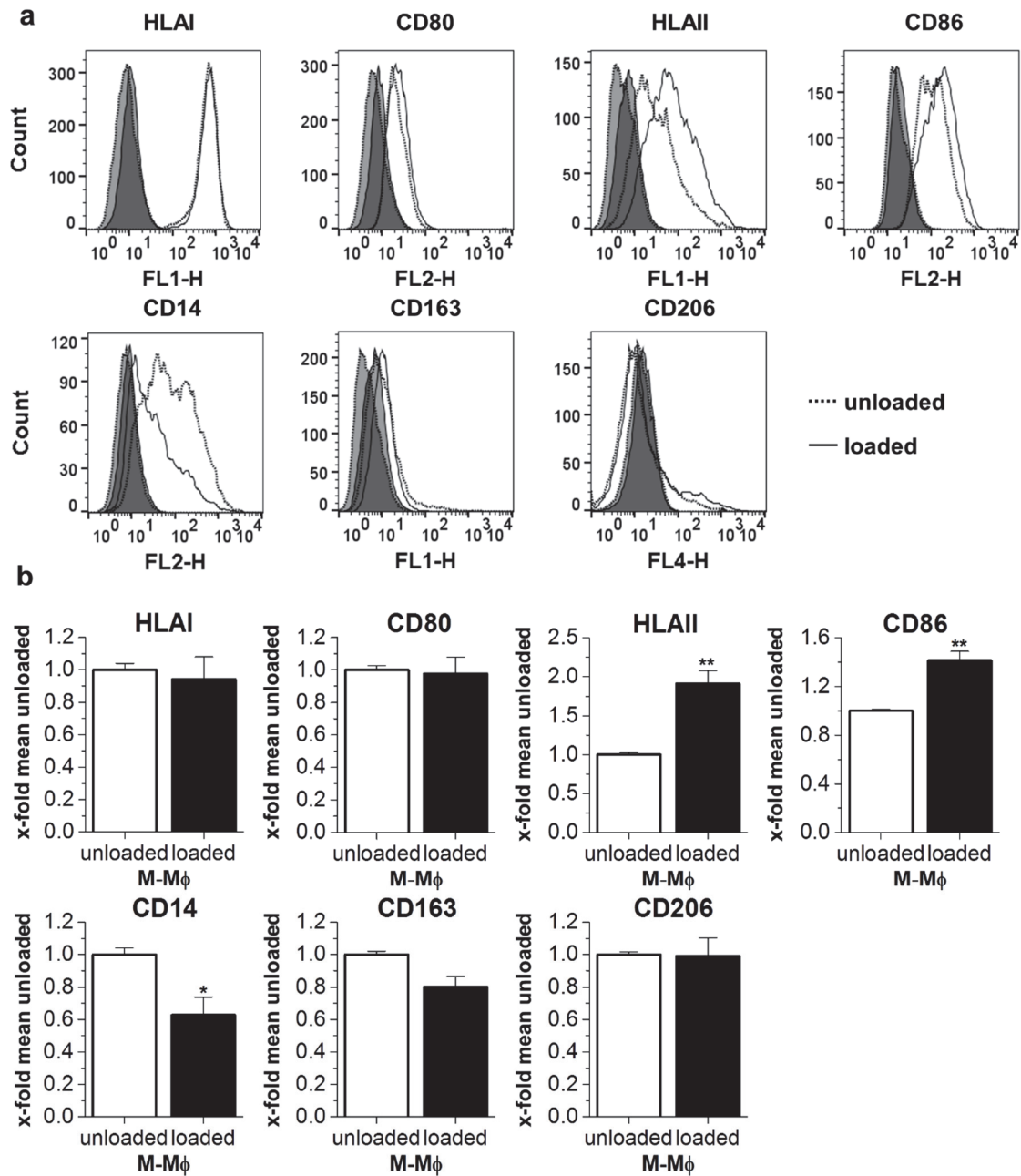


Figure 8: *S. cerevisiae* induces an M1 surface markers expression in M-M Φ . M-M Φ were incubated with opsonized *S. cerevisiae* at MOI 7 for 40 h. Surface expression of HLA I, CD80, HLA II, CD86, CD14, CD163 and CD206 was analyzed by flow cytometry. (A) One representative histogram is shown. Dark gray: isotype control, white: specific staining. (B) GMFI values. Data represent GMFI means + SEM of yeast-loaded cells normalized to the mean of GMFI of unloaded cells. Data were obtained from 4 independent experiments performed in duplicate. p-values were generated by two sample t-test except for CD86 where Mann-Whitney was used. *p < 0.05, **p < 0.01.

Chapter I

To further evaluate the yeast-facilitated induction of an M1-like phenotype suggested by surface marker expression, we determined cytokine mRNA levels by real-time RT-PCR. The pro-inflammatory cytokines TNF- α , IL-12p40 and IL-6 were used as M1 markers, whereas the anti-inflammatory cytokine IL-10 was used as an M2 marker (Biswas *et al.*, 2010; Krausgruber *et al.*, 2011; Verreck *et al.*, 2006; Hamilton *et al.*, 2014; Rey-Giraud *et al.*; 2012; Martinez *et al.*, 2006). The expression of the anti-inflammatory regulator GILZ (Glucocorticoid-Induced Leucine Zipper) was also studied since GILZ has been reported to be upregulated in human and murine M2-like macrophages (Hoppstädter and Kiemer, 2015; Berrebi *et al.*, 2003; Vago *et al.*, 2015; Hoppstädter *et al.*, 2015). *TNF* mRNA was significantly induced in both GM-M Φ and M-M Φ after 2 h of co-culture and decreased afterward (Figure 9 A). *IL12B* mRNA was also induced after 2 h, reaching a peak at 4 h in M-M Φ and still increasing after 16 h in GM-M Φ (Figure 9 B). In addition, *IL6* mRNA was upregulated with a maximum at 4 h of co-culture (Figure 9 C). On the other hand, no significant changes of *IL10* or *GILZ* mRNA were observed (Figure 9 D, E). Taken together, our data suggest that yeast can induce M1 cytokine expression in GM-M Φ and M-M Φ . Incubation with non-opsonized yeast also resulted in cytokine mRNA upregulation, although to a lesser extent (Figure 10), suggesting that Fc-receptor engagement contributes to the overall effect.

Chapter I

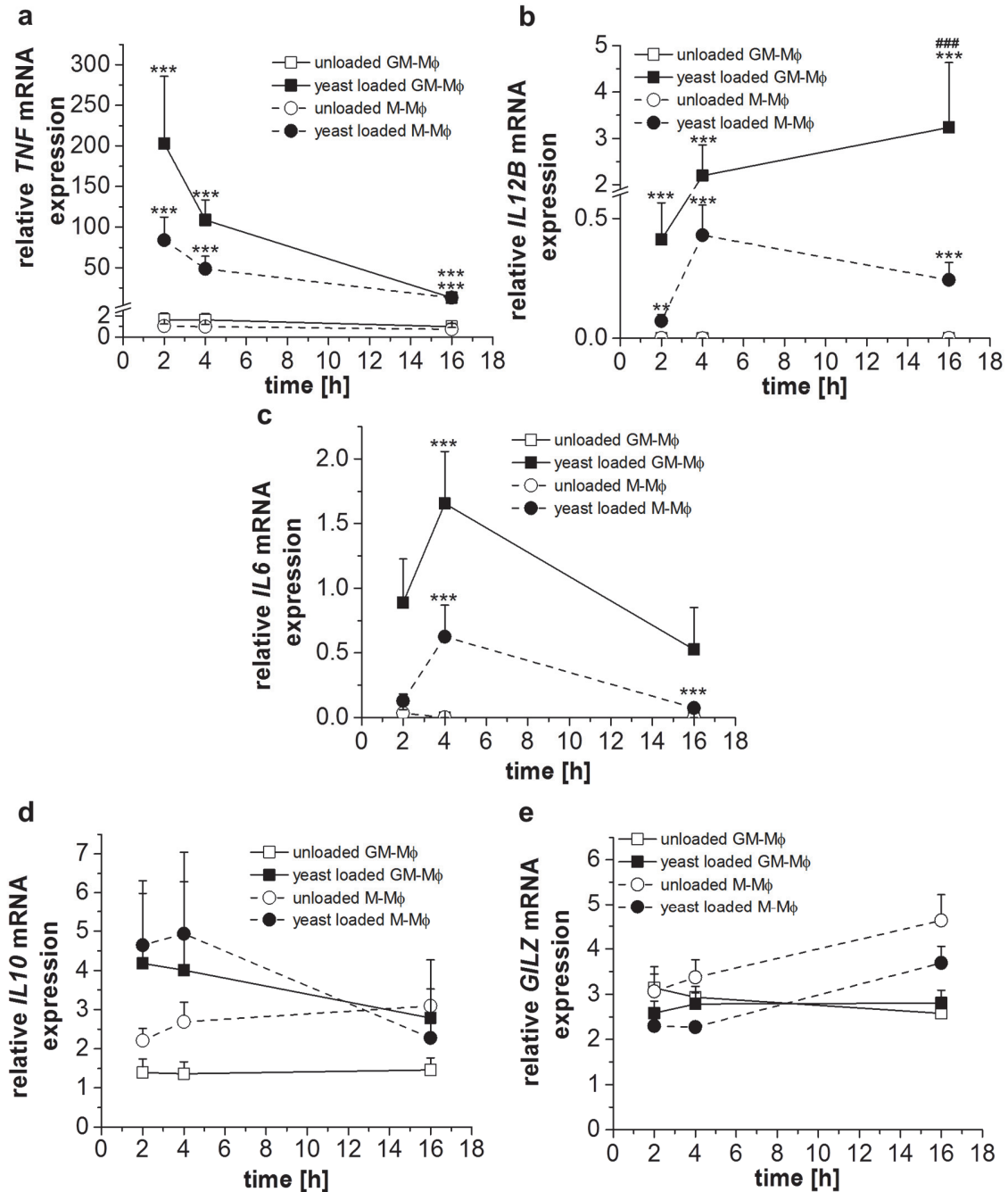


Figure 9: *S. cerevisiae* induces cytokine expression in GM-Mφ and M-Mφ. GM-Mφ and M-Mφ were left unloaded or loaded with opsonized *S. cerevisiae* at an MOI of 7 for the indicated periods of time. mRNA expression levels of *TNFα*, *IL6*, *IL12B*, *IL10*, and *GILZ*, were quantified by real-time RT-PCR, normalized to *ACTB* and multiplied by 104. Data show means + SEM of 4 independent experiments performed in duplicate. p-values were generated by Mann-Whitney test. **p < 0.01, ***p < 0.001. (*) Yeast-loaded cells compared to unloaded cells at the same time point. (#) yeast-loaded GM-Mφ compared to yeast-loaded M-Mφ.

Chapter I

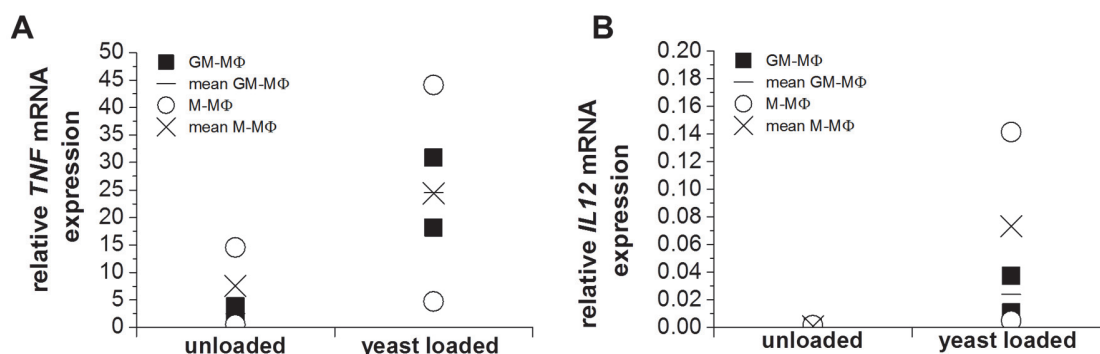


Figure 10: *S. cerevisiae* induces cytokine expression in GM-MΦ and M-MΦ. GM-MΦ and M-MΦ were left unloaded or loaded with unopsonized *S. cerevisiae* at an MOI of 7 for 4 h. mRNA expression levels of *TNF α* and *IL12B* were quantified by real-time RT-PCR, normalized to ACTB and multiplied by 10^4 . Data show 2 independent experiments with cells from different donors.

2.3 Discussion

The nonpathogenic yeast *S. cerevisiae* has been proposed as a promising candidate for biomedical applications, such as delivery of peptides and nucleic acids for vaccination (Ardiani *et al.*, 2010; Walch *et al.*, 2012; Kenngott *et al.*, 2016). *S. cerevisiae* can be specifically recognized by several receptors, mainly Toll-like receptors, mannose receptor, and dectin-1. After their recognition, yeast cells are engulfed by professional phagocytic cells, e.g. dendritic cells, neutrophils, and macrophages (Keppler-Ross *et al.*, 2010). Most *in vitro* studies focused on the interaction of *S. cerevisiae* with dendritic cells or the influence of *S. cerevisiae*-derived compounds on mouse macrophages (Liu *et al.*, 2016; Elcombe *et al.*, 2013). Therefore, information on the interaction of the whole *S. cerevisiae* with differently polarized human macrophages is still lacking.

2.3.1 Characterization of GM-MΦ and M-MΦ

It is well established that macrophages can adopt different phenotypes depending on the surrounding signals, with the pro-inflammatory phenotype (M1) and anti-inflammatory phenotype (M2) representing two extremes of a broad phenotypic spectrum. *In vitro* M1- and M2- like macrophages can be generated by differentiating peripheral blood monocytes using GM-CSF and M-CSF,

Chapter I

respectively. While GM-CSF induces the expression of M1 markers like HLAII and CD86, M-CSF induces the expression of M2 markers such as CD163 and CD14. Although the mannose receptor CD206 is widely used as an M2 surface marker, we and others (Rey-Giraud *et al.*, 2012; Xu *et al.*, 2006; Bender *et al.*, 2004; Kittan *et al.*, 2013) observed that it is highly expressed on GM-CSF derived M1 like-macrophages. In fact, CD206 expression was reported to be induced by GM-CSF in early studies on macrophage phenotypes (Chroneos *et al.*, 1995). The usage of CD206 as an M2 marker is actually being reconsidered lately, as at least 3 newer studies (Kittan *et al.*, 2013; Jaguin *et al.*, 2013; Ambarus *et al.*, 2012) suggested that this marker used for mouse macrophages could not be used to discriminate between human M1 and M2 macrophages.

The assumption that GM-CSF and M-CSF-derived macrophage populations can be considered as M1-like and M2-like, respectively, is supported by the observation that both cell types exhibit distinct reactions upon stimulation. After LPS treatment, GM-M Φ secrete high amounts of pro-inflammatory cytokines, whereas M-M Φ increase IL-10 expression (Verreck *et al.*, 2006; Reales-Calderon *et al.*, 2014; Bender *et al.*, 2004; Martinez *et al.*, 2006). Furthermore, exposure to the same material can result in distinct uptake patterns depending on the macrophage phenotype. For example, M-M Φ are more potent regarding the uptake of apoptotic cells when compared with GM-M Φ (Xu *et al.*, 2006).

2.3.2 *S. cerevisiae* uptake by *in vitro* polarized macrophages

To comparatively evaluate the initial interaction between human GM-M Φ or M-M Φ and *S. cerevisiae*, we first determined the percentage of macrophages that internalized yeast. While De Souza Silva *et al.* showed that *P. brasiliensis* was internalized more efficiently by murine M-M Φ than GM-M Φ (De souza Silva *et al.*, 2015). Our data indicate that human GM-M Φ have a higher uptake potential for *S. cerevisiae* than M-M Φ . This difference in yeast uptake between GM-M Φ and M-M Φ might be explained by the high expression of the mannose receptor on GM-M Φ since this receptor is critically involved in yeast recognition (Giaimis *et*

Chapter I

al., 1993; Porcaro *et al.*, 2003). The yeast uptake capacity by GM-M Φ was similar to human dendritic cells when compared with previous reports on yeast internalization in this cell type. In fact, under similar experimental conditions Boschi Bazan *et al.* have shown that 92% of human dendritic cells internalized at least one yeast cell (Boschi *et al.*, 2011). However, opsonized yeast cells were engulfed to a similar extent by both GM-M Φ and M-M Φ . In both types of macrophages, yeast uptake was enhanced by opsonizing the yeast cells in human serum before performing the macrophage/yeast co-culture. Human serum contains opsonins, such as complement-derived proteins and immunoglobulins. Coating of yeast cells with opsonins allows their recognition and subsequent ingestion by complement receptors and Fc receptors (Underhill *et al.*, 2012).

2.3.3 *S. cerevisiae* polarizes both M-CSF and GM-CSF-differentiated macrophages towards an M1-like phenotype

Two recent studies have focused on the response of GM-M Φ and M-M Φ to different pathogenic yeast strains, such as *C. albicans* (Reales-Calderón *et al.*, 2014) and *P. brasiliensis* (De Souza Silva *et al.*, 2015). *C. albicans* induced an M2 proteomic profile in both GM-M Φ and M-M Φ , indicating that the interaction with *C. albicans* promotes a switch towards an anti-inflammatory phenotype. In line with these findings, *C. albicans* exposure did not result in the induction of pro-inflammatory cytokines, such as IL-12, TNF- α , and IL-6 (Jouault *et al.*, 2006). In contrast to these observations, we showed that *S. cerevisiae* promotes an M1-like macrophage phenotype. Both GM-M Φ and M-M Φ upregulated the M1-associated surface markers HLAII and CD86, whereas M2 markers were downregulated. Furthermore, *S. cerevisiae* induced an upregulation of pro-inflammatory cytokines, suggesting that *S. cerevisiae* skews macrophages toward an M1 phenotype. These results are in line with the observation for mouse macrophage cell lines and human dendritic cells. In particular, *S. cerevisiae* exposure leads to TNF- α secretion by mouse macrophages (Jouault *et al.*, 2006) and can induce human dendritic cell activation and maturation as evidenced by upregulation of CD80, CD83, and HLAII (Remondo *et al.*, 2009).

Chapter I

The influence of *S. cerevisiae* uptake on the macrophage phenotype is of particular interest, as *S. cerevisiae* might be used as a vehicle to deliver peptides and nucleic acids *in vivo*. In veterinary medicine, *S. cerevisiae* expressing antigens on its surface is being investigated as a promising vaccine for oral administration. Several antigens for immunization against hepatitis B virus, porcine epidemic diarrhea virus, and *Actinobacillus pleuropneumoniae* are currently being tested (Shin *et al.*, 2013). Furthermore, yeast expressing tumor-associated antigens are presently evaluated in clinical trials as therapeutic anti-cancer vaccines. The application of two genetically modified *S. cerevisiae* strains, yeast-ras, and yeast-CEA expressing a mutant of ras pro-oncogene and carcinoembryonic antigen, respectively, has led to promising results. In phase I clinical trials, yeast-ras, and yeast-CEA had minimal toxicity and induced antigen-specific T-cell responses (Ardiani *et al.*, 2010; Bilusic *et al.*, 2015). *S. cerevisiae* may also be a suitable vaccine carrier against fungal diseases since *S. cerevisiae* expressing gp43 was able to immunize mice against paracoccidioidomycosis (Assis-Marques *et al.*, 2015). Moreover, vaccination with yeast-HCV led to the induction of HCV-specific T-cell responses in HCV-infected patients and reduction in the viral load (Ardiani *et al.*, 2010). Besides these peptide antigens, yeast cells can deliver antigen-encoding DNA and mRNA to phagocytic cells, which was previously described *in vitro* and *in vivo* (Walch *et al.*, 2012; Walch-Rückheim *et al.*, 2015; Kiflmariam *et al.*, 2013) Furthermore, *S. cerevisiae* could also deliver shRNA *in vivo* after yeast oral administration (Zhang *et al.*, 2014).

2.4 Conclusion

In conclusion, our study suggests that opsonized *S. cerevisiae* can induce an M1-like phenotype in macrophages. This inflammatory response was stronger in GM-M Φ than in M-M Φ . Moreover, opsonized *S. cerevisiae* might be used as a delivery system for therapeutic agents targeting macrophages. These findings

Chapter I

may be of particular interest for the treatment of pathologic conditions that would benefit from reprogramming M2 towards M1 macrophages, such as solid tumors.

Parts of the results presented in this chapter have been published in:

Yeast (*Saccharomyces cerevisiae*) polarizes both M-CSF and GM-CSF differentiated macrophages towards an M1-like phenotype.

Seif M, Philippi A, Breinig F, Kiemer AK, Hoppstädter J. *Inflammation* 2016

Reprinted with permission of Springer.

3 Chapter II

Yeast-mediated *MYD88* or *TNF* mRNA delivery
re-educates M2 macrophages towards an
M1-like phenotype

Chapter II

Chapter II

3.1 Introduction

Cell-specific gene delivery represents a promising therapeutic approach, but limited bioavailability is still a major obstacle. Macrophages as critical players in inflammatory diseases have gained increasing attention as potential targets for gene delivery strategies. Still, therapeutic approaches mostly aim to target the inflammatory macrophage phenotype (Singh *et al.*, 2014). Adenoviral vectors delivering cytokine DNA (such as IL-12 or IFN- γ) were able to induce an M1 phenotype in macrophages. Adoptive transfer of these genetically modified macrophages into tumor-bearing mice showed promising results (Satoh *et al.*, 2003; Tabata *et al.*, 2011; Hagemann *et al.*, 2008). Due to the lack of specificity and potential toxicity of these viral vectors, several non-viral gene delivery approaches (e.g. polymers, liposomes) are currently being tested (Singh *et al.*, 2014; Nayerossadat *et al.*, 2012). Specificity, stability, and clearance are major challenges in designing a novel gene delivery system (Singh *et al.*, 2014)

Recent studies have shown that *S. cerevisiae* can be used as vehicle for DNA/RNA vaccination (Walch *et al.*, 2012; Walch-Rückheim *et al.*, 2016). We hypothesized that yeast might also be used as a gene delivery vehicle targeting phagocytic cells.

In this chapter, we analyzed the potency of *S. cerevisiae* to deliver nucleic acids to primary human macrophages and determined whether this approach might be used to re-educate M2 macrophages towards an M1 phenotype.

Chapter II

3.2 Results

3.2.1 Polarization of human monocyte-derived macrophages

To establish an *in vitro* model for pro- and anti-inflammatory macrophages, peripheral blood monocytes were isolated from buffy coats and differentiated into macrophages using GM-CSF (GM-M Φ) or M-CSF (M-M Φ). The pro-inflammatory macrophage phenotype (M1) was induced by stimulation of GM-M Φ with LPS/IFN- γ . To generate anti-inflammatory M2a and M2c macrophages, M-M Φ were exposed to IL-4 or IL-10, respectively. The expression of surface markers was analyzed by flow cytometry. No significant difference was observed in CD80 expression between the three macrophages populations (Figure 11). As reported previously (Rey-Giraud *et al.*, 2012), M1 cells displayed an increased surface expression of CD86, HLA I, and HLA II, especially when compared with M2c (Figure 11). We also observed an increased expression of the mannose receptor CD206 as well as CD86 on M2a cells. M2c macrophages showed the highest expression of CD14 and the scavenger receptor CD163, which was paralleled by low CD206, HLA II and CD86 expression (Figure 11).

To further characterize the macrophage phenotype, we measured the mRNA expression of pro- and anti-inflammatory mediators. Consistent with their pro-inflammatory phenotype, M1 cells expressed *TNF*, *IL6*, and *IL12B* (Figure 12 A-C). M2a macrophages expressed higher amounts of *IL10* when compared with M1 cells. M2c cells expressed the highest amount of the anti-inflammatory mediators *IL10* and *GILZ* (Figure 12 D, E).

Taken together, both surface marker and cytokine expression confirmed the pro-inflammatory phenotype of *in vitro* generated M1 and the anti-inflammatory phenotype of M2a and M2c cells. The anti-inflammatory phenotype was more pronounced in M2c cells when compared with M2a macrophages.

Chapter II

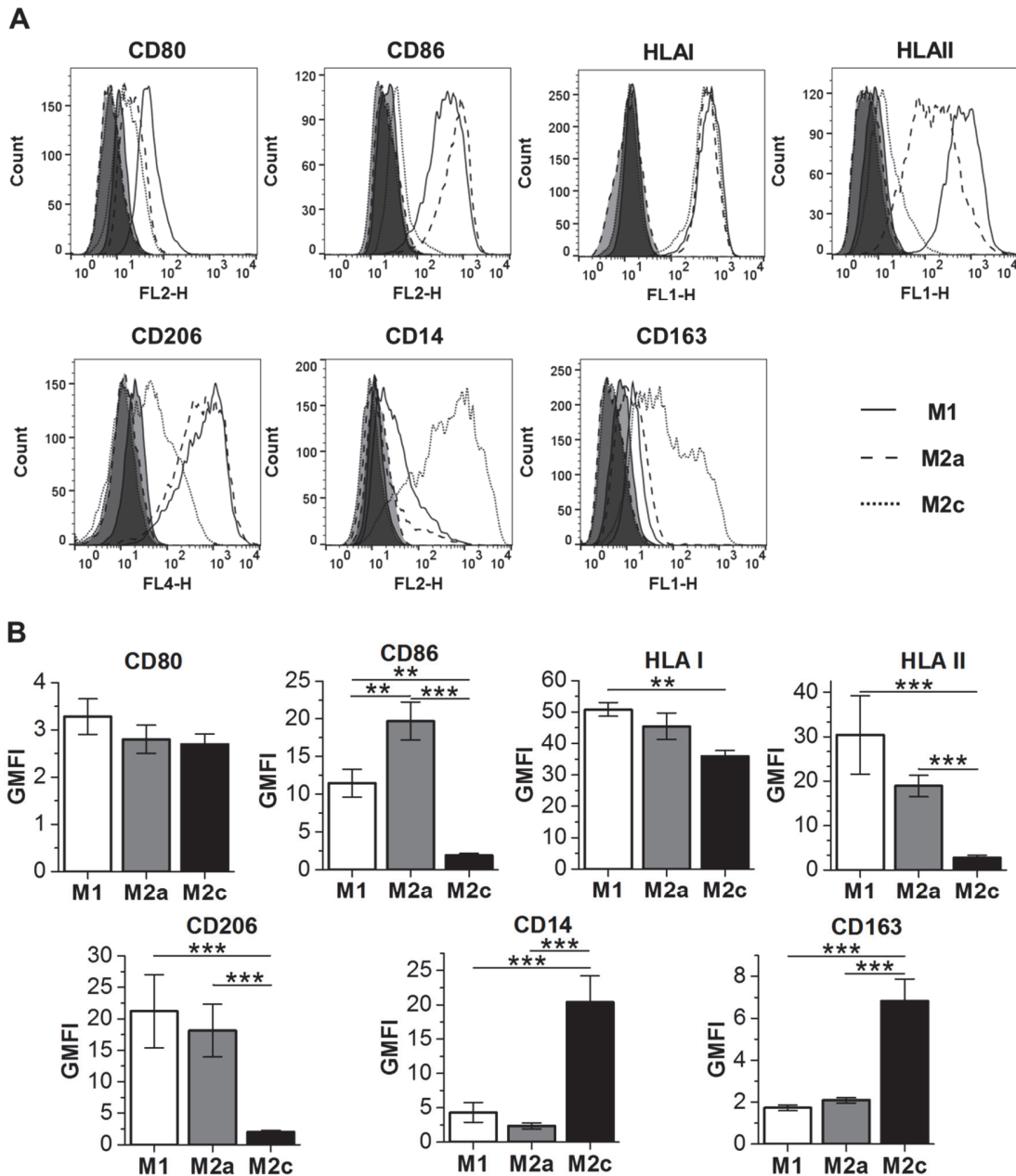


Figure 11: Surface markers expression on *in vitro* polarized macrophages. Human peripheral blood monocytes were differentiated into macrophages with either GM-CSF (GM-M Φ) or M-CSF (M-M Φ). GM-M Φ were polarized to M1 by stimulation with LPS/IFN- γ . M-M Φ were polarized towards M2a or M2c by the addition of IL-4 or IL-10, respectively. Surface expression of CD80, CD86, HLA I, HLA II, CD206, CD14 and CD163 was analyzed by flow cytometry. (A) Representative histograms are shown. Dark grey: isotype control, white: specific staining. (B) Relative GMFI values. Data represent relative GMFI values \pm SEM obtained from 7 independent experiments with cells from different donors. p-values were generated by Mann-Whitney test except for CD80 and HLA I where one way ANOVA with Bonferroni's post hoc test was used. **p < 0.01, ***p < 0.001.

Chapter II

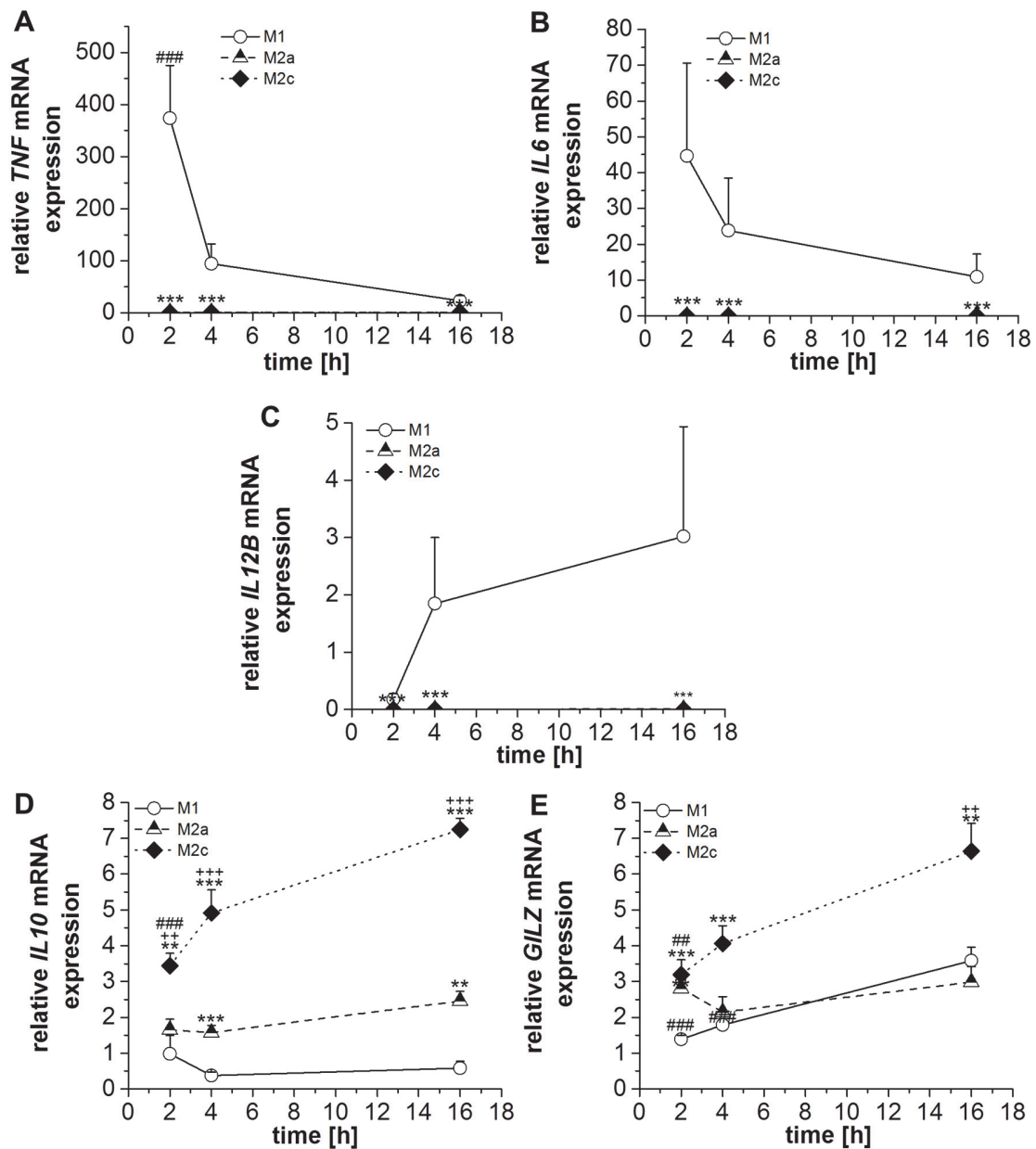


Figure 12: Cytokine mRNA levels in *in vitro* polarized macrophages. GM-M Φ were polarized into M1 cells by stimulation with LPS/IFN- γ . M-M Φ were polarized towards M2a or M2c by the addition of IL-4 or IL-10, respectively, for the indicated periods. mRNA expression levels of *TNF*, *IL12B*, *IL6*, *IL10*, and *GILZ* were quantified by real-time RT-PCR, normalized to ACTB and multiplied by 10^4 . Data show means \pm SEM of 4 independent experiments performed in duplicate. p-values were generated by Mann Whitney test. **p < 0.01, ***p < 0.001. (*) M2a or M2c compared to M1 at the same time point. (+) M2c compared with M2a. (#) 2 h or 4 h compared with 16 h.

Chapter II

3.2.2 Uptake of yeast by differently polarized macrophages

To be able to compare the yeast-based nucleic acid delivery to pro- and anti-inflammatory macrophages, we had to make sure that *S. cerevisiae* was internalized to a similar extent by all cell types. Thus, we compared the ability of human *in vitro* generated M1, M2a, and M2c macrophages to phagocytose *S. cerevisiae* S86c. Living *S. cerevisiae* S86c was stained with CFSE, and then left untreated or opsonized with human AB serum. Macrophages were co-cultured with yeast at an MOI of 7 for 4 h. All types of macrophages internalized untreated *S. cerevisiae* (Figure 13 A). M1 macrophages had the highest yeast uptake efficiency with 82% CFSE positive cells, followed by M2a (56% CFSE+ cells). M2c had the lowest uptake efficiency with only 31% CFSE positive cells (Figure 13 B). Yeast opsonization with human serum increased the percentage of cells internalizing yeast, especially in M2c cells (Figure 13 B). No significant difference in opsonized yeast uptake was observed between the differently polarized cells (Figure 13 B). M2a tended to have lower uptake efficiency than M1 and M2c macrophages. Since M2c macrophages represent the main macrophage population at tumor sites (Sica *et al.*, 2006) and show a more pronounced anti-inflammatory phenotype (Figure 11 and 12), we decided to focus on this cell type rather than M2a cells. Thus, M1 and M2c macrophages were loaded with opsonized yeast in the following experiments.

Chapter II

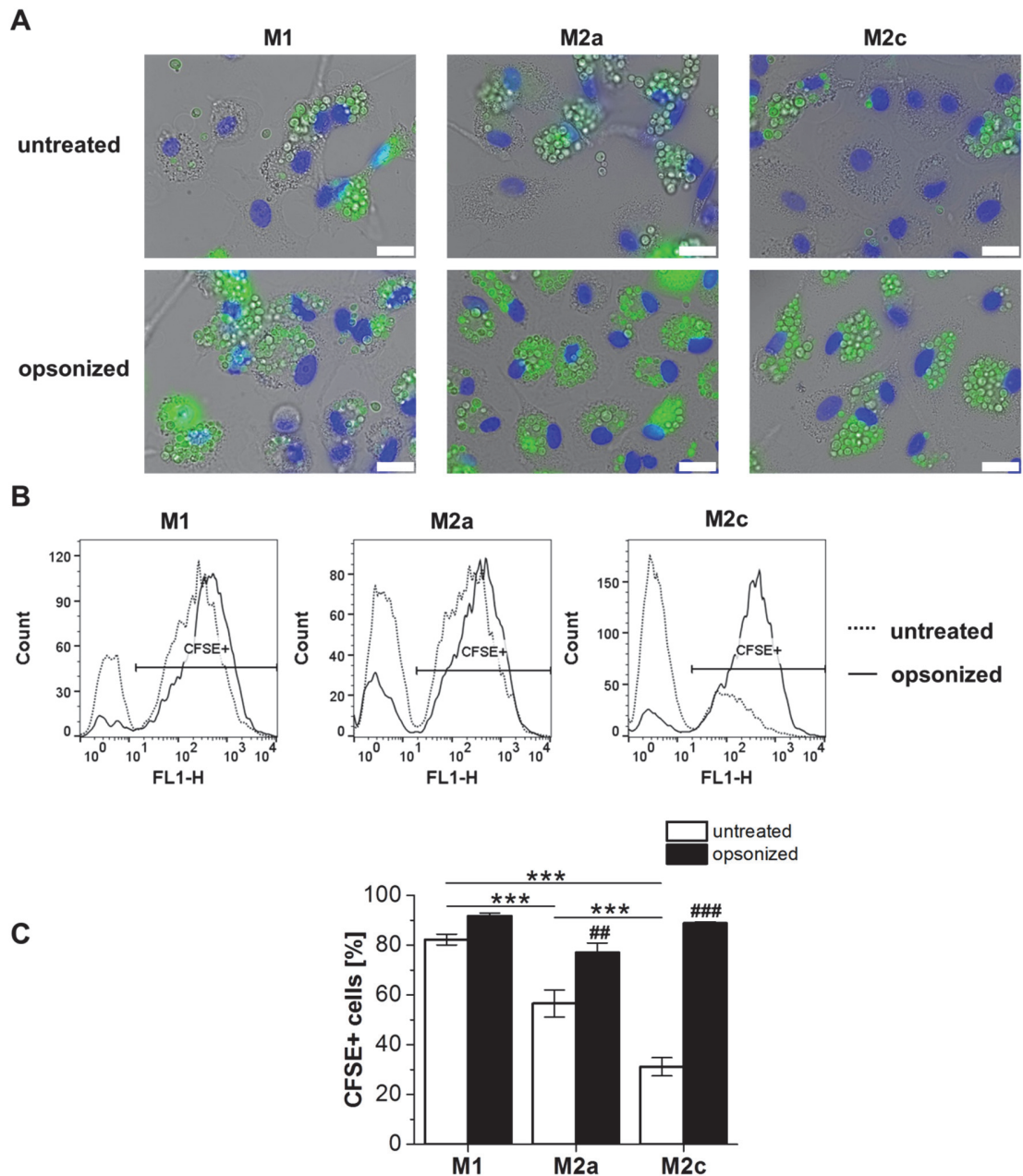


Figure 13: *S. cerevisiae* uptake by M1, M2a, and M2c. M1, M2a or M2c were incubated with untreated or opsonized *S. cerevisiae* at an MOI of 7 for 4 h. (A) Yeast uptake was verified by fluorescence microscopy. Green: *S. cerevisiae*, blue: nuclei, scale bar: 20 μ m. The percentage of CFSE+ macrophages was measured by flow cytometry. (B) One representative histogram is shown. (C) Percentage of CFSE+ macrophages. Data represent means \pm SEM from three independent experiments with cells from different donors performed in duplicate. p-values were calculated by one-way ANOVA with Bonferroni's post hoc test. ***p < 0.001. (#) cells loaded with opsonized yeast compared to cells loaded with untreated yeast.

Chapter II

3.2.3 *S. cerevisiae* uptake induces pro-inflammatory cytokine mRNA expression in M1 and M2c macrophages

Prior to gene delivery experiments, we assessed the effect of yeast uptake itself on the macrophage phenotype by comparing the expression of cytokine mRNA in yeast-loaded macrophages with unloaded cells (Figure 14). Yeast uptake induced a significant upregulation of *TNF* and *IL6* mRNA in M1 macrophages after 6 h, whereas no change in *IL12B* expression was observed (Figure 14 A-C). Yeast uptake also induced pro-inflammatory cytokine expression in M2c macrophages, with maximal expression values detected as early as 4 h for *TNF* (Figure 14 D) and *IL6* (Figure 14 E) and after 6 h for *IL12B* (Figure 14 F). No significant change was observed for anti-inflammatory mediators (Figure 15 B-D), except for *IL10* mRNA, which was induced in M1 macrophages 4 h after yeast uptake (Figure 15 A).

Chapter II

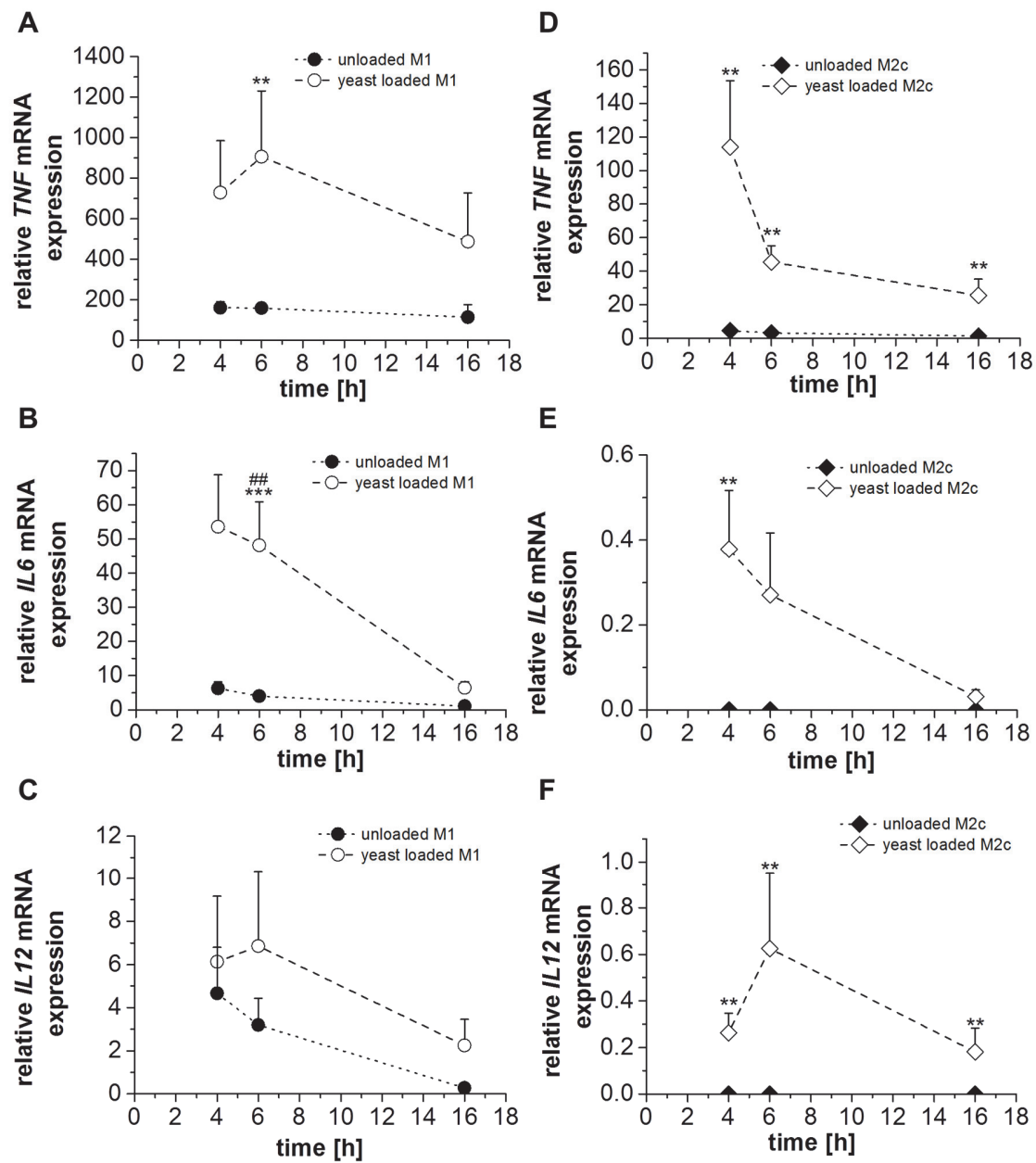


Figure 14: *S. cerevisiae* uptake induces pro-inflammatory cytokine mRNA expression in M1 and M2c macrophages. M1 (A, B,C) or M2c cells (D, E,F) were incubated with opsonized *S. cerevisiae* carrying the empty vector (YEp352) at an MOI of 7 for the indicated periods of time. mRNA expression levels of *TNF*, *IL12B*, and *IL6* were quantified by real-time RT-PCR, normalized to *ACTB*, and multiplied by 10^4 . Data show means + SEM of 3 independent experiments performed in duplicate. p-values were generated by Mann Whitney test. **p < 0.01, ***p < 0.001. (*) yeast-loaded cells compared to unloaded cells at the same time point. (#) yeast-loaded cells compared to yeast-loaded cells at 16 h.

Chapter II

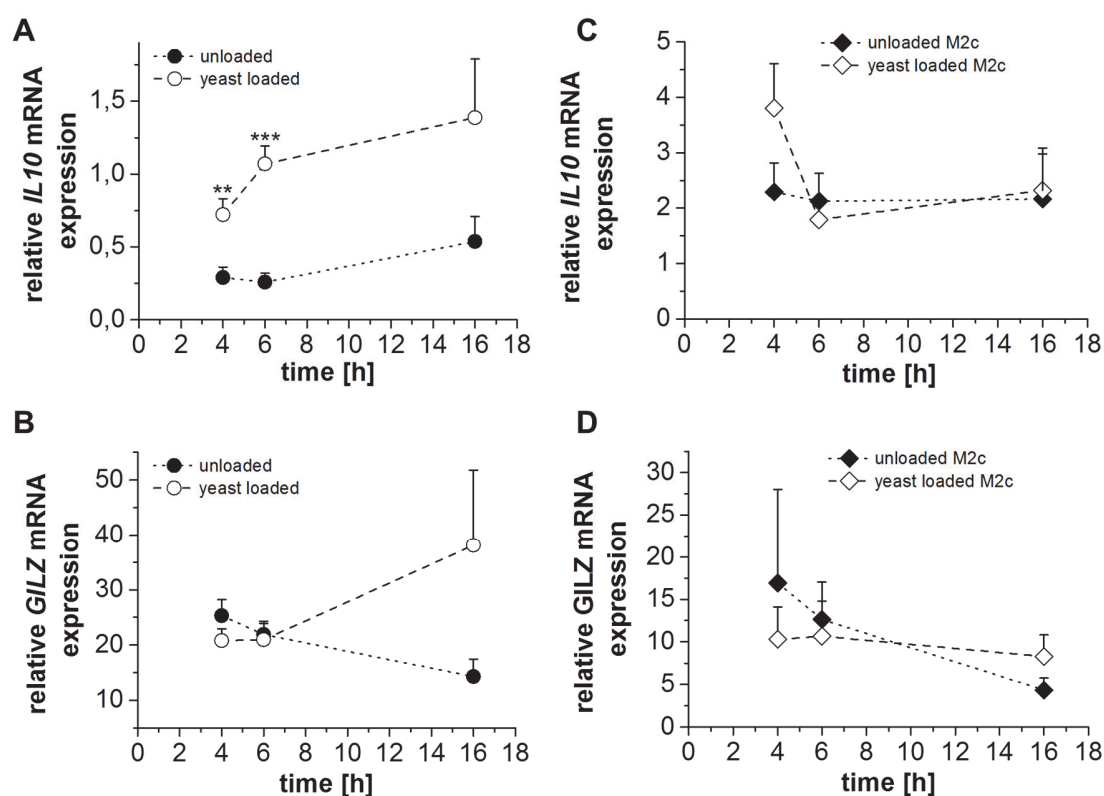


Figure 15: *S. cerevisiae* uptake induces *IL10* mRNA in M1 macrophages. M1 (A, B) or M2c cells (C, D) were incubated with opsonized *S. cerevisiae* carrying the empty vector (YEp352) at an MOI of 7 for the indicated periods of time. mRNA expression levels of *IL10* and *GILZ* were quantified by real-time RT-PCR and normalized to *ACTB* and multiplied by 10^4 . Data show means + SEM of 3 independent experiments performed in duplicate. p-values were generated by Mann Whitney test. **p < 0.01, ***p < 0.001. (*) yeast-loaded cells compared to unloaded cells at the same time point. (#) yeast-loaded cells compared with yeast-loaded cells at 16 h.

3.2.4 *S. cerevisiae* delivers functional DNA and mRNA to human M1 and M2c macrophages

To compare the ability of recombinant yeast to deliver either DNA or mRNA to human M1 and M2c macrophages, we used yeast strains carrying an eGFP gene (Walch *et al.*, 2012). All vectors contained an internal ribosomal entry site (IRES) of the encephalomyocarditis virus upstream of the eGFP encoding sequence. This approach prevents translation in yeast while enhancing it in macrophages (Walch *et al.*, 2012; Evstafieva *et al.*, 1993). For DNA delivery, a vector containing the mammalian CMV promoter was used. This made sure that transcription was facilitated by macrophages. For mRNA delivery, several yeast promoters were tested. The yeast phosphoglycerate kinase promoter (PGK) induces constitutive eGFP mRNA expression in yeast. For inducible mRNA

Chapter II

expression after yeast uptake by macrophages, the promoters of the yeast malate synthase (MLS1) and isocitrate lyase (ICL1) were used (Walch *et al.*, 2012). Both promoters are derived from genes involved in the yeast glyoxylate cycle, a metabolic pathway which permits the use of two-carbon compounds as carbon sources in absence of complex carbon sources such as glucose. The yeast glyoxylate cycle was shown to be induced in yeast isolated from macrophage phagolysosomes, most probably because the phagolysosome is poor in complex carbon compounds (Lorenz *et al.*, 2001; Lorenz *et al.*, 2004).

M1 or M2c macrophages were co-cultured for 16 h with yeast carrying the eGFP vectors. eGFP expression was observed in both M1 and M2c macrophages under all conditions tested (Figure 16). Comparison of transfection efficiencies revealed that both DNA and mRNA delivery were more efficient in M2c than in M1 cells. DNA delivery was less effective than mRNA delivery (Figure 16). The highest transfection efficiency was obtained with the constitutive PGK promoter, yielding $7.7 \pm 0.6\%$ transfected M1 and $22.7 \pm 2.5\%$ M2c cells (Figure 16). Thus, constitutive expression of mRNA in yeast was the most efficient method to deliver nucleic acids to human macrophages. This approach was used for all subsequent experiments.

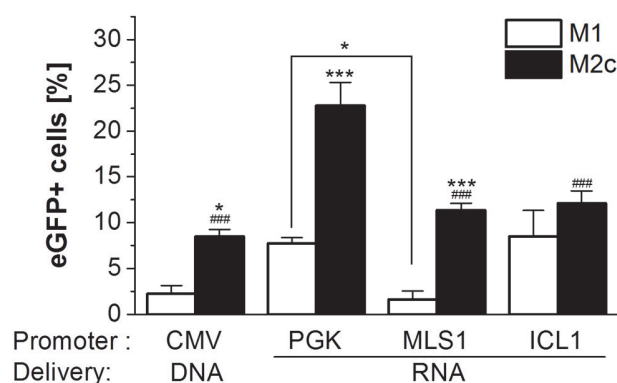


Figure 16: *S. cerevisiae* delivers functional DNA and mRNA to human M1 and M2c macrophages. M1 or M2c macrophages were incubated with opsonized *S. cerevisiae* carrying the indicated vector at an MOI of 7 for 16 h. The percentage of eGFP+ macrophages was measured by flow cytometry. (*) M2c compared to M1, (#) M2c compared to M2c loaded with yeast carrying the pPGK-IRES-eGFP vector. p-values were calculated by Mann Whitney test. *p < 0.05, ***p < 0.001. Data show means + SEM of 4 independent experiments performed in duplicate.

Chapter II

3.2.5 *S. cerevisiae*-mediated *MYD88* mRNA delivery repolarizes M2c macrophages towards a pro-inflammatory phenotype

In order to re-educate M2c macrophages towards an M1 phenotype, we aimed to deliver *MYD88* mRNA. MyD88 is an adaptor protein implicated in the signal transmission induced by most Toll-like receptor agonists, and is therefore involved in the induction of pro-inflammatory cytokine expression in macrophages (Martinez *et al.*, 2014; Wang *et al.*, 2014).

M1 and M2c cells were incubated with yeast carrying the vector pPGK-IRES-MyD88 for 16 h. *MYD88* mRNA delivery was verified by real-time RT-PCR, and MyD88 expression was evaluated by Western blot. Yeast-mediated mRNA delivery resulted in an at least 3-fold increase in the abundance of the delivered mRNA in M1 macrophages (Figure 17 A) and 2-fold increase in M2c macrophages (Figure 17 D).

In M1 macrophages, yeast uptake itself tended to induce a downregulation of MyD88 expression, but a significant up-regulation was observed upon yeast-mediated mRNA delivery (Figure 17 B, C). In M2c macrophages, yeast uptake induced an upregulation of MyD88, which was further enhanced after *MYD88* mRNA delivery by yeast (Figure 17 E, F).

Chapter II

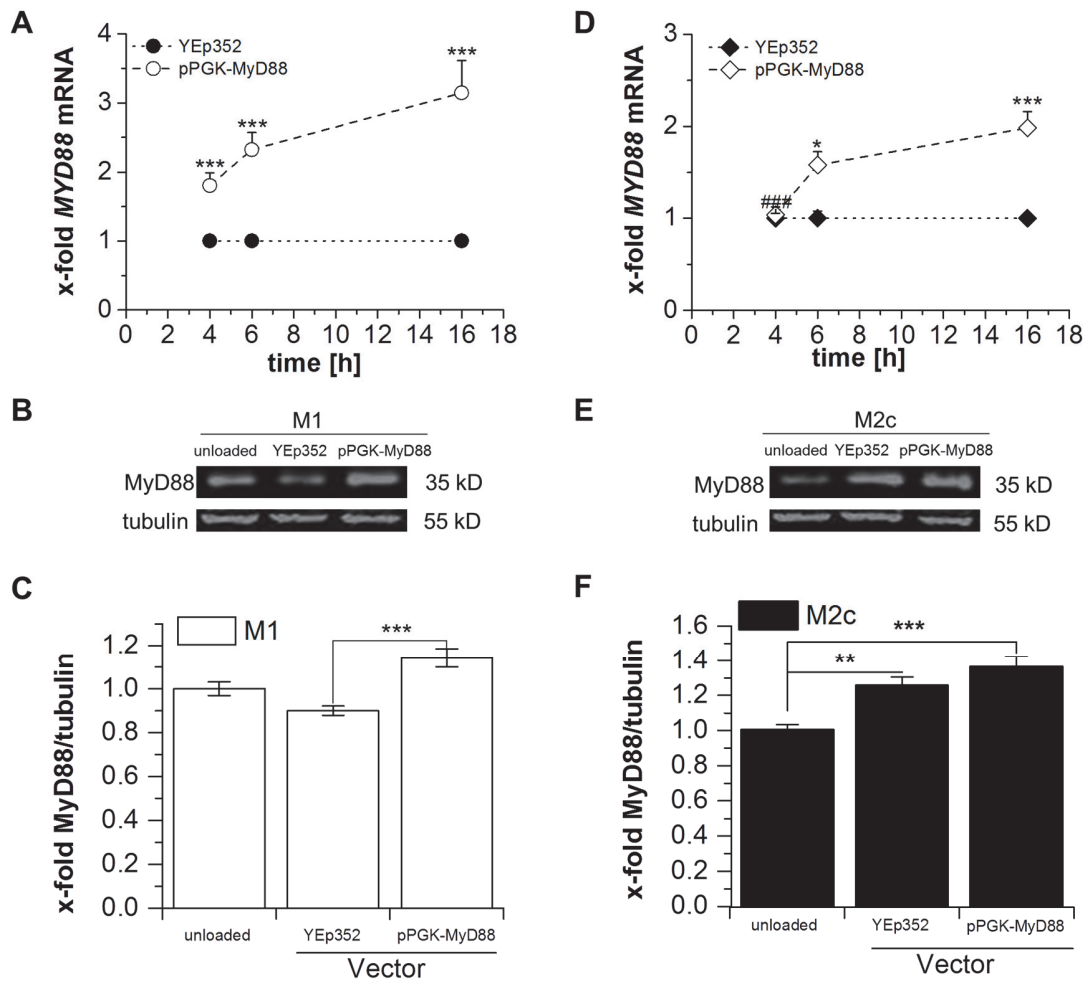


Figure 17: *S. cerevisiae* delivers functional *MYD88* mRNA to human M1 and M2c macrophages. (A, D) *MYD88* mRNA delivery was verified by real-time RT-PCR and normalized to *ACTB*. Data are presented as x-fold, with cells loaded with yeast carrying YEp352 set to 1. p-values were generated by Mann Whitney test. (*) pPGK-MyD88 compared to YEp352. (#) pPGK-MyD88 compared to pPGK-MyD88 at 16 h. (B, E) MyD88 expression was measured by Western blot. One representative blot is shown. (C, F) MyD88 quantification. Data are presented as x-fold, with unloaded cells set to 1. (C) p-values were calculated by Mann Whitney test (F) p-values were calculated using one-way ANOVA with Bonferroni's post hoc test. * $p < 0.05$, ** $p < 0.01$, *** $p < 0.001$. Data show means \pm SEM of 3 independent experiments.

Chapter II

We then compared the expression of pro- and anti-inflammatory mediators in macrophages loaded either with yeast carrying the empty vector or with yeast producing *MYD88* mRNA. *MYD88* mRNA delivery did not affect the phenotype of M1 macrophages (Figure 18 A-F). In contrast, the *MYD88* vector induced a significant up-regulation of *TNF* mRNA in M2c macrophages (Figure 18 A). Furthermore, it significantly induced the secretion of TNF- α by these cells 16 h after yeast addition (Figure 18 B). This effect was still detectable after 40 h (Figure 18 B). *MYD88* delivery induced an upregulation of *IL12B* and *IL6* after 16 h in M2c cells (Figure 18 C, D), but did not have any significant effect on anti-inflammatory mediators (Figure 18 E, F).

These results indicate that yeast-based *MYD88* mRNA delivery induced pro-inflammatory cytokine expression in M2c macrophages, suggesting a re-education of these cells towards an M1-like phenotype.

Chapter II

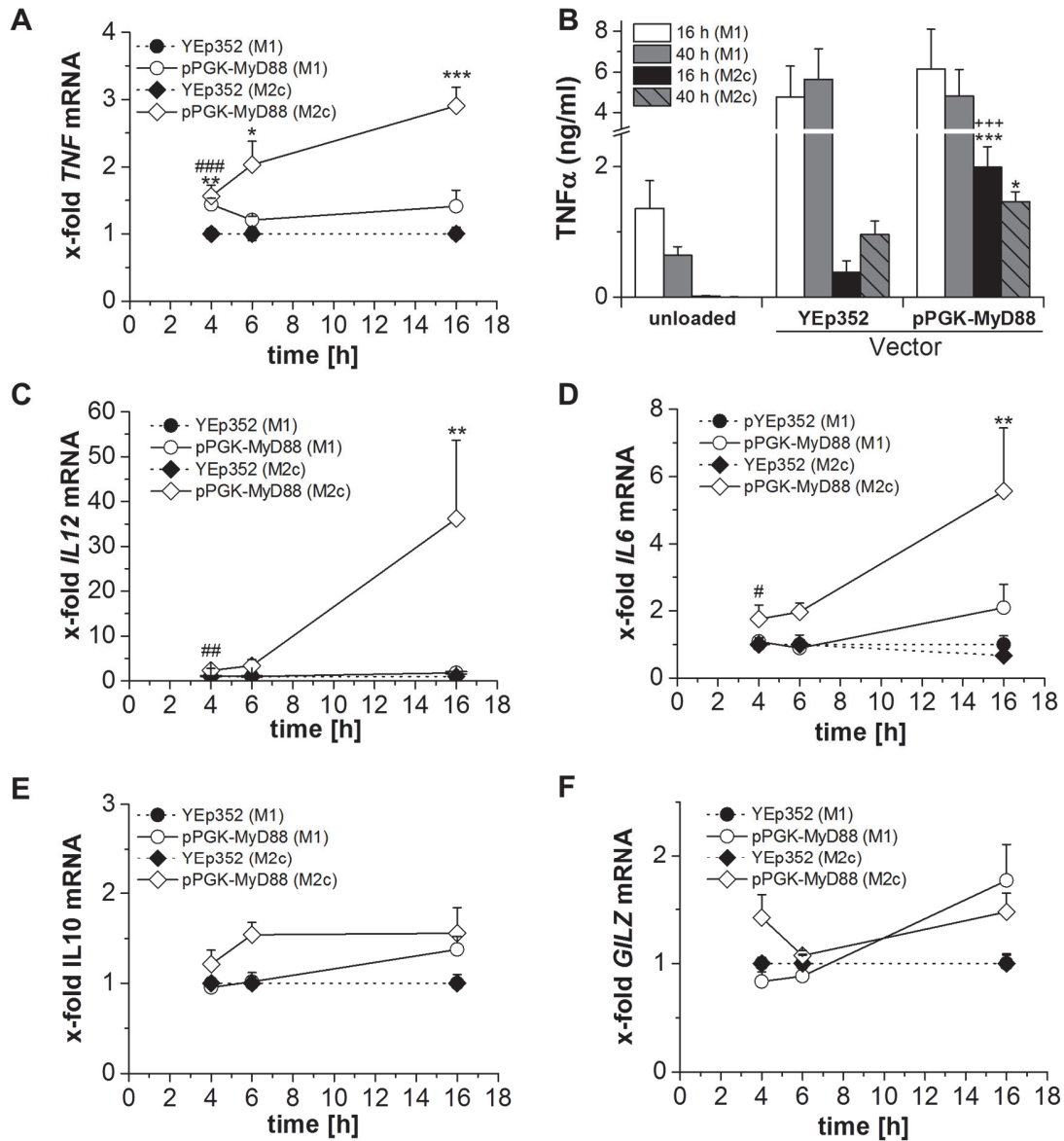


Figure 18: *S. cerevisiae*-mediated *MYD88* mRNA delivery induces pro-inflammatory cytokine expression in M2c macrophages. M1 or M2c macrophages were incubated with opsonized *S. cerevisiae* carrying the indicated vector at an MOI of 7 for 16h or the indicated period of time. (A C-F) mRNA expression levels of *TNF*, *IL12B*, *IL6*, *IL10*, and *GILZ*, were quantified by real-time RT-PCR and normalized to *ACTB*. Data are presented as x-fold, with cells loaded with yeast carrying YEp352 set to 1. Data show means + SEM of 3 independent experiments performed in duplicate. p-values were generated by Mann Whitney test, except for *IL10*, *GILZ* (for M1), *IL6*, *TNF* and *IL12B* (for M2) where one way ANOVA with Bonferroni's post hoc test was used. * $p < 0.05$, ** $p < 0.01$, *** $p < 0.001$. (*) pPGK-MyD88 compared to YEp352. (B) $TNF-\alpha$ was measured in the macrophage supernatant by ELISA after 16 h or 40 h of yeast co-culture. Data represent means + SEM from three (16 h) or two (40 h) independent experiments performed in duplicate. p-values were calculated by one-way ANOVA with Bonferroni's post hoc test. * $p < 0.05$, *** $p < 0.001$. (*) yeast-loaded cells compared to unloaded cells. (+) yeast-loaded cells compared to cells loaded with yeast carrying the vector YEp352.

Chapter II

3.2.6 *S. cerevisiae*-mediated *TNF* mRNA delivery repolarizes M2c macrophages towards a pro-inflammatory phenotype

TNF- α is considered as an M1 macrophage stimulus (Martinez *et al.*, 2014). Recently Kratochvill *et al.* have shown that the loss of type I TNF receptor signaling enhanced the M2-like phenotype of tumor-associated macrophages, suggesting that TNF- α can act as a repressor of M2 signaling in TAM (Kratochvill *et al.*, 2015). Using yeast-mediated mRNA delivery, we aimed to overexpress TNF- α in M2c macrophages.

Yeast-mediated *TNF* mRNA delivery was successful in both M1 and M2c macrophages, as indicated by a 3-fold and 4.5-fold induction of *TNF* mRNA, respectively (Figure 19 A). TNF- α was measured in the cell culture supernatants by ELISA after short-term (16 h) and long-term (40 h) incubation. The delivery of *TNF* mRNA tended to increase the TNF- α secretion by M1 macrophages (Figure 19 B), although not significantly so. However, *TNF* mRNA delivery significantly induced the secretion of TNF- α in M2c cells after short term and long term exposure (Figure 19 B).

TNF overexpression resulted in an induction of *IL12B* and tended to induce *IL6* (Figure 19 C, D) in both M1 and M2c macrophages. Interestingly, the pro-inflammatory effect of yeast-mediated delivery of *TNF* mRNA was more pronounced in M2c cells. In addition to pro-inflammatory cytokines, TNF delivery induced the expression of the anti-inflammatory mediators *IL10* (Figure 19 E) and *GILZ* (Figure 19 F), in M1 macrophages, possibly within a regulatory feedback loop. No significant change in *IL10* expression was observed in M2c macrophages (Figure 19 E), although an upregulation of *GILZ* mRNA was induced (Figure 19 F).

Taken together, these results indicate that yeast carrying the pPGK-IRES-TNF boosts the M1 pro-inflammatory activation state and can induce pro-inflammatory cytokine expression in M2c macrophages.

Chapter II

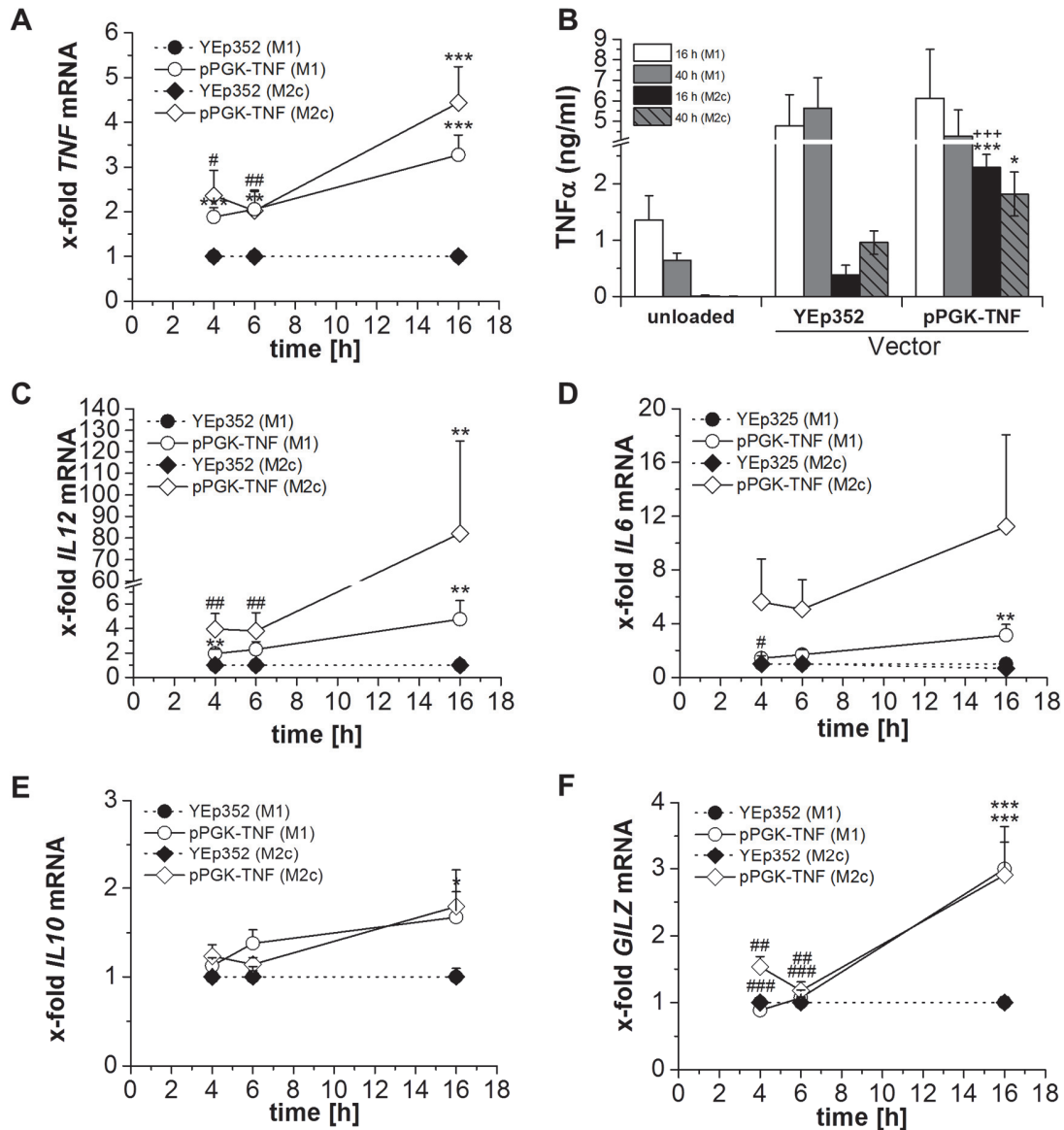


Figure 19: *S. cerevisiae*-mediated TNF mRNA delivery induces cytokine expression in M1 and M2c macrophages. M1 or M2c macrophages were incubated with opsonized *S. cerevisiae* carrying the indicated vector at an MOI of 7 for 16 h or the indicated period of time. (A-C-F) mRNA expression levels of *TNF*, *IL12B*, *IL6*, *IL10*, and *GILZ*, were quantified by real-time RT-PCR and normalized to *ACTB*. Data are presented as x-fold, with cells loaded with yeast carrying YEp352 set to 1. Data show means + SEM of 3 independent experiments performed in duplicate. p-values were generated by Mann Whitney test, except for *IL10* and *IL6* (for M1), *GILZ*, *IL12B* and *TNF* (for M2) where one way ANOVA with Bonferroni's post hoc test was used. * $p < 0.05$, ** $p < 0.01$, *** $p < 0.001$. (*) pPGK-MyD88 compared to YEp352. (B) TNF- α was measured in the macrophage supernatant by ELISA after 16 h or 40 h of yeast co-culture. Data represent means + SEM from three (16 h) or two (40 h) independent experiments performed in duplicate. p-values were calculated by one-way ANOVA with Bonferroni's post hoc test. * $p < 0.05$, *** $p < 0.001$. (*) yeast-loaded cells compared to unloaded cells. (+) yeast-loaded cells compared to cells loaded with yeast carrying the vector YEp352.

Chapter II

3.3 Discussion

Recently, *S. cerevisiae* was proposed as a novel live DNA/RNA vaccine vehicle (Walch *et al.*, 2012; Walch-Rückheim *et al.*, 2016; Kiflmariam *et al.*, 2013). Since yeast can also be internalized by macrophages (Seif *et al.*, 2016), we hypothesized that this novel approach might also be useful for gene delivery into macrophages. In this study, we show for the first time that recombinant yeast cells can be used to genetically modify macrophages and to manipulate their functional phenotype.

3.3.1 *In vitro* model of pro- and anti-inflammatory macrophages

In response to surrounding signals, macrophages can acquire different phenotypes. With reference to Th1-Th2 activation of T cells, macrophages exposed to Th1 cytokines, such as IFN- γ , were termed M1 and the ones exposed to Th2 cytokines, such as IL-4 and IL-10, were referred to as M2. Several other stimuli inducing a pro-inflammatory or anti-inflammatory phenotype were grouped as M1 or M2 stimuli, respectively (Martinez *et al.*, 2014). The notion of macrophage polarization is of particular importance due to their influence on disease progression (Murray and Wynn, 2011). In solid tumors, for example, the presence of tumor-associated macrophages with an anti-inflammatory M2 phenotype is related to a poor prognosis (Bingle *et al.*, 2002). Rey-Giraud *et al.* (Rey-Giraud *et al.*, 2012) described a method to generate *in vitro* M1 and M2 macrophages, with M2c macrophages showing a significant pro-tumor activity. As an *in vitro* model of M1 and M2 macrophages, we cultured human peripheral blood monocytes with GM-CSF/LPS/IFN- γ (for M1), M-CSF/IL-4 (for M2a) or M-CSF/IL-10 (for M2c). In our hands, macrophages differentiated with GM-CSF and stimulated by subsequent LPS/IFN- γ treatment expressed M1 macrophages surface markers, mainly HLAII and CD86. M-CSF differentiation followed by IL-4 treatment led to a high expression of the mannose receptor CD206. Finally, M-CSF differentiation followed by IL-10 treatment induced the expression of the M2 marker CD163. The pro-inflammatory phenotype of the *in vitro* differentiated M1

Chapter II

cells was confirmed by their high expression of pro-inflammatory cytokines. Both M2a and M2c cells expressed the anti-inflammatory cytokine IL-10. Thus, our treatment scheme successfully generated differentially polarized macrophages, as previously described in the literature (Rey-Giraud *et al.*, 2012; Seif *et al.*, 2016; Hoppstädter and Kiemer, 2015).

3.3.2 Yeast uptake by differently polarized macrophages

One main function of macrophages is phagocytosis. The efficiency of this process can vary depending on their phenotype. M2 macrophages have for example been described as more potent regarding cell debris clearance when compared with M1 macrophages (Xu *et al.*, 2006). While it is well known that yeast can be taken up by phagocytic cells including macrophages (Seif *et al.*, 2016), its uptake by fully polarized pro- and anti-inflammatory macrophages was not described. In this study, we showed that M1 macrophages were more potent in yeast uptake when compared to M2a or M2c cells. Interestingly, M2a macrophages internalized *S. cerevisiae* more efficiently than M2c cells. This difference in yeast uptake capacity might be related to the differential expression of the mannose receptor CD206 in M1, M2a, and M2c macrophages. The mannose receptor is well known to be involved in yeast uptake (Giaimis *et al.*, 1993). However, opsonized *S. cerevisiae* was internalized to the same extent by the three macrophage populations, suggesting that different types of macrophages can be targeted by yeast-based delivery systems. Opsonization enhanced yeast uptake is due to the involvement of Fc and complement receptors in the internalization of yeast coated with antibodies and complement fragments (Underhill *et al.*, 2012).

3.3.3 Yeast mediated nucleic acids delivery to human macrophages

To find the optimal vector for nucleic acid delivery to polarized human macrophages, we compared DNA, constitutively expressed mRNA or inducible mRNA delivery using the model protein eGFP. All treatment schemes resulted in a higher percentage of eGFP-expressing cells in M2c macrophages when

Chapter II

compared with M1 cells. The maximal amount of eGFP-expressing cells was obtained by delivering eGFP mRNA constitutively expressed in yeast using the PGK promoter. These results were in contrast to the observation made in dendritic cells where inducible mRNA using the MLS promoter and DNA using the CMV promoter led to the highest number of eGFP positive cells (Walch *et al.*, 2012). These differences might be due to differential phagolysosome maturation and acidification processes upon particle uptake in M1/M2 macrophages and dendritic cells (Cerovic *et al.*, 2014; Canton *et al.*, 2014).

Several studies using adenoviral vectors to deliver genes, such as *IFNG*, *IL12B* or *IRF5*, suggested inducing an M1 phenotype in macrophages as a promising strategy for cancer therapy (Singh *et al.*, 2014). We used the biosynthetic mRNA mycofection described here and earlier (Walch *et al.*, 2012) to deliver *MYD88* or *TNF*. Both MyD88 and TNF- α are involved in the polarization of macrophages towards an M1 phenotype (Martinez *et al.*, 2014). Furthermore, loss of type I TNF receptor and MyD88 in TAM has been reported to induce an M2 phenotype and an increase in tumor size (Kratochvill *et al.*, 2015).

First, we compared cytokine expression profiles between yeast-loaded and unloaded cells to determine the unspecific effects of mycofection. Yeast uptake induced a pro-inflammatory phenotype in M1 and M2c macrophages, as indicated by the upregulation of the pro-inflammatory cytokines *IL12B*, *TNF*, and *IL6*. These results are in line with our previous observations for GM-CSF and M-CSF differentiated macrophages. In fact, we recently showed that *S. cerevisiae* exposure leads to the upregulation of pro-inflammatory cytokine mRNA in both cell types (Seif *et al.*, 2016).

We then compared the expression profiles of macrophages loaded with yeast carrying the empty vector as a negative control and yeast delivering *MYD88* or *TNF* mRNA. Both *MYD88* and *TNF* mRNA were expressed in M1 and M2c cells after yeast-mediated mRNA delivery. Since M1 cells were already secreting TNF- α , mRNA delivery did not induce TNF- α much further. In contrast, a remarkable increase in TNF- α secretion was observed after yeast-mediated *MYD88* and *TNF* mRNA delivery in M2c macrophages. Interestingly, the concentration measured

Chapter II

was similar to TNF- α concentrations that have previously been shown to be sufficient to induce a 50% reduction of cell viability in MCF7 cells, a human breast adenocarcinoma cell line (Machuca *et al.*, 2006).

The delivery of *MYD88* mRNA did not affect the M1 macrophage phenotype. In contrast, the upregulation of MyD88 after mycofection induced a high and long lasting expression of pro-inflammatory mediators in M2c macrophages. *TNF* delivery led to a significantly higher expression of pro-inflammatory cytokine mRNA in both M1 and M2c cells but also induced the anti-inflammatory cytokine IL-10 in M1 and GILZ in both M1 and M2c macrophages. Recently, the elevated expression of GILZ in macrophages was reported to occur in the late stage of inflammation (Hoppstädter and Kiemer, 2015; Hoppstädter *et al.*, 2015; Vago *et al.*, 2015). Thus, GILZ and IL-10 upregulation might indicate the initialization of the resolution phase. Since this effect is lacking in MyD88-overexpressing cells, a MyD88-based strategy may be more efficient.

In summary, we showed for the first time that *S. cerevisiae*-mediated mRNA delivery can be used to overexpress cytosolic (MyD88) or secreted proteins (TNF- α) in both M1 and M2c macrophages.

3.4 Conclusion

In conclusion, we show for the first time that mycofection can be used to overexpress proteins in macrophages and manipulate their phenotype. mRNA mycofection could be a good strategy to target tumor-associated macrophages and repolarize them toward an M1 phenotype.

4 Chapter III

M2 polarization enhances silica
nanoparticle uptake by macrophages

Chapter III

Chapter III

4.1 Introduction

Numerous types of nanomaterials, such as quantum dots or silica, carbon, zinc oxide and gold nanoparticles, have been shown to induce inflammatory responses both *in vitro* and *in vivo* (Roy *et al.*, 2014; Wu and Tang, 2014; Autengruber *et al.*, 2014; Deng *et al.*, 2011; Kusaka *et al.*, 2014). Macrophages represent critical regulators of inflammatory processes and also exhibit a high uptake potential for nanoparticles (Amoozgar and Goldberg, 2014; Diesel *et al.*, 2013; Klein *et al.*, 2013; Kusaka *et al.*, 2014; Sica and Mantovani, 2012). Therefore, the investigation of macrophage responses upon nanoparticle exposure is highly relevant for the prediction of potentially harmful effects.

Most cellular models used so far to investigate nanoparticle-associated inflammation do not take macrophage heterogeneity into account. A study by Jones *et al.* (2013) recently reported that the rate of nanoparticle clearance *in vivo* differs largely between mouse strains dependent on their preference for either Th1- or Th2-responses. C57BL/6 mice preferentially produce T helper type 1 (Th1) cytokines, such as interferon (IFN)- γ , whereas those from Balb/c mice favor T helper type 2 (Th2) cytokine production, e.g. interleukin (IL)-10. In addition to their distinct T-cell responses, *in vitro* investigations have demonstrated that macrophages from these mouse strains exert different reactions in response to the bacterial cell wall component and activator of the innate immune response lipopolysaccharide (LPS) (Watanabe *et al.*, 2004). Using depletion strategies, Jones *et al.* (2013) demonstrated that macrophages are involved in the enhanced clearance of 300 nm cylindrical PEG hydrogel nanoparticles observed in Th2-prone mice. In accordance, macrophages isolated from Th1 strains showed a lower capacity than macrophages from Th2 strains to take up these nanoparticles. *In vitro* polarization led to similar results, suggesting that macrophage polarization critically affects nanoparticle uptake.

Other factors influencing cellular uptake include nanoparticle morphology, i.e. size and shape, and the materials used (Truong *et al.*, 2014; Albanese *et al.*, 2012; Kusaka *et al.*, 2014). Therefore, the findings by Jones *et al.* might not

Chapter III

apply to other types of nanoparticles. Among different nanomaterials, silica nanoparticles are widely used in various applications, ranging from additives for plastics or food to targeted drug carrier systems. Worldwide, 1.5 million tons of amorphous silica nanoparticles are produced annually. This enormous production rate is even expected to rise due to growth sectors such as energy and information technology as well as nanomedicine (BMBF, 2013).

Despite the increasing number of applications for silica nanoparticles, the influence of macrophage polarization on their uptake and thereby their clearance has not been characterized yet. Thus, we examined the uptake potential of differentially polarized human macrophages for silica nanoparticles by employing fluorescently labeled particles.

4.2 Results

4.2.1 Silica nanoparticle toxicity

We used silica nanoparticles preparations having 26 nm or 41 nm size. Viability tests by MTT assay showed no significant cytotoxicity of both nanoparticle preparations on GM-M Φ , M-M Φ in concentrations up to 50 $\mu\text{g/ml}$ (Figure 20). Controls for unspecific interactions of nanoparticles with the assay were performed as previously described (Astania *et al.*, 2014; Diesel *et al.*, 2013).

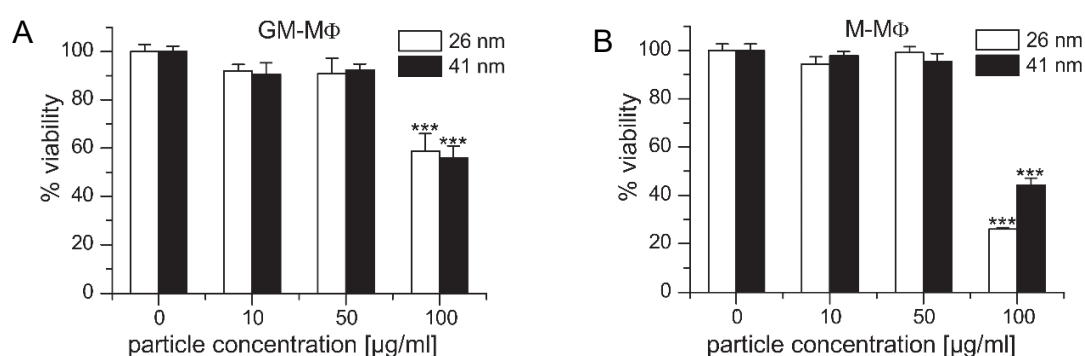


Figure 20: Nanoparticle cytotoxicity. Cell viability upon nanoparticle exposure as determined by MTT assay. GM-M Φ (A) or M-M Φ (B) were treated with nanoparticles for 24 h at the indicated concentrations. Data represent means + SEM from two independent experiments performed at least in quadruplicate with cells originating from different donors. Values obtained for untreated cells were set as 100%. p-values were calculated by one way ANOVA with Bonferroni's post hoc test. ***p < 0.001 compared with untreated cells.

Chapter III

4.2.2 Uptake of nanoparticles and microparticles in *in vitro* polarized macrophages

Particle uptake by M1 and M2 polarized primary human monocyte-derived macrophages was assessed by flow cytometry (Figure 21 A and B). M1 and M2 cells internalized 1.75 μm microspheres to a similar extent, as shown by comparable values for relative geometric mean fluorescence intensity. Likewise, no significant difference was observed between M1 and M2 cells regarding the percentage of macrophages positive for particle-associated fluorescence ($63.8 \pm 5.1\%$ for M1 vs. $69.6 \pm 3.3\%$ for M2). In contrast, both M1 and M2 macrophages were $> 98\%$ positive for particle-associated fluorescence after incubation with nanoparticles. GMFI values were significantly higher in M2 macrophages compared with M1 polarized cells, indicating that both 26 and 41 nm silica particles were taken up more efficiently in M2 cells. Visualization of particle uptake by fluorescence microscopy further confirmed these assumptions and indicated that nanoparticles were in fact localized inside the cells and not merely attached to their surface (Figure 21 C).

In addition to monocyte-derived macrophages, the macrophage-like cell line THP-1 is widely used to investigate the impact of M1 and M2 polarization on distinct cell functions (Chanput *et al.*, 2013; Tjiu *et al.*, 2009). Therefore, we also analyzed nanoparticle uptake in these cells after treatment with LPS/IFN- γ or IL-10 to induce an M1 or M2 phenotype, respectively. As observed in primary MDM, the uptake potential for nanoparticles was increased in M2-polarized THP-1 macrophages when compared with M1 cells, as suggested by significantly increased GMFI values (Figure 22).

Chapter III

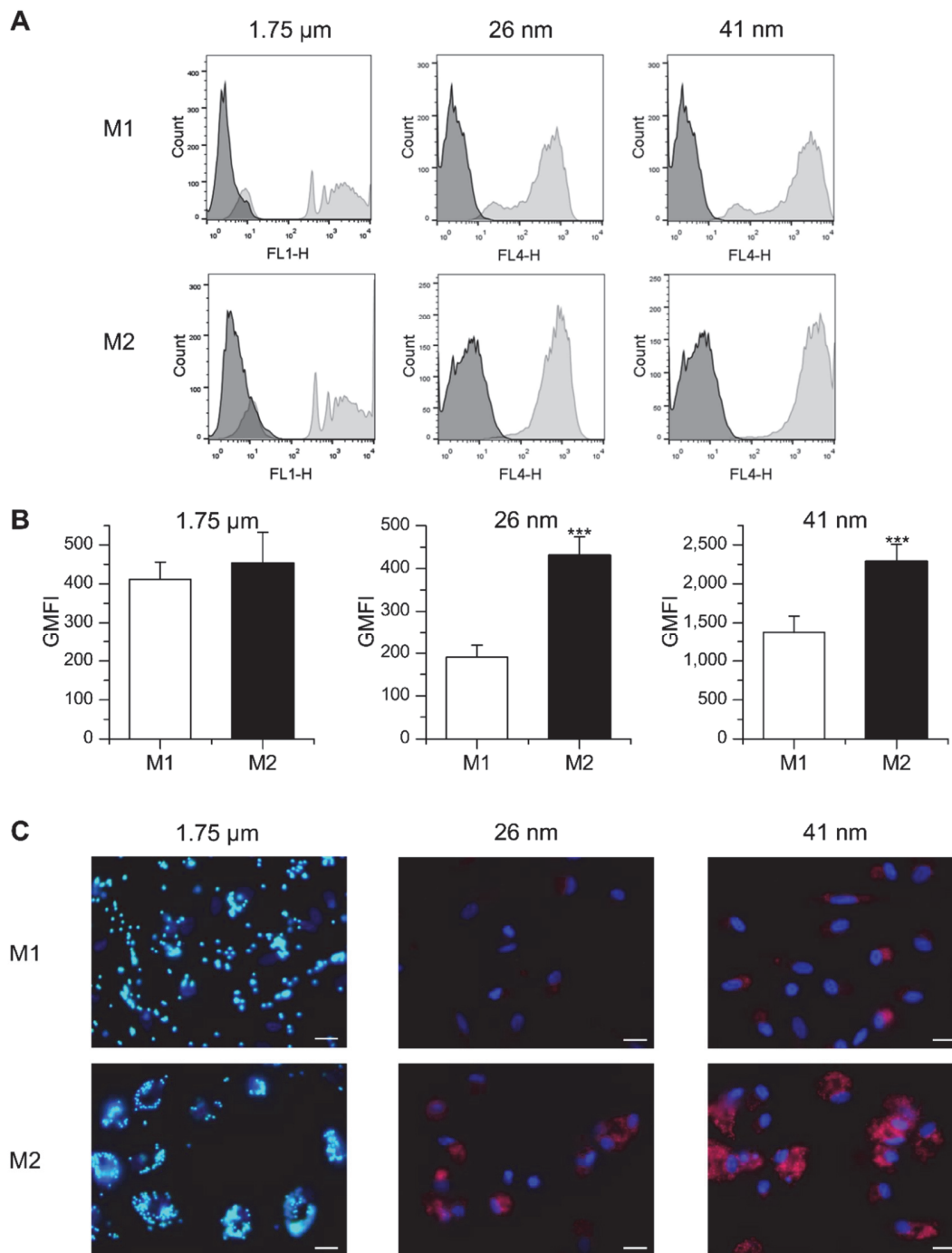


Figure 21: Particle uptake in M1- and M2-polarized monocyte-derived macrophages. (A, B) Macrophages were incubated for 1 h with FITC-labelled 1.75 μm latex beads (100 beads/cell) or fluorescent nanoparticles (26 or 41 nm, 50 $\mu\text{g}/\text{ml}$) and uptake efficiency was assessed by flow cytometry. (A) Representative histograms are given. (B) GMFI values. Data represent means + SEM of 3 independent experiments performed in duplicate or triplicate with cells derived from different donors. p-values were generated by Student's t-test. ***p < 0.001 compared with M1-polarized cells. (C) Representative images of M1 and M2 macrophages 3 h after particle addition. Green: microparticles, red: nanoparticles, blue: nucleus, scale bar: 20 μm . Imaging was done by Anna Dembek.

Chapter III

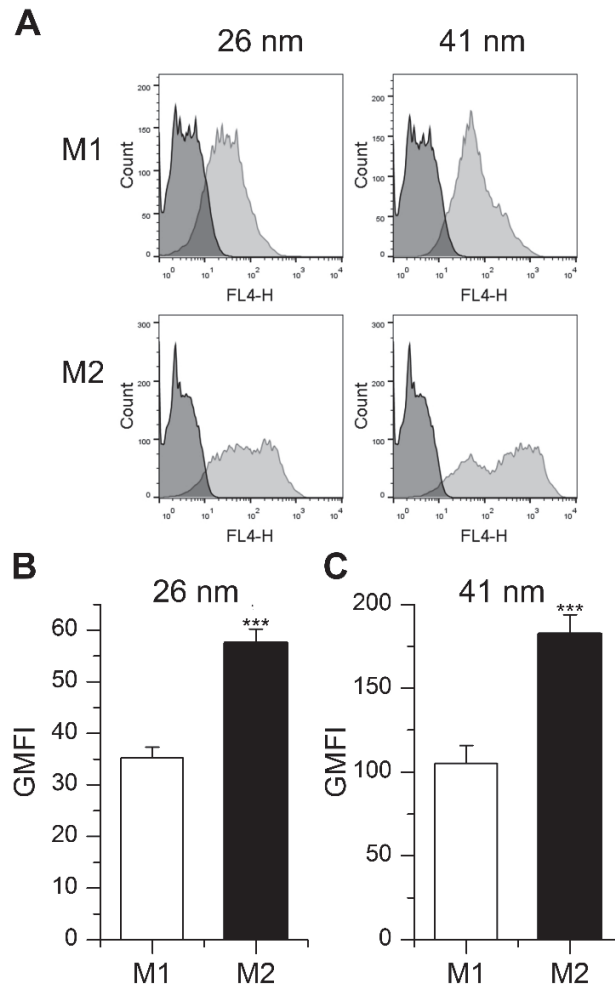


Figure 22: Particle uptake in M1- and M2-polarized THP-1 macrophages. (A, B, C) Cells were incubated for 1 h with fluorescent nanoparticles (26 or 41 nm, 50 $\mu\text{g/ml}$) and uptake efficiency was assessed by flow cytometry. (A) Representative histograms are given. (B, C) GMFI mean values + SEM of 3 independent experiments performed in triplicate. p-values were generated by Student's t-test. *** $p < 0.001$ compared with M1-polarized cells.

Chapter III

4.2.3 Nanoparticle uptake in primary human alveolar macrophages (AM) and tumor-associated macrophages (TAM)

In general, TAM represent M2-like macrophages promoting tumor cell proliferation, angiogenesis, matrix turnover, and repression of adaptive immunity (Solinas *et al.*, 2009). In contrast, AM are considered to exhibit a more pro-inflammatory, M1-like phenotype (Hoppstädter *et al.*, 2010). Therefore, we hypothesized that the capacity to take up nanoparticles might differ between those two cell types. TAM were obtained after digestion of tumor tissue from patients undergoing lung resection, whereas AM were isolated from the surrounding non-tumor lung tissue. AM populations mostly consisted of large, round cells whereas TAM were more heterogenous in size and shape (Figure 23 A). Intracellular CD68, often used as a marker specific for macrophages (Hoppstädter *et al.*, 2010; Holness and Simmons, 1993), was detected in over 95% of the cells contained in AM and TAM preparations, thereby identifying them as macrophages (Figure 23 B). The uptake of 26 nm silica particles was indeed enhanced in TAM when compared to AM, as assessed by flow cytometry (Figure 23 C), suggesting that our findings for *in vitro* polarized macrophages also translate to the *in vivo* situation.

Chapter III

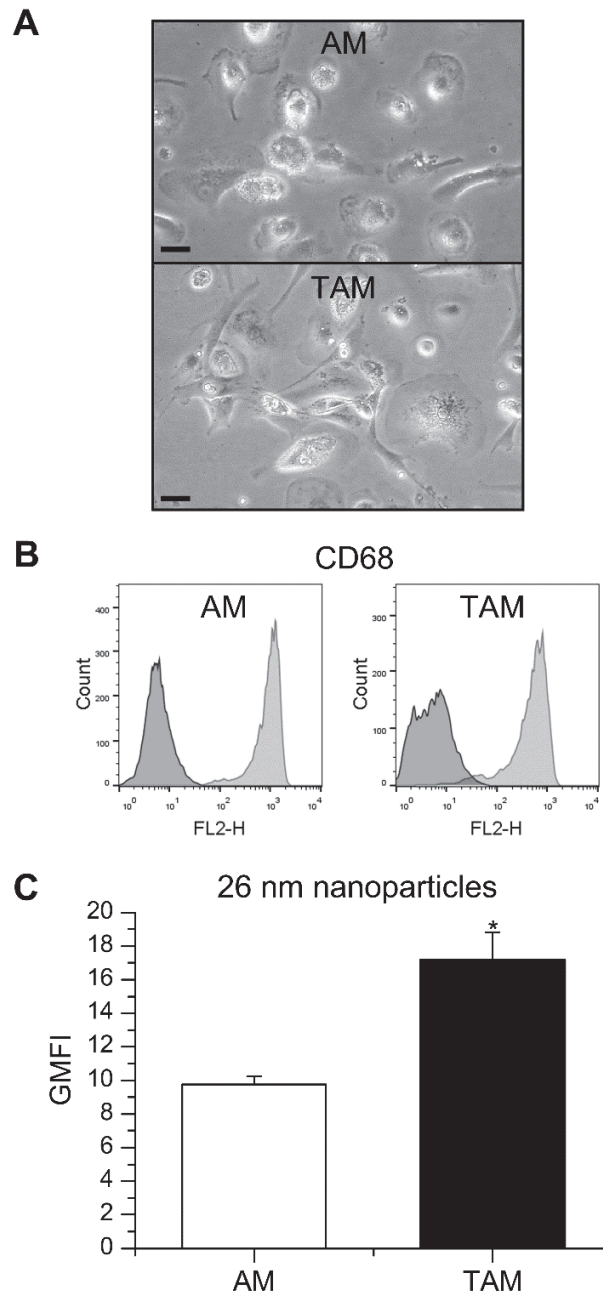


Figure 23: Nanoparticle uptake in AM and TAM. (A) AM and TAM morphology were examined by light microscopy. One representative image is given. Scale bar: 20 μ m. (B) CD68 expression in AM and TAM. Data show one histogram representative for 4 independent experiments. Dark grey: isotype control; light grey: specific staining. (C) GMFI mean values + SEM obtained from independent experiments with AM obtained from two and TAM obtained from 4 different donors. P-values were calculated by Student's t-test. * $p < 0.05$ compared with AM. This experiment was performed by Anna Dembek.

Chapter III

4.3 Discussion

The use of silica-based nanomaterials in commercial products, e.g. as additives to food, cosmetics, varnishes or printer toners, is rapidly increasing. In addition, silica or silica coated engineered nanoparticles have been suggested as promising candidates for biomedical applications, such as gene transfection, drug delivery, biosensing, and imaging applications (Probst *et al.*, 2012; Korzeniowska *et al.*, 2013; Knopp *et al.*, 2009; Montalti *et al.*, 2014; Ravi Kumar *et al.*, 2004; Rosenholm *et al.*, 2010). The growing commercialization of nanotechnology products has raised concerns about their safety. The physico-chemical properties of silica nanoparticles that make them attractive for industrial use might represent potential hazards to human health, due to an enhanced ability to penetrate tissues or even cells and their interactions with biomolecules. Investigations on their potential to induce cell death or inflammation led to divergent results. Apart from the composition and size of nanomaterials, the target cell type critically affects intracellular responses and the degree of cytotoxicity (Napierska *et al.*, 2010; Sohaebuddin *et al.*, 2010; Izak-Nau *et al.*, 2013).

4.3.1 Nanoparticles clearance

After entering the body, nanoparticles are rapidly cleared by macrophages and other cells of the mononuclear phagocyte system (MPS) (Amoozgar and Goldberg, 2014; Yoo *et al.*, 2010). Besides tissue macrophages present in every organ of the body, the MPS includes committed precursors in the bone marrow and circulating blood monocytes (Jenkins and Hume, 2014). Nanoparticles entering tissues or circulating in the blood make direct contact with various MPS cells. Previous studies have shown that the MPS is responsible for the clearance of most nanoparticles larger than 10 nm, regardless of their shape and surface chemistry (Longmire *et al.*, 2008).

Nanoparticle uptake by MPS cells can occur through various pathways In macrophages, phagocytosis, and macropinocytosis, as well as clathrin-

Chapter III

caveolae-, and scavenger receptor-mediated endocytic pathways have been suggested to be involved in nanoparticle internalization (Diesel *et al.*, 2013; Kuhn *et al.*, 2014; Roy *et al.*, 2014). Nanoparticle exposure can lead to pro-inflammatory responses, most of which are associated with macrophages. The avid uptake of nanoparticles by these cells might make them more susceptible to particle overload and cell death (Napierska *et al.*, 2010; Sohaebuddin *et al.*, 2010). Thus, the characterization of nanoparticle uptake in macrophages is a major step in the assessment of nanoparticle toxicity.

4.3.2 Macrophage polarization influences particle uptake

In the present study, we demonstrated that macrophage polarization influences particle uptake in primary human macrophages and human macrophage-like THP-1 cells. M1 macrophages are considered to be more involved in inflammatory and microbicidal processes and have been shown to be more phagocytic towards bacteria (Krysko *et al.*, 2011; Varin *et al.*, 2010). In contrast, M2 macrophages are thought to exert anti-inflammatory functions and to promote wound healing. They might also be more involved in debris clearance, since they exhibit a greater phagocytic activity towards cell debris compared with M1 (Rey-Giraud *et al.*, 2012), indicating that the influence of macrophage polarization on phagocytosis largely depends on the properties of the phagocytosed material. Accordingly, phagocytosis has been suggested as a general property of macrophages, but not a reliable predictor of M1 or M2 responses (Mills and Ley, 2014). In fact, we did not detect any differences between primary M1 and M2 macrophages regarding the phagocytic uptake of latex microparticles. In line with our findings, microparticle clearance has been reported to be similar in Th1- and Th2-prone mouse strains (Jones *et al.*, 2013).

On the other hand, we observed a markedly increased uptake of both 26 and 41 nm silica nanoparticles following M2 polarization compared to M1 cells in primary as well as THP-1 macrophages. M2 macrophages have been shown to internalize FITC-dextran and 300 nm PEG hydrogel nanoparticles more efficiently when compared to M1 polarized cells, indicating that M2 polarization

Chapter III

leads to a higher endocytic capacity (Edin *et al.*, 2013). This might be due to increased expression of receptors facilitating endocytosis, i.e. scavenger and lectin receptors, in M2-polarized cells (Jones *et al.*, 2013; Martinez *et al.*, 2006; Rey-Giraud *et al.*, 2012). Furthermore, the Th1-biased mouse strain C57BL/6 has been reported to clear nanoparticles more slowly than the Th2-prone Balb/c strain, which might be mainly due to the prevalence of M2 macrophages in Balb/c mice (Jones *et al.*, 2013).

The unique physical and chemical properties associated with potentially detrimental effects of nanoparticles on cells and tissues might be beneficial in the context of nanomedicine. In fact, nanomaterials offer many advantages, such as improved bioavailability and feasibility of incorporation of both hydrophilic and hydrophobic substances, and may be used in various biomedical applications ranging from diagnostics to therapeutics (Latterini and Amelia, 2009; Chang *et al.*, 2014; Vijayanathan *et al.*, 2014; Zhao *et al.*, 2009). Due to their hydrophilicity, stability in physiological environment, ease of production, and relatively low cost, silica nanoparticles display a great potential for biomedical applications (Bitar *et al.*, 2012).

However, rapid elimination from the systemic circulation by cells from the MPS constitutes a major challenge for the application of nanoparticles as intravenous drug delivery platforms, as it significantly reduces the number of nanoparticles available at the target site, thereby impairing the efficacy of the drug (Amoozgar and Goldberg, 2014; Yoo *et al.*, 2010). At the same time, nanoparticle accumulation in macrophages has been considered to be an advantage for therapeutic strategies based on macrophage reprogramming towards a stimulatory/destructive or a suppressive/protective phenotype (Chellat *et al.*, 2005).

A recently published meta-analysis revealed that the inter-patient pharmacokinetic variability of nanoparticulate formulations is higher compared with small molecule agents (Schell *et al.*, 2014). The patients' immune status and thereby their dominant macrophage phenotype can be influenced by various immune-priming events such as allergies or infections (Sica and Mantovani,

Chapter III

2012). Thus, our data suggest that the macrophage phenotype might contribute to the high inter-individual pharmacokinetic variability of nanoparticulate drugs, with analogous implications for the clearance of potentially harmful nanoparticles taken up from the environment.

4.3.3 Silica nanoparticles uptake is enhanced in tumor-associated macrophages

We previously reported that distinct macrophage populations residing in the human lung exhibit different phenotypic and functional characteristics: alveolar macrophages (AM) resemble inflammatory M1 macrophages, whereas lung interstitial macrophages display a more regulatory phenotype (Hoppstädter *et al.*, 2010). Macrophages are also one of the major populations of infiltrating leukocytes in solid lung tumors. These tumor-associated macrophages (TAM) play a major role in tumor initiation, development, and metastasis. TAM are considered to be a polarized M2-like macrophage population with potent immunosuppressive functions. High numbers of TAM are associated with a poor prognosis, accelerated lymphangiogenesis, and lymph node metastasis (Ma *et al.*, 2010; Solinas *et al.*, 2009; Sica *et al.*, 2008). In the present study, we compared the nanoparticle uptake capacity of human primary TAM from non-small cell lung cancer tissue samples with AM from non-tumor tissue. As observed for *in vitro* differentiated M2 macrophages, the internalization of 26 nm silica nanoparticles was clearly enhanced in TAM. Since TAM retain functional plasticity, reprogramming TAM in order to eliminate their support for tumor growth or to induce cytotoxic activity has been considered as a strategy to improve tumor therapy (Amoozgar and Goldberg, 2014; Sica *et al.*, 2007; Chakraborty *et al.*, 2012; Stout *et al.*, 2009). Considering the high potential for nanoparticle uptake observed in TAM, such therapeutic approaches might benefit from the use of nanoparticulate formulations.

Chapter III

4.4 Conclusion

In summary, our data suggest that the interaction of nanoparticles with differentially polarized macrophages should be taken into consideration when investigating the potentially toxic health effects of nanomaterials. What is more, the preferential uptake of nanoparticles by M2-like macrophages might offer new therapeutic approaches aimed at targeting M2 macrophages.

Parts of the results presented in this chapter have been published in:

M2 polarization enhances silica nanoparticle uptake by macrophages.
Hoppstädter J, Seif M, Dembek A, Cavelius C, Huwer H, Kraegeloh A
and Kiemer AK. (2015) *Front. Pharmacol.* 6:55. doi: 10.3389/fphar.2015.00055

Jessica Hoppstädter participated in writing this chapter.

5 Materials and methods

Materials and methods

Materials and methods

5.1 Cell culture

5.1.1 Human monocyte-derived macrophages (MDM)

Peripheral blood monocyte isolation

Buffy coats were obtained from healthy adult blood donors (Blood Donation Center, Saarbrücken, Germany). The use of human material for the isolation of primary cells was approved by the local ethics committee (State Medical Board of Registration, Saarland, Germany; permission no. 130/08). Peripheral blood mononuclear cells (PBMC) were isolated by density gradient centrifugation following the protocol proposed by Miltenyi Biotec (Bergisch Gladbach, Germany). In brief, buffy coats were diluted 1:1 with endotoxin-free PBS (phosphate buffered saline, Sigma-Aldrich, Steinheim, Germany) containing 2 mM EDTA (ethylenediaminetetraacetic acid, Sigma-Aldrich). The diluted buffy coats were carefully layered on Pancoll (density 1.077g/ml, PAN Biotech, Aidenbach, Germany) and centrifuged (400 x *g*, 30 min, w/o break). The mononuclear cell layer was removed, washed with PBS/EDTA and centrifuged again (300 x *g*, 10 min). Remaining red blood cells were lysed in BD Pharm Lyse (BD Biosciences, Heidelberg, Germany). For removal of platelets, PBMCs were washed twice with PBS/EDTA, followed by centrifugation (200 x *g*, 10 min). Monocytes were isolated from PBMC using magnetic anti-CD14 microbeads (Miltenyi Biotec) following the manufacturer instructions. Briefly, PBMCs were resuspended in isolation buffer (PBS, 2 mM EDTA, 0.5% FBS) and incubated with CD14 microbeads (8 μ l CD14 microbeads for 10^7 total cells) for 15 min at 4°C. Cells were subsequently washed (300 x *g*, 10 min, 4°C), resuspended in isolation buffer and applied to an LS column (Miltenyi Biotec) attached to a MidiMACS separator (Miltenyi Biotec). After washing the column three times with isolation buffer, the column was removed from the separator and magnetically labeled monocytes were eluted by firmly applying a plunger. Monocyte purity was > 95% as assessed by CD14 expression (Figure 24).

Materials and methods

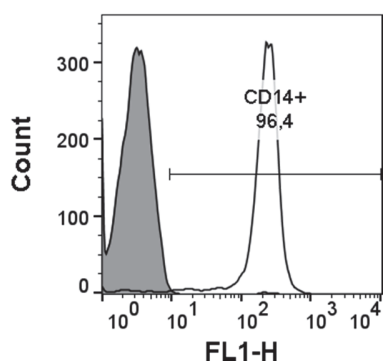


Figure 24: Monocyte purity. After isolation, Monocytes were stained with anti-CD14 (clone TÜK4, Miltenyi Biotec) as described in section 5.9.2. One representative histogram is shown. Gray: unstained cells, white: stained cells; the percentage of CD14+ cells is indicated.

Monocyte differentiation and polarization

For macrophage polarization, monocytes were cultured in 12-well plates at a density of 0.5×10^6 cells per well for 5 days at 37°C and 5% CO₂ in Macrophage-SFM (Life Technologies, Grand Island, NY, USA) supplemented with either 10 ng/ml human recombinant macrophage colony-stimulating factor (M-CSF) or granulocyte-macrophage colony-stimulating factor (GM-CSF). The medium was changed every other day. GM-CSF-differentiated macrophages (GM-MΦ) were stimulated for another 40 hours or as indicated with 1 µg/ml LPS (Sigma-Aldrich) and 20 ng/ml human recombinant interferon (IFN)-γ for M1 polarization. M-CSF-differentiated macrophages (M-MΦ) were stimulated for another 40 hours or as indicated with 50 ng/ml human recombinant IL-4 or 200 ng/ml human recombinant IL-10 for M2a or M2c polarization, respectively. All cytokines and growth factors were obtained by Miltenyi Biotec and dissolved in endotoxin-free water (Sigma-Aldrich).

For uptake experiments, monocytes were cultured in petri dishes (Ø 60 mm) at a density of 6×10^6 cells per dish for 4 days at 37°C and 5% CO₂ in Macrophage-SFM (Life Technologies) supplemented with GM-CSF or M-CSF as described above. On day 4, cells were detached from plates using PBS supplemented with 5 mM EDTA (Sigma-Aldrich). Cells were seeded into 24-well plates (for flow cytometry analysis) or SensiPlate™ 24-well glass-bottom plate (for fluorescence microscopy) at a density of 1.5×10^5 cells/well or into 12-well plates at a density of 5×10^5 cells/well (for real time RT-PCR or western blot). On the next day, cells were stimulated with LPS/IFN-γ, IL-4 or IL-10 as described above.

Materials and methods

In all experiments comparing GM-M Φ and M-M Φ , or M1, M2a and M2c cells were generated from monocytes obtained from the same donor.

5.1.2 THP-1 cell line

THP-1 cells were grown in RPMI1640 (PAN Biotech) medium supplemented with 10% [v/v] FBS (PAN Biotech) and kept at a density of $2 \times 10^5 - 1 \times 10^6$ cells / ml. For differentiation into macrophages, cells were cultured at a concentration of $5 \cdot 10^5$ cells/ml in the presence of 30 ng/ml PMA (Sigma-Aldrich) for 48 hours. For polarization, PMA-differentiated cells were harvested using PBS containing 5 mM EDTA (Sigma-Aldrich) and seeded overnight into 24-well plates at a density of 1.5×10^5 cells/well and cytokines were added as described in section 5.1.1.

Freezing

For freezing, cell suspensions were centrifuged ($250 \times g$, 5 min) and resuspended in ice-cold freezing medium (60 % [v/v] RPMI 1640, 30 % [v/v] FBS, 10 % [v/v] DMSO). Cells were stored at $-80 \text{ }^\circ\text{C}$ for 2-3 days and afterwards in liquid nitrogen at $-196 \text{ }^\circ\text{C}$.

Thawing

Cells were thawed by rapidly shaking for 1 min in a 37°C water bath and instantly transferred into pre-warmed cell culture medium. After centrifugation ($250 \times g$, 5 min), cells were resuspended in growth medium and cultured as described above.

5.1.3 Cell counting and viability

For routine cell culture, living cells were counted using an automated cell counter (CASY Model TT, OMNI Life Science, Bremen, Germany).

PI staining

Macrophages were co-cultured with yeast overnight and harvested using PBS/EDTA (Sigma-Aldrich). Cells were resuspended in MACS buffer (PBS pH

Materials and methods

7.2 containing 2 mM EDTA, 0.5% (w/v) BSA, and 0.09% (w/v) NaN₃, Miltenyi Biotec) containing 2 µg/mL PI (Propidium Iodide, Sigma-Aldrich). After incubation for 10 min at 4°C, cells were examined on a FACSCalibur (BD Biosciences, Heidelberg, Germany). Results were analyzed using FlowJo v10 software (Tree Star, Inc., Ashland, OR, USA) and are presented as % viable cells.

MTT assay

The MTT (3-(4,5-dimethyl-thiazol-2-)-2,5-diphenyl tetrazolium bromide) colorimetric assay was used to ensure the usage of non-toxic nanoparticle concentrations as described previously (Astanina *et al.*, 2014; Diesel *et al.*, 2013; Ziaei *et al.*, 2015). Briefly, culture medium was replaced by MTT solution (0.5 mg/ml in culture medium) after 24 hours of nanoparticle exposure in medium containing 5% FCS. After incubation for 2 h, the MTT solution was removed and cells were solubilized in dimethyl sulfoxide (DMSO). Absorbance measurements were performed at 550 nm with 630 nm as the reference wavelength using a microplate reader (Tecan Sunrise). The cell viability index was calculated relative to the untreated control and obtained from at least two independent experiments.

5.2 Yeast preparation

Saccharomyces cerevisiae S86c WT or recombinant (carrying the following vectors: pCMV-IRES-eGFP, pMLS1-IRES-eGFP, pICL1-IRES-eGFP, pPGK-IRES-eGFP and pPGK-IRES-MYD88), YPD medium, synthetic complete (SC) medium, uracil-deficient (*ura d/o*) SC medium and agar plates were kindly provided by Dr. Frank Breinig (Molecular and Cell Biology, Saarland University).

5.2.1 Culture

Saccharomyces cerevisiae S86c [MAT α *ura3-2 leu2 his3 pra1 prb2 prc1 cps1*] cells were grown overnight in synthetic complete (SC) medium (0.17% yeast nitrogen base, 0.5% ammonium sulfate, supplemented with amino acids, nucleotides, and 2% glucose) while shaking at 220 rpm at 30°C. Recombinant S.

Materials and methods

cerevisiae cells were grown in SC medium lacking uracil in flasks shaken at 220 rpm at 30°C until O.D.₆₀₀ \simeq 1 was reached.

5.2.2 Fluorescence labeling

10⁷ yeast cells were harvested by centrifugation (3,000 x g, 5 min), washed twice with endotoxin-free PBS (Sigma-Aldrich), and stained with 2.5 μ M carboxyfluorescein diacetate succinimidyl ester (CFSE, Life Technologies) for 30 min at 37°C. Yeast cells were washed twice with PBS containing 5% FBS to remove the residual dye.

5.2.3 Opsonization

Yeast cells were opsonized by incubation with 50% human AB serum (PAA, Pasching, Austria, diluted in PBS), for 30 min at 37°C. Subsequently, the cells were washed twice with PBS and resuspended in macrophage-SFM medium.

5.2.4 Plasmid generation for yeast transformation

The DNA sequences coding for the IRES-TNF fusion construct were synthesized by GeneArt (Life technologies). The IRES-TNF sequence was cloned into the pPGK-IRES-eGFP as XhoI/BglII fragments resulting in pPGK-IRES-TNF replacing the IRES-eGFP sequence. For cloning, ultracompetent *E. coli* cells (NEB 10-beta competent *E. coli*, New England BioLabs, MA, USA) were used following the manufacturer instructions. Transformants were selected on LB plates with 50 mg/ml ampicillin and the isolated plasmid was sequenced (Eurofins MWG Operon, Ebersberg, Germany).

5.2.5 Transformation

Yeast cells were transformed by the lithium acetate method (Ito *et al.*, 1983). In brief, *S. cerevisiae* was grown overnight at 30°C in YPD medium (1% yeast extract, 2% peptone, 2% glucose). Cells were centrifuged (7,000 rpm, 5 min) and washed with LiAc/TE (0.1 M lithium acetate, 10 mM Tris-HCL, 1 mM EDTA, pH 7.5). Yeast was resuspended in 100 μ l LiAc/TE and 10 μ l carrier DNA (salmon

Materials and methods

sperm DNA, 10 mg/ml, Serva, Heidelberg, Germany), 1 µg plasmid DNA, 600 µl PEG solution (0.1 M lithium acetate, 10 mM Tris-HCL, 1 mM EDTA, pH 7.5, PEG 4000 40% [w/v]) and 3 µl of 10x LiAc (lithium acetate 1 M, pH 7.5) were added. The cells were incubated for 30 min at 30°C under agitation at 220 rpm and heat-shocked at 42°C for 15 min. Yeast cells were washed twice with TE (10 mM Tris, 1 mM EDTA, pH 7.5), centrifuged (13,000 rpm, 5 min) and resuspended in TE buffer. To select the transformed yeast, cells were plated on synthetic complete (SC) medium lacking uracil and incubated for three days at 30°C.

5.3 Isolation of DNA

5.3.1 Plasmid DNA isolation

Plasmid DNA was isolated from overnight culture using the Mini plasmid isolation kit (Qiagen, Hilden, Germany) according to the manufacturer's instructions.

5.3.2 THP-1 DNA isolation

DNA was isolated using RiboZol RNA Extraction Reagents (AMRESCO VWR Life sciences, Solon, OH, USA) following the manufacturer instruction. In brief, 10^6 cells were centrifuged (300 x *g*, 5 min) and resuspended in 1 mL RiboZol. After homogenizing the cell lysate by several passage through the tip of a pipette, 200 µL of chloroform were added. Tubes were shaken vigorously for 15 seconds then incubate for 2 minutes at room temperature. Samples were centrifuged (12,000 x *g*, 15 min, 4 °C), the aqueous phase containing the RNA was removed. In order to precipitate the DNA, 300 µl of 100% ethanol were added to the interphase/organic phase and mixed. Samples were centrifuged (2,000 x *g*, 5 min, 4°C) and the pellet was washed twice with 1 mL sodium citrate 0.1 M /10% ethanol, then resuspended in 1 mL 75% ethanol. After 10 min incubation at room temperature, samples were centrifuged (2,000 x *g*, 5 min, 4°C) and pellet was air-dried for 5 minutes. DNA pellet was dissolved in 8 mM NaOH and stored at -20°C.

Materials and methods

5.4 Agarose gel electrophoresis

5.4.1 Detection of DNA

0.8 – 2 % [w/v] agarose (ultra-quality for DNA/RNA electrophoresis, Roth, Karlsruhe, Germany) gels containing 0.4 µg/ml ethidium bromide (Roth) were used depending on the DNA size. After adding 5 x loading buffer (30% [w/v] glycerol, 10 mM Tris (pH 8), 1 mM EDTA, 0.04 % bromphenol blue), DNA samples were loaded onto agarose gel and separated in TBE (9 mM Tris, 90 mM boric acid, 2 mM EDTA) at 100 V. A Quick-Load 2-Log DNA ladder (NEB) or GeneRuler 100 bp DNA Ladder (Thermo Scientific, Invitrogen, Carlsbad, CA, USA) was used in order to determine the DNA band size. Gels were imaged using a gel documentation system E-Box VX2 (Peqlab biotechnologies, Erlangen, Germany).

5.4.2 Detection of RNA

RNA samples were boiled at 68 °C for 10 min in loading buffer (2 x RNA-Ladepuffer Peqlab) then loaded on an agarose-formaldehyde gel (1.2% [w/v] agarose (Ultra-pure agarose, Invitrogen); 1% formaldehyde (roth); 10% MOPS buffer). RNA samples were separated in MOPS buffer (20 mM MOPS; 5 mM sodium acetate; 1 mM EDTA in DEPC-treated water) 1% formaldehyde at 80 v. Gels were imaged using a gel documentation system E-Box VX2 (Peqlab biotechnologies).

5.5 RNA isolation and reverse transcription

5.5.1 RNA isolation

Total RNA was extracted using the RNeasy plus mini kit (Qiagen) following the manufacturer's instructions. RNA quality was checked by agarose gel electrophoresis.

Materials and methods

5.5.2 Measurement of RNA concentration

RNA concentration was measured at 260 nm using a nanodrop 2000c UV-Vis spectrophotometer (Peqlab biotechnologies).

5.5.3 Alu PCR

To confirm the elimination of genomic DNA during the RNA isolation process, a PCR analysis for Alu elements was performed. Alu elements are very abundant and dispersed throughout the human genome. The following primer was used: 5'-TCATGTCGACGCGAGACTCCATCTCAAA-3'. 5 ng THP-1 genomic DNA were used as a positive control. The PCR reaction was performed using a 96 Universal Gradient Pqstar Thermocycler (Peqlab biotechnologies).

One reaction mixture composition:

Taq-Polymerase	2.5 U
10 x Taq-buffer	2.5 µl
MgCl ₂	5 mM
dNTPs	800 µM
primer	100 nM
template	100 ng RNA
H ₂ O	ad 25 µl

Reaction conditions:

Denaturation	5 min 94°C	
Denaturation	1 min 94°C	} 30 cycles
Annealing	1 min 56°C	
Elongation	1 min 72°C	
Final elongation	10 min 72°C	

Products were detected by agarose gel electrophoresis. If no product was detected in the samples, they were considered DNA-free and used for reverse transcription.

Materials and methods

5.5.4 Reverse transcription

200 ng of total RNA were reverse transcribed in a total volume of 20 µl using the High-Capacity cDNA Reverse Transcription Kit (Applied Biosystems, Foster City, CA, USA) according to the manufacturer's instructions. Samples were subsequently diluted with 80 µl of TE buffer (AppliChem, Darmstadt, Germany) and stored at -20°C until use for real-time RT-PCR.

5.6 Real Time RT-PCR

5.6.1 Primer and probes sequences

Primers and dual-labelled probes were obtained from Eurofins MWG Operon.

Primer sequences

mRNA	primer sense (5'→ 3')	primer antisense, (5'→ 3')
ACTB	TGCGTGACATTAAGGAGA AG	GTCAGGCAGCTCGTAGCTCT
IL12B	GTGCCCTGCAGTTAGTTCT	TGGGTCTATTCCGTTGTGTCTT
TNF	CTCCACCCATGTGCTCCTCA	CTCTGGCAGGGGCTCTTGAT
IL6	AATAATAATGGAAAGTGGCTATGC	AATGCCATTTATTGGTATAAAAAC
IL10	CAACAGAAGCTTCCATTCCA	AGCAGTTAGGAAGCCCCAAG
GILZ	TCCTGTCTGAGCCCTGAAGAG	AGCCACTTACACCGCAGAAC
MYD88	TTCGATGCCTTCATCTGCTAT T	CGGTCAGACACACACAACTT

Probe sequences

mRNA	probe, 5' FAM → 3' BHQ1
ACTB	CACGGCTGCTTCCAGCTCCTC
TNF	CACCATCAGCCGCATCGCCGTCTC
IL6	TCCTTTGTTTCAGAGCCAGATCATTCT
IL10	AGCCTGACCACGCTTTCTAGCTGTTGAG
GILZ	CCCGAATCCCCACAAGTGCCCGA

Materials and methods

ACTB, *TNF*, *IL6*, *IL10* and *GILZ* primers and probes sequences were already described (Hoppstädter *et al.*, 2010). *IL12B* primers sequences were provided by Dr. Jessica Hoppstädter (Department of Pharmacy, Pharmaceutical Biology, Saarland University). *MYD88* primers sequences were designed using Primer Quest Tool (Integrated DNA technologies, CA, USA).

5.6.2 Standard dilution series

To quantify the target cDNA and check the real-time RT-PCR efficiency, standard curves were generated by a serial dilution from 60 to 0.00006 attomoles of the PCR product cloned into pGEM-T easy vector (Promega, Madison, WI, USA). Plasmids were diluted in TE-buffer, using the following formula:

$$c \text{ (target-DNA) } [\mu\text{mol/ml}] = c \text{ (plasmid) } [\mu\text{g/ml}] / \text{MW} * L$$

MW: molecular weight of the DNA (approx. 660g/ml) and L: length of plasmid insert in bp.

All plasmids were provided by Dr. Jessica Hoppstädter except for *MYD88*. The standard plasmid for *MYD88* was generated by cloning the *MYD88* PCR product into the pGEM-T vector (Promega, Madison, WI, USA) according to the manufacturer's guidelines.

5.6.3 Experimental procedure

The CFX96 Touch™ Real-Time PCR Detection System (Bio-Rad, Richmond, CA, USA) was used for real-time RT-PCR. Standards were run alongside the samples to generate a standard curve. All samples and standards were analyzed in triplicate. Experiments were performed in 96 well plates using 5 µl of sample or standard.

Materials and methods

Real-time RT-PCR using dual-labeled probes

PCR reaction mix:

Taq-Polymerase	2.5 U
10 x Taq-buffer	2.5 µl
MgCl ₂	3-9 mM
dNTPs	200 µM
Primer forward	500 nM
Primer reverse	500 nM
Dual-labelled probe	2.5 or 1.5 pmol
Template	5 µl
H ₂ O	Up to 25 µl

Reaction conditions:

Denaturation	8 min 95°C	
Denaturation	15 s 95°C	} 40 cycles
Annealing	15 s 57-60°C	
Elongation	15s 72°C	

Target specific conditions:

mRNA	probe	MgCl₂	annealing
<i>ACTB</i>	60 nM	4 mM	60 °C
<i>TNF</i>	100 nM	3 mM	60 °C
<i>IL6</i>	100 nM	4 mM	59 °C
<i>IL10</i>	100 nM	4 mM	60 °C
<i>GILZ</i>	100 nM	4 mM	60 °C

Real-time RT-PCR using EvaGreen

For *IL12B* and *MYD88*, the EvaGreen qPCR Mix Plus (Solis Biodyne, Tartu, Estonia) was used.

Materials and methods

PCR reaction mix:

EvaGreen® mix	4 µl
Primer forward	500 nM
Primer reverse	500 nM
Template	5 µl
H ₂ O	Up to 20 µl

Reaction conditions:

Initial Denaturation	15 min 95°C	
Denaturation	15 s 95°C	} 40 cycles
Annealing	20 s 60°C	
Elongation	20s 72°C	

5.7 Western Blot

5.7.1 Preparation of protein samples

After co-culture with yeast, cells were washed with PBS and stored at -80°C until further use. Cells were then lysed in lysing buffer (50 mM Tris-HCl, 1% [m/v] SDS, 10% [v/v] glycerol, 5% [v/v] β-mercaptoethanol, 0.004% [m/v] bromophenol blue) supplemented with protease inhibitor (Complete; Roche Diagnostics, Basel, Switzerland). Cell lysates were sonicated, centrifuged (17,000 x g, 10 min, 4 °C), and denatured for 5 min at 95°C.

5.7.2 SDS-polyacrylamide gel electrophoresis (SDS-PAGE)

Equal sample volumes were used for SDS-PAGE and separated on 12% gels. A protein marker (Fermentas, St. Leon-Rot, Germany) was used to estimate the molecular masses.

Materials and methods

Composition of 12 % gels:

<u>resolving gel</u>		<u>stacking gel</u>	
H ₂ O	6.6 ml	H ₂ O	5.5 ml
30 % acrylamide Mix	8 ml	30 % acrylamide	1.3 ml
Tris (1.5 M, pH 8.0)	5 ml	Tris (1 M, pH 6.8)	1 ml
SDS (10 % [w/v])	200 µl	SDS (10 % [w/v])	80 µl
APS (10 % [w/v])	200 µl	APS (10 % [w/v])	80 µl
TEMED	20 µl	TEMED	8 µl

Proteins were separated in electrophoresis buffer (24.8 mM Tris, 1.92 mM glycine, 0.1 % [w/v] SDS) for 30 min at 80 V, followed by 2 hours at 100 V. The Mini PROTEAN system (Bio-Rad) was used for gel preparation and electrophoresis.

5.7.3 Blotting

Proteins were transferred to Immobilon FL-PVDF membranes (Millipore, Billerica, MA, USA) using the Mini-Transblot cell (Bio-Rad) system. The membrane was incubated for 30 s in methanol. Sponges, filter papers and membrane were equilibrated in transfer buffer (24.8 mM tris base, 1.92 mM glycine, 20% [v/v] methanol, 0.05% [w/v] SDS), followed by gel sandwich preparation. Blotting was performed overnight at 80 mA.

5.7.4 Immunodetection

After blocking for 1 h in Rockland Blocking Buffer for near- infrared Western Blotting (RBB, obtained from Rockland, Gilbertsville, PA, USA), the membranes were incubated overnight at 4°C with the primary polyclonal antibody anti-MyD88 (abcam, Cambridge, MA, USA) and anti-tubulin (DM1A) (Sigma-Aldrich) diluted 1:1000 in PBST (0.1 % [v/v] tween 20 in PBS) containing 5 % [m/v] dried milk. Subsequently, membranes were washed in PBST (4 times for 5 min) and incubated at room temperature for 1.5 h with the secondary antibodies, i.e. IRDye© 800CW conjugated goat anti-mouse IgG (1:10,000) and IRDye© 680

Materials and methods

conjugated mouse anti-rabbit IgG (1:5,000) diluted in RBB. Blots were washed twice with PBST and twice with PBS, followed by documentation on an Odyssey Infrared Imaging System (LI-COR Biosciences, Lincoln, NE, USA). Relative signal intensities were determined using Odyssey software.

5.8 Flow cytometry

5.8.1 Antibodies

<u>Antibody</u>	<u>Isotype control</u>
APC-labelled mouse anti-human CD206; clone DCN228	APC-IgG1, mouse
FITC-labelled mouse anti-human HLA-A, B, C; clone W6/32	FITC-IgG2a κ , mouse
FITC-labelled anti-human HLA-DR, DP, DQ; clone REA332	FITC-REA
FITC-labelled mouse anti-human CD163; clone GHI/61.1	FITC-IgG1, mouse
PE-labelled mouse anti-human CD14; clone TÜK4	PE-IgG2a, mouse
PE-labelled mouse anti-human CD80; clone 2D10	PE-IgG1, mouse
PE-labelled mouse anti-human CD86; clone B7-2	PE-IgG2b κ , mouse

CD14, CD80, CD163, CD206 and HLA-DR, DP, DQ antibodies and respective isotype control were obtained from Miltenyi Biotec. CD86, HLA-A, B, C antibodies with respective isotype controls were obtained from eBioscience (San Diego, CA, USA). All antibodies were used at concentrations recommended by the supplier.

5.8.2 Cell staining and analysis

Macrophages were harvested using PBS containing 5 mM EDTA (Sigma-Aldrich). Cells were resuspended in MACS Buffer (PBS pH 7.2 containing 2 mM EDTA, 0.5% (w/v) BSA, and 0.09% (w/v) NaN₃, Miltenyi Biotec). FcR receptors were blocked using FcR Blocking Reagent (Miltenyi Biotec). Cells were stained for 10 min at 4°C with the following antibody combinations or respective isotype controls: anti-CD14; anti-HLA-A, B, C/anti-CD206; anti-CD163/ anti-CD80; anti-

Materials and methods

HLA-DR, DP, DQ/ anti-CD86. Stained cells were washed with MACS Buffer then analyzed using FACSCalibur (BD Biosciences) and FlowJo software. Results are reported as relative geometric mean of fluorescence intensity (GMFI; geometric mean of fluorescence intensity of specifically stained cells related to geometric mean of fluorescence intensity of isotype controls)

5.9 Uptake studies

5.9.1 Sample preparation

Particle uptake

Fluorescently labeled (Atto647N) 25 nm or 41 nm silica nanoparticles were provided by Dr. Annette Kraegeloh (Nano Cell Interactions Group, INM – Leibniz Institute for New Materials).

Cells were incubated with nanoparticles (50 µg/ml), or 1.75 µm microparticles (Fluoresbrite carboxylated YG microspheres, Polysciences, Warrington, PA, USA. 100 particles/cell) in RPMI 5% FCS at 37°C, 5% CO₂ for 1 (for flow cytometry) or 3 (fluorescence microscopy) hours.

Yeast uptake

Macrophages were incubated with CFSE-stained yeast cells at an MOI of 7 unless stated otherwise in a total volume of 1 ml at 37°C in 5% CO₂ for 4 hours or the indicated period of time. Plates were briefly centrifuged to ensure that yeast and macrophages were in close contact.

5.9.1 Uptake evaluation by fluorescence microscopy

Cells were washed three times with ice cold PBS and fixed with fixing solution (Cell Biolabs, San Diego, CA, USA) for 15 min at room temperature. Subsequently, cells were washed three times with PBS again and nuclei were counterstained with DAPI (Cell Biolabs) in PBS for 10 min. Cells were kept in PBS for microscopy analysis and stored at 4°C. Particle uptake was analyzed by Anna Dembek with an Axio Observer Zeiss microscope (Carl Zeiss, Göttingen,

Materials and methods

Germany) equipped with a MRM Axiocam at a 63× magnification using AxioVision software. Yeast uptake was imaged using an IX71 inverted microscope (Olympus, Hamburg, Germany) equipped with a 60× PlanApo N oil-immersion objective (Olympus; NA of 1.42). Image overlays were generated using AnalySIS Life Science software (version 2.8, Build1235, Olympus Soft Imaging Solutions).

5.9.2 Uptake quantification by flow cytometry

After incubation with particles or yeast, macrophages were washed 2 times with PBS and detached from plates using PBS containing 5 mM EDTA. Cells were resuspended in MACS buffer and examined on a FACSCalibur (BD Biosciences). Results were analyzed using FlowJo software and are presented as relative geometric mean fluorescence intensity (GMFI; mean fluorescence intensity of particle-loaded cells related to mean fluorescence intensity of untreated controls) for particles uptake and as % CFSE positive macrophages for yeast uptake.

5.10 Cytokine measurement

TNF- α was measured in cell culture supernatant using a TNF alpha ELISA Kit (Invitrogen) according to the manufacturer's instructions. Absorbance was measured using a Tecan sunrise absorbance reader (Tecan, Austria).

5.11 Statistics

If not stated otherwise, data represent the means + SEM of at least 3 independent experiments with cells from different donors, each performed in duplicates. Data distribution was determined by the Shapiro-Wilk test. For normally distributed data, means of two groups were compared with non-paired two-tailed Student's t-test. Whenever the data were not normally distributed, means of two groups were compared using the Mann-Whitney test. Means of

Materials and methods

more than two groups were compared by one-way ANOVA with Bonferroni's post hoc test (normal distribution) or Kruskal-Wallis ANOVA followed by Mann-Whitney test (no normal distribution). Statistical significance was set at a p-value of < 0.05 , < 0.01 , or < 0.001 . Data analysis was performed using Origin software (OriginPro 8.6G; OriginLabs).

6 Summary and outlook

Summary and outlook

Summary and outlook

Macrophages can adopt different phenotypes depending on the surrounding signals, with the pro-inflammatory phenotype (M1) and anti-inflammatory phenotype (M2) representing two extremes of a broad phenotypic spectrum. Tumor-associated macrophages are predominantly M2-polarized and have tumor-promoting functions. Re-educating tumor-associated macrophages towards an M1 phenotype with anti-tumor activity by gene therapy is a promising approach for cancer treatment. For successful gene therapy, several gene delivery systems are being investigated. The ideal gene delivery carrier would be stable, specific and biodegradable. Recently, nanoparticles and whole yeast were suggested as potential nucleic acid carriers.

In this work, we described the interaction of yeast and macrophages. We studied the possibility of using yeast as a gene delivery system to re-educate M2 macrophages towards an M1 phenotype. Finally, we investigated the influence of macrophages polarization on particles uptake.

First, we established and characterized an *in vitro* model of human M1/M2-polarized macrophages. GM-CSF-differentiated macrophages (GM-M Φ) expressed M1 surface markers such as HLAII and CD86, whereas M-CSF-differentiated macrophages (M-M Φ) expressed the scavenger receptor CD163. Further polarization was achieved by the addition of LPS and IFN- γ to GM-M Φ or IL-10 to M-M Φ , thereby generating fully polarized M1 and M2 macrophages, respectively. M1 macrophages were characterized by high amounts of HLAII and CD86, low expression of CD14 and absence of CD163. The M1 pro-inflammatory phenotype was confirmed by the expression of pro-inflammatory cytokines, such as IL-12, TNF- α , and IL-6. M2 macrophages had a high expression of CD14 and CD163, whereas HLAII and CD86 were only slightly expressed. Furthermore, M2 macrophages showed an up-regulation of the anti-inflammatory mediators IL-10 and GILZ, which correlated with their anti-inflammatory phenotype.

Then we studied the interaction between yeast and differently polarized macrophages. M1 macrophages showed a higher yeast uptake capacity when compared with M2 cells. In contrast, opsonized yeast was taken up to the same extent by all *in vitro* polarized macrophages. Opsonized *S. cerevisiae* promoted

Summary and outlook

an M1-like phenotype, as indicated by the induction of pro-inflammatory cytokines.

We also showed that biosynthetic mRNA mycofection is more efficient than DNA delivery in macrophages and established for the first time that *S. cerevisiae*-mediated mRNA delivery can be used to overexpress cytosolic (MyD88) or secreted proteins (TNF- α) in both M1 and M2 macrophages. Furthermore, both MyD88 and TNF- α overexpression re-educated M2 macrophages towards an M1 phenotype. Interestingly, while the upregulation of MyD88 did not show any effect on the M1 macrophages phenotype, it induced a high and long lasting expression of pro-inflammatory cytokines (TNF- α and IL-12) in M2 macrophages. TNF- α delivery had a stronger effect, as it boosted the pro-inflammatory mediator expression in both M1 and M2 cells to a considerable extend. Furthermore, TNF- α overexpression also induced GILZ mRNA upregulation in both M1 and M2 macrophages, possibly indicating the initialization of the resolution phase. Taken together these results suggest the use of mRNA mycofection as a novel strategy repolarize M2 macrophages toward an M1 phenotype. This system can still be improved due the versatility of *S. cerevisiae* as a gene carrier. New studies have shown that co-expression of human perforin in yeast can ameliorate the mRNA delivery efficiency (Walch-Rückheim *et al.*, 2016). It would also be possible to modify the surface properties of the yeast cells in order to enhance their uptake by a specific kind of cells (Kenngott *et al.*, 2016).

Finally, we demonstrated that macrophage polarization influences particle uptake in human macrophages. We employed three different models of human M1/M2 polarized macrophages. Whereas we did not detect any differences between primary M1 and M2 monocyte-derived macrophages regarding the phagocytic uptake of latex microparticles, we showed that M2 polarization enhanced nanoparticle uptake. M2 polarization was also associated with increased nanoparticle uptake in the macrophage-like THP-1 cell line. In accordance, *in vivo* polarized M2-like primary human tumor-associated macrophages (TAM) obtained from lung tumors took up more nanoparticles than M1-like alveolar macrophages isolated from the surrounding lung tissue. Our data indicate that

Summary and outlook

the M2 polarization of macrophages promotes nanoparticle internalization. Therefore, the phenotypical differences between macrophage subsets should be taken into consideration in future investigations on nanosafety, but might also open up therapeutic perspectives allowing to specifically target M2 polarized macrophages.

Taken together, these findings may be of particular interest for the treatment of pathologic conditions that would benefit from reprogramming M2 towards M1 phenotype, such as solid tumors. Both yeast and silica nanoparticles are promising vectors for targeting M2 macrophages, silica nanoparticles due to their preferential uptake by M2 cells and yeast because of their ability of to induce an M1 phenotype in M2 macrophages which can be further enhanced by gene delivery.

This work was supported by KIST-Europe basic research program.

References

7 References

References

References

- Albanese, A., Tang, P. S., and Chan, W. C. (2012) The effect of nanoparticle size, shape, and surface chemistry on biological systems. *Annu Rev Biomed Eng* **14**, 1-16.
- Ambarus, C.A., Krausz, S., van Eijk, M., Hamann, J., Radstake, T.R.D.J., Reedquist, K.A., *et al.* (2012) Systematic validation of specific phenotypic markers for in vitro polarized human macrophages. *J Immunol Methods* **375**, 196–206.
- Amoozgar, Z., and Goldberg, M. S. (2014) Targeting myeloid cells using nanoparticles to improve cancer immunotherapy. *Adv Drug Deliv Rev.*
- Ardiani, A., Higgins, J.P., Hodge, J. W. (2010) Vaccines based on whole recombinant *Saccharomyces cerevisiae* cells, *FEMS Yeast Res.* **10**, 1060–1069.
- Assis-marques, M.A., Oliveira, A.F., Ruas, L.P., Reis, F., Roque-barreira, M.C., Sergio, P., *et al.* (2015) *Saccharomyces cerevisiae* Expressing Gp43 Protects Mice against *Paracoccidioides brasiliensis* Infection. *PLoS One* **10**, 1–13.
- Astanina, K., Simon, Y., Cavelius, C., Petry, S., Kraegeloh, A., and Kiemer, A. K. (2014) Superparamagnetic iron oxide nanoparticles impair endothelial integrity and inhibit nitric oxide production. *Acta Biomater* **10**, 4896-4911.
- Autengruber, A., Sydlik, U., Kroker, M., Hornstein, T., le-Agha, N., Stockmann, D., Bilstein, A., Albrecht, C., Paunel-Gorgulu, A., Suschek, C. V., Krutmann, J., and Unfried, K. (2014) Signalling-dependent adverse health effects of carbon nanoparticles are prevented by the compatible solute mannosylglycerate (firoin) in vitro and in vivo. *PLoS One* **9**, e111485.
- Beier, R. and Gebert, A. (1998) Kinetics of particle uptake in the domes of Peyer's patches. *Am J Physiol* **275**, G130–G137.
- Bender, A.T., Ostenson, C.L., Giordano, D., Beavo, J.A. (2004) Differentiation of human monocytes in vitro with granulocyte – macrophage colony-stimulating factor and macrophage colony-stimulating factor produces distinct changes in cGMP phosphodiesterase expression. *Cellular Signaling* **16**, 365–374.
- Berrebi, D., S. Bruscoli, N. Cohen, A. Foussat, G. Migliorati, L. Bouchet-Delbos, *et al.* (2003) Synthesis of glucocorticoid-induced leucine zipper (GILZ) by macrophages: an anti-inflammatory and immunosuppressive mechanism shared by glucocorticoids and IL- 10. *Blood* **101**, 729–738.
- Bharali, D.J., Klejbor, I., Stachowiak, E.K., Dutta, P., Roy, I., Kaur, N., Bergey, E., Prasad, P., Stachowiak, M.K. (2005) Organically modified silica nanoparticles: a

References

nonviral vector for in vivo gene delivery and expression in the brain. *Proc Natl Acad Sci USA* **102**, 11539–11544

Bilusic, M., Heery, C.R., Arlen, P.M., Rauckhorst, M., Tsang, K.Y., Tucker, J.A., *et al.* (2015) Phase I Trial of a recombinant yeast-CEA vaccine (GI-6207) in adults with metastatic CEA-expressing carcinoma, *Cancer Immunol Immunother* **63**, 225–234.

Bingle, L., Brown, N.J., Lewis, C.E. (2002) The role of tumour-associated macrophages in tumour progression: implications for new anticancer therapies. *J Pathol* **196**, 254–65.

Biswas, S.K., Mantovani, A. (2010) Macrophage plasticity and interaction with lymphocyte subsets: cancer as a paradigm. *Nat Immunol* **11**, 889–896.

Bitar, A., Ahmad, N. M., Fessi, H., and Elaissari, A. (2012) Silica-based nanoparticles for biomedical applications. *Drug Discov Today* **17**, 1147-1154.

BMBF . nano.de-report 2013: status quo of nanotechnology in Germany. 2013. German Federal Ministry of Education and Research.

Boorsma, C. E., Draijer, C., and Melgert, B. N. (2013) Macrophage heterogeneity in respiratory diseases. *Mediators Inflamm* **2013**, 769214.

Boschi, S., Geginat, G., Breinig, T., Schmitt, M.J., Breinig, F. (2011) Uptake of various yeast genera by antigen-presenting cells and influence of subcellular antigen localization on the activation of ovalbumin-specific CD8 T lymphocytes. *Vaccine* **29**, 8165–8173.

Brown, G.D., Gordon, S. (2001) Immune recognition. A new receptor for β -glucans. *Nature* **413**, 36-37.

Canton, J., Khezri, R., Glogauer, M., Grinstein, S. (2014) Contrasting phagosome pH regulation and maturation in human M1 and M2 macrophages. *MBoC* **25**, 3330-3341.

Carta, L., Pastorino, S., Melillo, G., Bosco, M.C., Massazza, S., Varesio, L. (2001) Engineering of macrophages to produce IFN-gamma in response to hypoxia. *J Immunol* **166**, 5374–5380.

Cerovic, V., Bain, C. C., Mowat, A. M., Milling, S. W. F. (2014) Intestinal macrophages and dendritic cells: what's the difference? *Cell* **35**, 270-277.

Chakraborty, P., Chatterjee, S., Ganguly, A., Saha, P., Adhikary, A., Das, T., Chatterjee, M., and Choudhuri, S. K. (2012) Reprogramming of TAM toward

References

proimmunogenic type through regulation of MAP kinases using a redox-active copper chelate. *J Leukoc Biol* **91**, 609-619.

Chang, F. P., Hung, Y., Chang, J. H., Lin, C. H., and Mou, C. Y. (2014) Enzyme encapsulated hollow silica nanospheres for intracellular biocatalysis. *ACS Appl Mater Interfaces* **6**, 6883-6890.

Chanput, W., Mes, J. J., Savelkoul, H. F., and Wichers, H. J. (2013) Characterization of polarized THP-1 macrophages and polarizing ability of LPS and food compounds. *Food Funct* **4**, 266-276.

Chellat, F., Merhi, Y., Moreau, A., and Yahia, L. (2005) Therapeutic potential of nanoparticulate systems for macrophage targeting. *Biomaterials* **26**, 7260-7275.

Chronos, Z., Shepherd, V. L. (1995) Differential regulation of the mannose and SP-A receptors on macrophages. *Am J Physiol* **269**.

De Souza Silva, C., Tavares, A.H., Sousa Jeronimo, M., Soares De Lima, Y., Da Silveira Derengowski, L., Lorenzetti Bocca, A., *et al.* (2015) The Effects of *Paracoccidioides brasiliensis* Infection on GM-CSF-and M-CSF-Induced Mouse Bone Marrow-Derived Macrophage from Resistant and Susceptible Mice Strains. *Mediators Inflamm* 17–19.

Deng, Z. J., Liang, M., Monteiro, M., Toth, I., and Minchin, R. F. (2011) Nanoparticle-induced unfolding of fibrinogen promotes Mac-1 receptor activation and inflammation. *Nat Nanotechnol* **6**, 39-44.

Diesel, B., Hoppstadter, J., Hachenthal, N., Zarbock, R., Cavelius, C., Wahl, B., Thewes, N., Jacobs, K., Kraegeloh, A., and Kiemer, A. K. (2013) Activation of Rac1 GTPase by nanoparticulate structures in human macrophages. *Eur J Pharm Biopharm* **84**, 315-324.

Edin, S., Wikberg, M. L., Rutegard, J., Oldenborg, P. A., and Palmqvist, R. (2013) Phenotypic skewing of macrophages in vitro by secreted factors from colorectal cancer cells. *PLoS One* **8**, e74982.

Elcombe, S.E., Naqvi, S., Van Den Bosch, M.W.M., MacKenzie, K.F., Cianfanelli, F., Brown, G.D., *et al.* (2013) Dectin-1 Regulates IL-10 Production via a MSK1/2 and CREB Dependent Pathway and Promotes the Induction of Regulatory Macrophage Markers. *PLoS One* **8**.

Evstafieva, A. G., Beletsky, A. V., Borovjagin, A. V., Bogdanov, A. A. (1993) Internal ribosome entry site of encephalomyocarditis virus RNA is unable to direct translation in *Saccharomyces cerevisiae*. *FEBS Lett* **335**, 273–6.

Gellissen, G., Hollenberg, C.P. (1997). Application of yeasts in gene expression studies: a comparison of *Saccharomyces cerevisiae*, *Hansenula polymorpha* and *Kluyveromyces lactis* - a review. *Gene* **190**, 87-97.

References

- Gaiomis, J., Lombard, Y., Fonteneau, P. (1993) Both mannose and betaglucan receptors are involved in phagocytosis of unopsonized, heat-killed *Saccharomyces cerevisiae* by murine macrophages. *J Leukoc Biol* **54**, 564–71.
- Gordon, S. and Mantovani, A. (2011) Diversity and plasticity of mononuclear phagocytes. *Eur J Immunol* **41**, 2470-2472.
- Gordon, S., Taylor, P.R. (2005) Monocyte and macrophage heterogeneity. *Nat Rev Immunol* **5**, 953–964.
- Hagemann, T., Lawrence, T., McNeish, I., Charles, K.A., Kulbe, H., Thompson, R.G., Robinson, S.C., and Balkwill, F.R. (2008) “Re-educating” tumor-associated macrophages by targeting NF-kappaB. *J Exp Med* **205**, 1261–1268.
- Hahn, R. T., Hoppstädter, J., Hirschfelder, K., Hachenthal, N., Diesel, B., Kessler, S. M., Huwer, H., and Kiemer, A. K. (2014) Downregulation of the glucocorticoid-induced leucine zipper (GILZ) promotes vascular inflammation. *Atherosclerosis* **234**, 391-400.
- Hamilton, T.A., Zhao, C., Pavicic Jr., P.G., Datta, S. (2014) Myeloid colony-stimulating factors as regulators of macrophage polarization. *Front Immunol* **5**, 1–6.
- Heusinkveld, M., van der Burg, S.H. (2011) Identification and manipulation of tumor associated macrophages in human cancers. *J Transl Med* **9**.
- Holness, C. L. and Simmons, D. L. (1993) Molecular cloning of CD68, a human macrophage marker related to lysosomal glycoproteins. *Blood* **81**, 1607-1613.
- Hoppstädter, J., Diesel, B., Eifler, L. K., Schmidt, T., Brüne, B., and Kiemer, A. K. (2012) Glucocorticoid-Induced Leucine Zipper is downregulated in human alveolar macrophages upon Toll-like receptor activation. *Eur J Immunol* **42**, 1-13.
- Hoppstädter, J., Diesel, B., Zarbock, R., Breinig, T., Monz, D., Koch, M., Meyerhans, A., Gortner, L., Lehr, C. M., Huwer, H., and Kiemer, A. K. (2010) Differential cell reaction upon Toll-like receptor 4 and 9 activation in human alveolar and lung interstitial macrophages. *Respir Res* **11**, 124.
- Hoppstädter, J., Kessler, S.M., Bruscoli, S., Huwer, H., Riccardi, C., Kiemer, A.K. (2015) Glucocorticoid-Induced Leucine Zipper: A Critical Factor in Macrophage Endotoxin Tolerance. *J Immunol* **194**, 6057–6067.
- Hoppstädter, J., Kiemer, A.K. (2015) Glucocorticoid-induced leucine zipper (GILZ) in immuno suppression: master regulator or bystander? *Oncotarget* 1–11.

References

- Izak-Nau, E., Voetz, M., Eiden, S., Duschl, A., and Puentes, V. F. (2013) Altered characteristics of silica nanoparticles in bovine and human serum: the importance of nanomaterial characterization prior to its toxicological evaluation. *Part Fibre Toxicol* **10**, 56.
- Jaguin, M., Houlbert, N., Fardel, O., Lecureur, V. (2013) Polarization profiles of human M-CSF-generated macrophages and comparison of M1-markers in classically activated macrophages from GM-CSF and M-CSF origin. *Cell Immunol* **281**, 51–61.
- Jenkins, S. J. and Hume, D. A. (2014) Homeostasis in the mononuclear phagocyte system. *Trends Immunol* **35**, 358-367.
- Jones, S. W., Roberts, R. A., Robbins, G. R., Perry, J. L., Kai, M. P., Chen, K., Bo, T., Napier, M. E., Ting, J. P., Desimone, J. M., and Bear, J. E. (2013) Nanoparticle clearance is governed by Th1/Th2 immunity and strain background. *J Clin Invest* **123**, 3061-3073.
- Jouault, T., El Abed-El Behi, M., Martínez-Esparza, M., Breuilh, L., Trinel, P.A., Chamailard, M., *et al.* (2006) Specific recognition of *Candida albicans* by macrophages requires galectin-3 to discriminate *Saccharomyces cerevisiae* and needs association with TLR2 for signaling. *J Immunol* **177**, 4679–4687.
- Kenngott, E. E., Kiefer, R., Schneider-daum, N., Hamann, A., Schneider, M., Schmitt, M.J., Breinig, F. (2016) Surface-modified yeast cells : A novel eukaryotic carrier for oral application. *J Control Release* **224**, 1–7.
- Keppler-Ross, S., Douglas, L., Konopka, J.B., Dean, N. (2010) Recognition of yeast by murine macrophages requires mannan but not glucan. *Eukaryot Cell* **9**, 1776–1787.
- Kiemer, A. K., Senaratne, R. H., Hoppstädter, J., Diesel, B., Riley, L. W., Tabeta, K., Bauer, S., Beutler, B., and Zuraw, B. L. (2009) Attenuated activation of macrophage TLR9 by DNA from virulent mycobacteria. *J Innate Immun* **1**, 29-45.
- Kiflmariam, M.G., Yang, H., Zhang, Z. (2013) Gene delivery to dendritic cells by orally administered recombinant *Saccharomyces cerevisiae* in mice. *Vaccine* **31**, 1360–1363.
- Kittan, N.A., Allen, R.M., Dhaliwal, A., Cavassani, K.A., Schaller, M., Gallagher, K.A., *et al.* Cytokine Induced Phenotypic and Epigenetic Signatures Are Key to Establishing Specific Macrophage Phenotypes. *PLoS One* **8**, 1–15.
- Klein, S. G., Serchi, T., Hoffmann, L., Blomeke, B., and Gutleb, A. C. (2013) An improved 3D tetraculture system mimicking the cellular organisation at the

References

- alveolar barrier to study the potential toxic effects of particles on the lung. *Part Fibre Toxicol* **10**, 31.
- Knopp, D., Tang, D., and Niessner, R. (2009) Review: bioanalytical applications of biomolecule-functionalized nanometer-sized doped silica particles. *Anal Chim Acta* **647**, 14-30.
- Komohara, Y., Jinushi, M., Takeya, M. (2014) Clinical significance of macrophage heterogeneity in human malignant tumors. *Cancer Sci* **105**, 1–8
- Korzeniowska, B., Nooney, R., Wencel, D., and McDonagh, C. (2013) Silica nanoparticles for cell imaging and intracellular sensing. *Nanotechnology* **24**, 442002.
- Kratochvill F., Neale, G., Haverkamp, J.M., Van de Velde, L.A., Smith, A. M., *et al.* (2015) TNF Counterbalances the Emergence of M2 Tumor Macrophages *Cell Reports* **12**, 1902–1914.
- Krausgruber, T., Blazek, K., Smallie, T., Alzabin, S., Lockstone, H., Sahgal, N. *et al.* (2011) IRF5 promotes inflammatory macrophage polarization and TH1-TH17 responses., *Nat. Immunol.* **12**, 231–238.
- Krysko, O., Holtappels, G., Zhang, N., Kubica, M., Deswarte, K., Derycke, L., Claeys, S., Hammad, H., Brusselle, G. G., Vandenabeele, P., Krysko, D. V., and Bachert, C. (2011) Alternatively activated macrophages and impaired phagocytosis of *S. aureus* in chronic rhinosinusitis. *Allergy* **66**, 396-403.
- Kuhn, D. A., Vanhecke, D., Michen, B., Blank, F., Gehr, P., Petri-Fink, A., and Rothen-Rutishauser, B. (2014) Different endocytotic uptake mechanisms for nanoparticles in epithelial cells and macrophages. *Beilstein J Nanotechnol* **5**, 1625-1636.
- Kusaka, T., Nakayama, M., Nakamura, K., Ishimiya, M., Furusawa, E., and Ogasawara, K. (2014) Effect of silica particle size on macrophage inflammatory responses. *PLoS One* **9**, e92634.
- Latterini, L. and Amelia, M. (2009) Sensing proteins with luminescent silica nanoparticles. *Langmuir* **25**, 4767-4773.
- Lawrence, T., Natoli, G. (2011) Transcriptional regulation of macrophage polarization: enabling diversity with identity. *Nat Rev Immunol* **11**, 750–761.
- Lesage, G., Bussey, H. (2006) Cell Wall Assembly in *Saccharomyces cerevisiae*. *Microbiology and molecular biology reviews* **70**, 317-343.

References

- Lesniak, A., Fenaroli, F., Monopoli, M. P., Aberg, C., Dawson, K. A., and Salvati, A. (2012) Effects of the presence or absence of a protein corona on silica nanoparticle uptake and impact on cells. *ACS Nano* **6**, 5845-5857.
- Lin, E.Y., Nguyen, A.V., Russell, R.G., Pollard, J.W. (2001) Colony-stimulating factor 1 promotes progression of mammary tumors to malignancy. *J Exp Med* **193**, 727–40.
- Liu, M., Luo, F., Ding, C., Albeituni, S., Hu, X., Ma, Y., *et al.* (2016) Dectin-1 Activation by a Natural Product β -Glucan Converts Immunosuppressive Macrophages into an M1-like Phenotype. *J Immunol*
- Longmire, M., Choyke, P. L., and Kobayashi, H. (2008) Clearance properties of nano-sized particles and molecules as imaging agents: considerations and caveats. *Nanomedicine (Lond)* **3**, 703-717.
- Lorenz, M.C., Bender, J. A., Fink, G.R. (2004) Transcriptional Response of *Candida albicans* upon Internalization by Macrophages Transcriptional Response of *Candida albicans* upon Internalization by Macrophages. *Eukaryot Cell* **3**, 1076–87.
- Lorenz, M.C., Fink, G.R. (2001) The glyoxylate cycle is required for fungal virulence. *Nature* **412**, 83–6.
- Ma, J., Liu, L., Che, G., Yu, N., Dai, F., and You, Z. (2010) The M1 form of tumor-associated macrophages in non-small cell lung cancer is positively associated with survival time. *BMC Cancer* **10**, 112.
- Machuca C., Mendoza-Milla, C., Córdova, E., Mejía, S., Covarrubias, L., Ventura, J., Zentella, A. (2006) Dexamethasone protection from TNF-alpha-induced cell death in MCF-7 cells requires NF-kappaB and is independent from AKT. *BMC Cell Biology* **7**
- Mantovani, A. Sica, A. Sozzani, S. Allavena, P. Vecchi, A. Locati, M. (2004) The chemokine system in diverse forms of macrophage activation and polarization. *Trends Immunol* **25**, 677-86.
- Mantovani, A., Sozzani, S., Locati, M., Allavena, P., Sica, A. (2002) Macrophage polarization: tumor-associated macrophages as a paradigm for polarized M2 mononuclear phagocytes. *Trends Immunol* **23**, 549–55.
- Martinez, F. O., Gordon, S., Locati, M., and Mantovani, A. (2006) Transcriptional profiling of the human monocyte-to-macrophage differentiation and polarization: new molecules and patterns of gene expression. *J Immunol* **177**, 7303-7311.

References

- Martinez, F.O. and Gordon, S. (2014) The M1 and M2 paradigm of macrophage activation : time for reassessment. *F1000Prime Rep* **6**, 1–13.
- Mills, C. D. and Ley, K. (2014) M1 and m2 macrophages: the chicken and the egg of immunity. *J Innate Immun* **6**, 716-726.
- Mills, C.D. Kincaid, K. Alt, J.M. Heilman, M.J. Hill, A.M. (2000) M-1/M-2 macrophages and the Th1/Th2 paradigm. *J Immunol* **164**, 6166-73.
- Montalti, M., Prodi, L., Rampazzo, E., and Zaccheroni, N. (2014) Dye-doped silica nanoparticles as luminescent organized systems for nanomedicine. *Chem Soc Rev* **43**, 4243-4268.
- Mosser, D. M. and Edwards, J. P. (2008) Exploring the full spectrum of macrophage activation. *Nat Rev Immunol* **8**, 958-969.
- Murray, P.J. and Wynn, T.A. (2011) Protective and pathogenic functions of macrophage subsets., *Nat Rev Immunol* **11**, 723–37.
- Napierska, D., Thomassen, L. C., Lison, D., Martens, J. A., and Hoet, P. H. (2010) The nanosilica hazard: another variable entity. *Part Fibre Toxicol* **7**, 39.
- Nayerossadat, N., Maedeh, T., Ali, P. A. (2012) Viral and nonviral delivery systems for gene delivery. *Adv Biomed Res*
- Pollard, J.W. (2004) Tumour-educated macrophages promote tumour progression and metastasis. *Nat Rev Cancer* **4**, 71–8.
- Porcaro, I., Vidal, M., Jouvert, S., Stahl, P.D., Giaimis, J. (2003) Mannose receptor contribution to *Candida albicans* phagocytosis by murine E-clone J774 macrophages. *J Leukoc Biol* **74**.
- Probst, J., Dembski, S., Milde, M., and Rupp, S. (2012) Luminescent nanoparticles and their use for in vitro and in vivo diagnostics. *Expert Rev Mol Diagn* **12**, 49-64.
- Ravi Kumar, M. N., Sameti, M., Mohapatra, S. S., Kong, X., Lockey, R. F., Bakowsky, U., Lindenblatt, G., Schmidt, H., and Lehr, C. M. (2004) Cationic silica nanoparticles as gene carriers: synthesis, characterization and transfection efficiency in vitro and in vivo. *J Nanosci Nanotechnol* **4**, 876-881.
- Reales-Calderón, J.A., Aguilera-Montilla, N., Corbí, Á.L., Molero, G., Gil, C. (2014) Proteomic characterization of human pro-inflammatory M1 and anti-inflammatory M2 macrophages and their response to *Candida albicans*. *Proteomics* **14**, 1503–1518.

References

- Remondo, C., Cereda, V., Mostböck, S., *et al.* (2009) Human dendritic cell maturation and activation by a heat-killed recombinant yeast (*Saccharomyces cerevisiae*) vector encoding carcinoembryonic antigen. *Vaccine* **27**, 987–994.
- Rey-Giraud, F., Hafner, M., and Ries, C. H. (2012) In vitro generation of monocyte-derived macrophages under serum-free conditions improves their tumor promoting functions. *PLoS One* **7**, e42656.
- Rosenholm, J. M., Sahlgren, C., and Linden, M. (2010) Towards multifunctional, targeted drug delivery systems using mesoporous silica nanoparticles--opportunities & challenges. *Nanoscale* **2**, 1870-1883.
- Roy, R., Parashar, V., Chauhan, L. K., Shanker, R., Das, M., Tripathi, A., and Dwivedi, P. D. (2014) Mechanism of uptake of ZnO nanoparticles and inflammatory responses in macrophages require PI3K mediated MAPKs signaling. *Toxicol In Vitro* **28**, 457-467.
- Satoh, T., Saika, T., Ebara, S., Kusaka, N., Timme, T.L, Yang, G., Wang, J., Mouraviev, V., Cao, G., Fattah el, M.A., Thompson, T.C. (2003) Macrophages transduced with an adenoviral vector expressing interleukin 12 suppress tumor growth and metastasis in a preclinical metastatic prostate cancer model. *Cancer Res.* **63**, 7853–7860.
- Schell, R. F., Sidone, B. J., Caron, W. P., Walsh, M. D., White, T. F., Zamboni, B. A., Ramanathan, R. K., and Zamboni, W. C. (2014) Meta-analysis of inter-patient pharmacokinetic variability of liposomal and non-liposomal anticancer agents. *Nanomedicine* **10**, 109-117.
- Seif, M., Philippi, A., Breinig, F., Kiemer, A.K., Hoppstädter, J. (2016) Yeast (*Saccharomyces cerevisiae*) Polarizes Both M-CSF- and GM-CSF-Differentiated Macrophages Toward an M1-Like Phenotype. *Inflammation*
- Shin, M., Yoo, H.S. (2013) Animal vaccines based on orally presented yeast recombinants. *Vaccine* **31**, 4287–4292.
- Sica, A. and Mantovani, A. (2012) Macrophage plasticity and polarization: in vivo veritas. *J Clin Invest* **122**, 787-795.
- Sica, A., Larghi, P., Mancino, A., Rubino, L., Porta, C., Totaro, M. G., Rimoldi, M., Biswas, S. K., Allavena, P., and Mantovani, A. (2008) Macrophage polarization in tumour progression. *Semin Cancer Biol* **18**, 349-355.
- Sica, A., Rubino, L., Mancino, A., Larghi, P., Porta, C., Rimoldi, M., Solinas, G., Locati, M., Allavena, P., and Mantovani, A. (2007) Targeting tumour-associated macrophages. *Expert Opin Ther Targets* **11**, 1219-1229.

References

- Sica, A., Schioppa, T., Mantovani, A., Allavena, P. (2006) Tumour-associated macrophages are a distinct M2 polarised population promoting tumour progression: Potential targets of anti-cancer therapy. *European journal of cancer* **42**, 717-727.
- Sicard, D., Legras, J.L. (2011) Bread, beer and wine: yeast domestication in the *Saccharomyces sensu stricto* complex. *Comptes Rendus Biologies* **334**, 229-236.
- Singh, A., Talekar, M., Raikar, A., Amiji, M. (2014) Macrophage-targeted delivery systems for nucleic acid therapy of inflammatory diseases. *Journal of Controlled Release* **190**, 515–530
- Smith, R.A., Duncan, M.J., Moir, D.T. (1985) Heterologous protein secretion from yeast. *Science* **229**, 1219-1224.
- Sohaebuddin, S. K., Thevenot, P. T., Baker, D., Eaton, J. W., and Tang, L. (2010) Nanomaterial cytotoxicity is composition, size, and cell type dependent. *Part Fibre Toxicol* **7**, 22.
- Solinas, G., Germano, G., Mantovani, A., and Allavena, P. (2009) Tumor-associated macrophages (TAM) as major players of the cancer-related inflammation. *J Leukoc Biol* **86**, 1065-1073.
- Staples, K. J., Smallie, T., Williams, L. M., Foey, A., Burke, B., Foxwell, B. M., and Ziegler-Heitbrock, L. (2007) IL-10 induces IL-10 in primary human monocyte-derived macrophages via the transcription factor Stat3. *J Immunol* **178**, 4779-4785.
- Stout, R. D., Watkins, S. K., and Suttles, J. (2009) Functional plasticity of macrophages: in situ reprogramming of tumor-associated macrophages. *J Leukoc Biol* **86**, 1105-1109.
- Tabata, K., Kurosaka, S., Watanabe, M., Edamura, K., Satoh, T., Yang, G., Abdelfattah, E., Wang, J., Goltsov, A., Floryk, D., Thompson, T.C.(2011) Tumor growth and metastasis suppression by Glipr1 gene-modified macrophages in a metastatic prostate cancer model, *Gene Ther* **18**, 969–978.
- Tang, X., Mo, C., Wang, Y., Wei, D., Xiao, H. (2013) Anti-tumour strategies aiming to target tumour-associated macrophages. *Immunology* **138**, 93–104.
- Tjiu, J. W., Chen, J. S., Shun, C. T., Lin, S. J., Liao, Y. H., Chu, C. Y., Tsai, T. F., Chiu, H. C., Dai, Y. S., Inoue, H., Yang, P. C., Kuo, M. L., and Jee, S. H. (2009) Tumor-associated macrophage-induced invasion and angiogenesis of human basal cell carcinoma cells by cyclooxygenase-2 induction. *J Invest Dermatol* **129**, 1016-1025.

References

- Truong, N. P., Whittaker, M. R., Mak, C. W., and Davis, T. P. (2014) The importance of nanoparticle shape in cancer drug delivery. *Expert Opin Drug Deliv* 1-14.
- Uematsu, S., Akira, S. (2008) Toll-like receptors (TLRs) and their ligands. *Handbook of Experimental Pharmacology* **183**.
- Underhill, D.M., Goodridge, H.S. (2012) Information processing during phagocytosis. *Nat Rev Immunol* **12**, 492–502.
- Vago, J.P., Tavares, L.P., Garcia, C.C., Lima, K.M., Perucci, L.O., Vieira, É.L., *et al.* (2015) The role and effects of glucocorticoid-induced leucine zipper in the context of inflammation resolution. *J Immunol* **194**, 4940–50.
- Valenzuela, P., Medina, A., Rutter, W.J. (1982) Synthesis and assembly of hepatitis B virus surface antigen particles in yeast. *Nature* **298**, 347-350.
- Varin, A., Mukhopadhyay, S., Herbein, G., and Gordon, S. (2010) Alternative activation of macrophages by IL-4 impairs phagocytosis of pathogens but potentiates microbial-induced signalling and cytokine secretion. *Blood* **115**, 353-362.
- Verreck, F. A. W., De Boer, T., Langenberg, D.M.L., Van Der Zanden, L., Ottenhoff, T.H.M. (2006) Phenotypic and functional profiling of human proinflammatory type-1 and anti-inflammatory type-2 macrophages in response to microbial antigens and IFN- γ - and CD40L-mediated costimulation. *J Leukoc Biol* **79**, 285–293.
- Verreck, F.A.W. Boer, T. de. Langenberg, D.M.L. Hoeve, M.A. Kramer, M. Vaisberg, E. Kastelein, R. Kolk, A. Waal-Malefyt, R. de. Ottenhoff, T.H.M. (2004) Human IL-23-producing type 1 macrophages promote but IL-10-producing type 2 macrophages subvert immunity to (myco) bacteria. *Proc Natl Acad Sci USA* **101**, 4560-5.
- Vijayanathan, V., Agostinelli, E., Thomas, T., and Thomas, T. J. (2014) Innovative approaches to the use of polyamines for DNA nanoparticle preparation for gene therapy. *Amino Acids* **46**, 499-509.
- Walch, B., Breinig, T., Schmitt, M.J., Breinig, F. (2012) Delivery of functional DNA and messenger RNA to mammalian phagocytic cells by recombinant yeast. *Gene Ther* **19**, 237–45.
- Walch-Rückheim, B., Kiefer, R., Geginat, G., Schmitt, M.J., Breinig, F. (2015) Coexpression of human perforin improves yeast-mediated delivery of DNA and mRNA to mammalian antigen- presenting cells. *Gene Ther* **23**, 103–107.

References

- Wang, J. Q., Jeelall, Y.S., Ferguson, L.L., Horikawa, K. (2014) Toll-like receptors and cancer: MYD88 mutation and inflammation. *Front Immunol* **5**
- Watanabe, H., Numata, K., Ito, T., Takagi, K., and Matsukawa, A. (2004) Innate immune response in Th1- and Th2-dominant mouse strains. *Shock* **22**, 460-466.
- Wu, T. and Tang, M. (2014) Toxicity of quantum dots on respiratory system. *Inhal Toxicol* **26**, 128-139.
- Xu, W., Schlagwein, N., Roos, A., van den Berg, T.K., Daha, M.R., van Kooten, C. (2007) Human peritoneal macrophages show functional characteristics of M-CSF-driven anti-inflammatory type 2 macrophages. *Eur J Immunol* **37**, 1594–1599.
- Yoo, J. W., Chambers, E., and Mitragotri, S. (2010) Factors that control the circulation time of nanoparticles in blood: challenges, solutions and future prospects. *Curr Pharm Des* **16**, 2298-2307.
- Zhang, B., Yao, G., Zhang, Y., Gao, J., Yang, B., Rao, Z., Gao, J. (2011) M2-polarized tumor-associated macrophages are associated with poor prognoses resulting from accelerated lymphangiogenesis in lung adenocarcinoma. *Clinics* **66**, 1879-1886.
- Zhang, L., Zhang, T., Wang, L., Shao, S., Chen, Z., Zhang, Z. (2014) In vivo targeted delivery of CD40 shRNA to mouse intestinal dendritic cells by oral administration of recombinant *Saccharomyces cerevisiae*. *Gene Ther* **21**, 709–714.
- Zhao, B., Yin, J. J., Bilski, P. J., Chignell, C. F., Roberts, J. E., and He, Y. Y. (2009) Enhanced photodynamic efficacy towards melanoma cells by encapsulation of Pc4 in silica nanoparticles. *Toxicol Appl Pharmacol* **241**, 163-172.
- Ziaei, A., Hoppstadter, J., Kiemer, A. K., Ramezani, M., Amirghofran, Z., and Diesel, B. (2015) Inhibitory effects of teuclatriol, a sesquiterpene from *salvia mirzayanii*, on nuclear factor-kappaB activation and expression of inflammatory mediators. *J Ethnopharmacol* **160**, 94-100.

8 Publications

Original Publications

Hoppstädter J, **Seif M**, Dembek A, Cavelius C, Huwer H, Kraegeloh A and Kiemer AK. M2 polarization enhances silica nanoparticle uptake by macrophages. *Front. Pharmacol.* 2015; 6:55. doi: 10.3389/fphar.2015.00055

Seif M, Philippi A, Breinig F, Kiemer AK, Hoppstädter J. Yeast (*Saccharomyces cerevisiae*) polarizes both M-CSF and GM-CSF differentiated macrophages towards an M1-like phenotype. *Inflammation* 2016. doi:10.1007/s10753-016-0404-5

Seif M, Hoppstädter J., Breinig F, Kiemer A.K. Yeast-mediated *MYD88* or *TNF* mRNA delivery re-educates M2 macrophages towards an M1-like phenotype (in preparation).

Abstracts to poster presentations

Seif M, Philippi A, Hoppstädter J, Breinig F, Kiemer AK. Yeast (*Saccharomyces cerevisiae*) polarizes both M-CSF and GM-CSF differentiated macrophages towards an M1-like phenotype. 44th annual meeting of the German society for immunology, Bonn, Germany, 2014.

Seif M, Philippi A, Hoppstädter J, Breinig F, Kiemer AK. Yeast (*Saccharomyces cerevisiae*) polarizes both M-CSF and GM-CSF differentiated macrophages towards an M1-like phenotype. 28th international conference of the European macrophage and dendritic cell society, Vienna, Austria, 2014.

Publications

Seif M, Hoppstädter J, Dembek A, Cavellius C, Huwer H, Kraegeloh A and Kiemer AK. M2 polarization enhances silica nanoparticle uptake by macrophages. 13th Annual Meeting of the Association for Cancer Immunotherapy, Mainz, Germany, 2015

Seif M, Breinig F, Kiemer AK, Hoppstädter J. *Saccharomyces cerevisiae* induces an M1 phenotype and can be used to deliver functional mRNA and DNA to human macrophages. Keystone Symposia conference, Myeloid Cells (D3), Killarney, Ireland, 2016.

Acknowledgment

9 Acknowledgment

I am very grateful to Prof. Dr. Alexandra Kiemer for supervising this work and giving me the opportunity to be part of her working group. I appreciate her continuous support and encouragement during tough times in the Ph.D. pursuit, and all her contributions of time, guidance and ideas to make my Ph.D. experience productive and stimulating.

To Prof. Dr. Manfred Schmitt for kindly consenting to provide the second expert report and for the fruitful discussions during my progress reports.

To Dr. Jessica Hoppstädter for the scientific input, valuable suggestions and discussions, for her time, patience and encouragement.

To Dr. Frank Breinig for providing the knowledge and material for yeast experiments.

I acknowledge KIST Europe for the financial support and laboratory facilities.

Dr. Anja Philippi for giving me the opportunity to work on this topic in KIST-Europe, for initiating the study and helping me preparing my move to Germany.

Anna Dembek for performing the microscopy for nanoparticle uptake and the experiments with lung macrophages, for helping with the MTT assay and always offering help in the lab.

Ruth Kiefer for preparing yeast culture medium and plates.

Dr. Annette Kraegeloeh and Dr. Christian Cavelius for providing the silica nanoparticles and Dr. Hanno Huwer for providing lung and tumor tissue.

Acknowledgment

Birgit Wiegand for all the help in administrative issues since the very beginning of my stay in Germany and for technical assistance.

Daniela Vanni-Strassner and Tim Mehlhorn for technical assistance.

The whole “AG Kiemer” for the friendly working atmosphere and for always being ready to help.

All members of KIST-Europe, specially Dr. Nuriye Korkmaz and Ruth Eggers for the warm and friendly atmosphere in the office and for scientific discussions.

My friends specially Rita, Alice, Oras, Elie and Antoine for always giving me motivation.

Finally, I would like to thank my family for their love, encouragement and support.